

NUREG/CR-4260

LA-10435-M

Manual

Los Alamos National Laboratory is operated by the University of California for the United States Department of Energy under contract W-7405-ENG-36.

For Reference

Not to be taken from this room

*USER'S Manual*

*Computer Code for Analyzing Tornado-Induced Flow*

*and Material Transport in Nuclear Facilities*



**Los Alamos** Los Alamos National Laboratory  
Los Alamos, New Mexico 87545

An Affirmative Action/Equal Opportunity Employer

Edited by M. C. Timmers, Group Q-6

Prepared by L. C. Duncan and O. E. Garnica, Group Q-6

**NOTICE**

This report was prepared as an account of work sponsored by an agency of the United States Government. Neither the United States Government nor any agency thereof, or any of their employees, makes any warranty, expressed or implied, or assumes any legal liability or responsibility for any third party's use, or the results of such use, of any information, apparatus, product or process disclosed in this report, or represents that its use by such third party would not infringe privately owned rights.

NUREG/CR-4260  
LA-10435-M  
Manual

RZ

## TORAC User's Manual

### A Computer Code for Analyzing Tornado-Induced Flow and Material Transport in Nuclear Facilities

R. W. Andrae  
P. K. Tang  
R. A. Martin  
W. S. Gregory

Manuscript submitted: April 1985  
Date published: May 1985

Prepared for  
Division of Risk Analysis  
Office of Nuclear Regulatory Research  
US Nuclear Regulatory Commission  
Washington, DC 20555

NRC FIN No. A7029



**Los Alamos** Los Alamos National Laboratory  
Los Alamos, New Mexico 87545

## CONTENTS

	<u>Page</u>
ABSTRACT.....	1
I. INTRODUCTION.....	1
II. THE COMPUTER CODE.....	3
III. MODELING.....	4
A. General Information.....	4
B. System Modeling.....	4
C. Gas Dynamics Modeling.....	11
D. Material Transport Models.....	16
E. Initial Conditions.....	20
F. Accident Description.....	20
G. Expected Results.....	22
IV. INPUT PREPARATION.....	22
A. Data Deck Organization.....	22
B. Input Card Description.....	24
C. Restart Procedure.....	46
V. CODE OUTPUT.....	46
A. Input Return.....	46
B. Output Lists and Summaries.....	46
C. Printer Plots.....	47
D. Diagnostic Messages.....	47
VI. SAMPLE PROBLEMS.....	48
APPENDIX A. GAS DYNAMICS SUMMARY.....	102
APPENDIX B. MATERIAL TRANSPORT THEORY.....	105
REFERENCES.....	134

# TORAC USER'S MANUAL

## A Computer Code for Analyzing Tornado-Induced Flow and Material Transport in Nuclear Facilities

by

R. W. Andrae, P. K. Tang,  
R. A. Martin, and W. S. Gregory

### ABSTRACT

This manual describes the TORAC computer code, which can model tornado-induced flows, pressures, and material transport within structures. Future versions of this code will have improved analysis capabilities. In addition, it is part of a family of computer codes that is designed to provide improved methods of safety analysis for the nuclear industry. TORAC is directed toward the analysis of facility ventilation systems, including interconnected rooms and corridors.

TORAC is an improved version of the TVENT computer code. In TORAC, blowers can be turned on and off and dampers can be controlled with an arbitrary time function. The material transport capability is very basic and includes convection, depletion, entrainment, and filtration of material. The input specifications for the code and a variety of sample problems are provided.

---

### I. INTRODUCTION

This user's manual supports the computer code TORAC, which can simulate tornado-induced flows, pressures, and material transport within structures. Its use is directed toward nuclear fuel cycle facilities and their primary release pathway—the ventilation system. However, it is applicable to other structures and can be used to model other airflow pathways within a facility.

This computer code is essentially the TVENT computer code, but it has been modified to include material transport, particularly transport of radioactive material. This is the first of a number of versions that will evolve into more refined and improved codes. In addition, it is part of a family of computer codes that are designed to provide improved methods of safety analysis for the nuclear fuel cycle industry. The family of accident analysis codes also will include codes to address fire, explosion, criticality, and equipment failure within nuclear facilities.

This manual is similar to the TVENT user's manual, and we suggest that the reader obtain a copy of it for reference.<sup>1</sup> TORAC retains all the gas-dynamic features of TVENT plus gives the user an additional basic ability to simulate the transport of material through and out of the facility. TORAC is written in FORTRAN IV and is designed to run on a CDC 7600 computer. As in TVENT, the free-format and film-plotting options are precluded but can be added easily to fit particular computer installations.

TORAC simulates steady-state and transient pressure and flow distributions in complex airflow pathways within structures. System pressures, flows, and material transport in this version of the code are based on the following assumptions.

- Isothermal flow
- Lumped-parameter formulation
- Incompressible flow with compressibility at nodes
- Gas dynamics decoupled from material transport
- No material interaction, phase change, or chemical reaction allowed during transport
- Homogeneous mixture and dynamic equilibrium
- Material deposition only by the mechanism of gravitational settling
- Material entrainment based on the resuspension factor and other concepts for rooms and on semi-empirical entrainment rate equations and wind tunnel data for ducts

A problem can be stopped and restarted; this is especially advantageous when modeling systems with changing time steps or analyzing complex systems requiring long computing times. This feature was used in TVENT to simulate the failure of components or system changes during a transient. A detailed description of the modeling necessary to simulate the facility system and the tornado accident

event will be given. Detailed discussions of the gas dynamics and material transport theory are in Appendixes A and B, respectively.

## II. THE COMPUTER CODE

TORAC is designed to be used on large computers. It is portable; that is, it should be installed easily on most computers with a minimum of changes required. Three BCD and four binary files are used: input (unit 5), standard printed output (unit 6), special printed output for restart (unit 18), temporary read/write (units 10, 17, and 59), and saved output (unit 23). (The latter four files are binary.) CRT plots can be made using an auxiliary program based on the DISSPLA language (input unit 10). Standard printed plots and the unit 10 file can be made after the run from the information on unit 23.

This version of TORAC uses five special utilities that are on the Los Alamos National Laboratory's LTSS computer system. They have a convenient, but not vital, role. If at all possible, these callouts should be replaced by their counterparts in the user's computer system. These five utilities and their line locations are given in the "Glossary of Variables" appearing at the end of the code. They are defined as follows.

1. CALL FEXIST (IFILE,IFLAG)  
Routine to see whether a given file exists  
IFILE = Name of File  
IFLAG = 0 does not exist  
1 exists
2. CALL DESTROY  
Routine to destroy a file
3. CALL SECOND(T)  
Routine to return the difference between the initial time limit and the time remaining for the job.
4. CALL DATEH(IDATE)  
Routine to return the current date
5. CALL TIMEH (ITIME)  
Routine to return the current time

Information that will make it easy for a programmer to modify the code also is given at the end of the code. This includes an index of subroutines, a summary of read-in statements, and a glossary of variables.

### III. MODELING

#### A. General Information

TORAC is designed to predict airflows in an arbitrarily connected network system. In a nuclear facility, this network system could include process cells, canyons, laboratory offices, corridors, and offgas systems. The ventilation system is an integral part of this network; it moves air into, through, and out of the facility. Therefore, TORAC must be able to predict flow through a network system that also includes ventilation system components such as filters, dampers, ducts, and blowers. These ventilation system components are connected to the rooms and corridors of the facility to form a complete network for moving air through the structure and perhaps maintaining pressure levels in certain areas.

#### B. System Modeling

The first and most critical step in setting up a model of the air pathways in a nuclear facility requires a comprehensive schematic of the system components and their interconnections. Drawings, specifications, material lists, safety analysis reports, and existing schematics can be used in deriving a system description. A physical inspection of the facility and consultations with the designer(s) before and after it is drawn may be necessary to verify that the schematic is correct. (At this stage, there frequently is a lack of data.) Although there is no substitute for accurate data, certain assumptions, averaging, or conservative estimates can be used to make the problem manageable. Figures 1 and 2 show how a simple ventilation system within a facility structure can be transformed into a network schematic. We will illustrate the system-modeling concepts in the next section and then provide additional modeling detail for the flow and material transport modeling.

1. System Definitions. Three terms are used to describe the construction of a model, and they are used extensively in the remainder of this report.

- System. A network of components (branches) joined together at points called nodes.
- Branch. A connecting member between upstream and downstream nodal points. A branch contains one component. (Ducts, dampers, filters, and blowers are components that can exist in a branch. Flow is defined for a branch.)



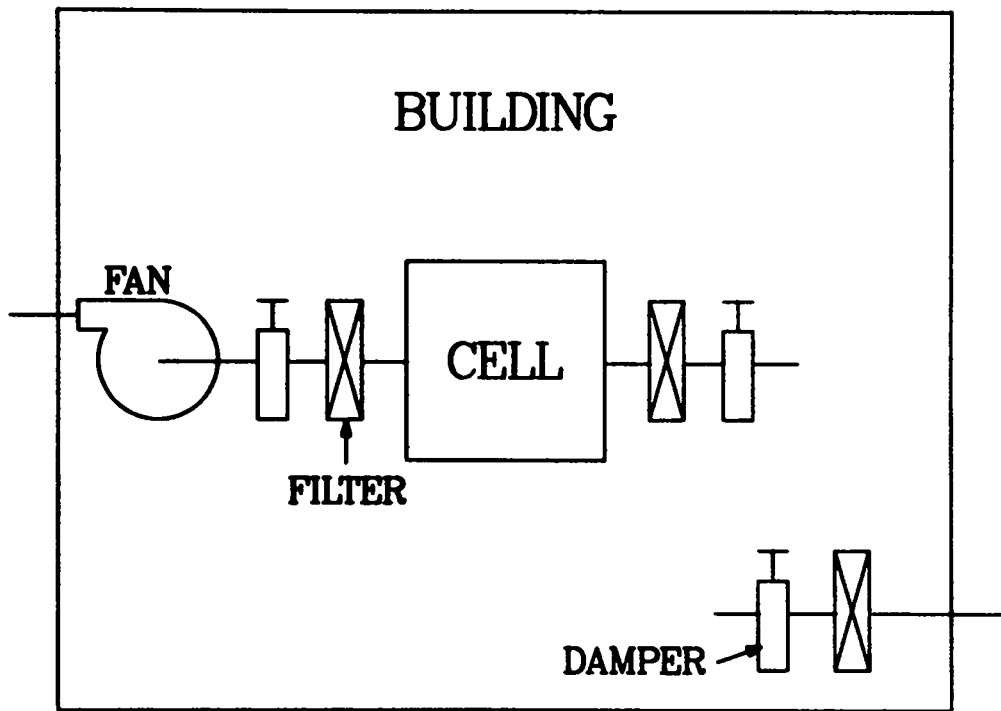


Fig. 1.  
Facility with ventilation system.

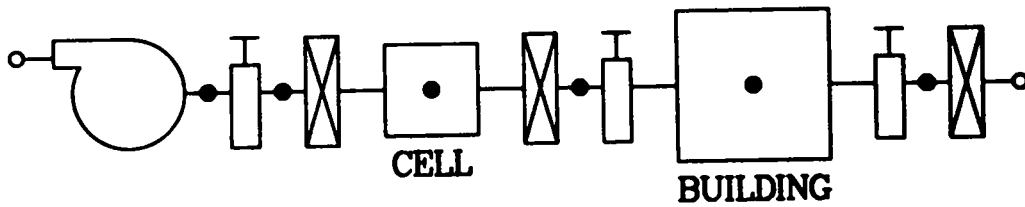


Fig. 2.  
Network schematic of facility with ventilation system.

- Node. A connection point or junction for one or more branches. Volume elements such as rooms, gloveboxes, and plenums are defined as capacitance nodes. The compressibility of the system fluid is accounted for at these capacitance nodes. Boundary points (inlet and exhaust) are defined at nodes. System pressure and material concentration also are defined at nodes.

2. System Modeling Examples. Network systems for airflow through a nuclear facility can be constructed using a building block approach. The building blocks used to construct network systems are shown in Fig. 3 and can be arranged to form arbitrary systems (Fig. 4). The building block symbols will be used throughout this report. An example of the correspondence of the building block schematic to a simple network system is presented in Fig. 5.

Nodes 1 and 9 in Fig. 5 are boundary nodes. A capacitance node, 4, represents the sampling room. Branches are shown in Fig. 5 at the tips of arrows. The branch numbers are in parentheses adjacent to their corresponding branches. Note that branch 3 is connected on the upstream side by node 3 and on the downstream side by capacitance node 4. Duct resistance is shown separately in branch 2, whereas it is lumped or combined with damper resistance for branches 4 through 8.

Thus far, we have discussed extremely simple network systems. A slightly more complex system is shown in Fig. 6, and its corresponding schematic is shown in Fig. 7. This system shows a room (node 2) with three connected branches (1, 2, and 3). Also illustrated, using branch 5 and node 5, is the leakage path around the cell access hatch.

Additional network complexity is shown in Fig. 8. Figure 8 is a single frame from a computer-generated movie that shows the tornado-induced flow through a system. Figure 9 is the network schematic for the system shown in Fig. 8. Although the system shown in Fig. 9 is quite small when compared with many network systems in nuclear facilities, it contains most of the elements common to larger facilities. This system features the following.

- Natural bypass around rooms
- Recirculation
- Combinations of series and parallel component arrangements
- Rooms (confinement volumes) with multiple inlets and outlets
- Duct friction
- A network consisting of 30 components and 25 nodal points

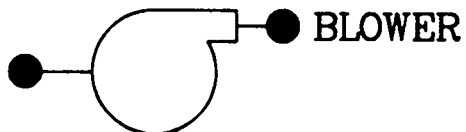
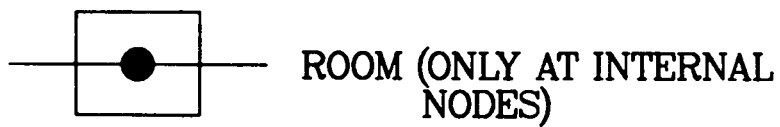
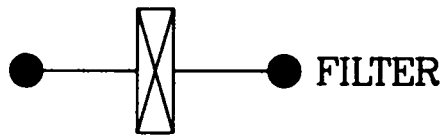
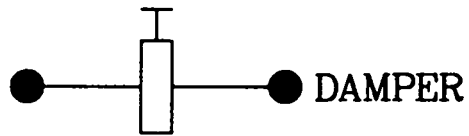


Fig. 3.  
Network system building blocks.

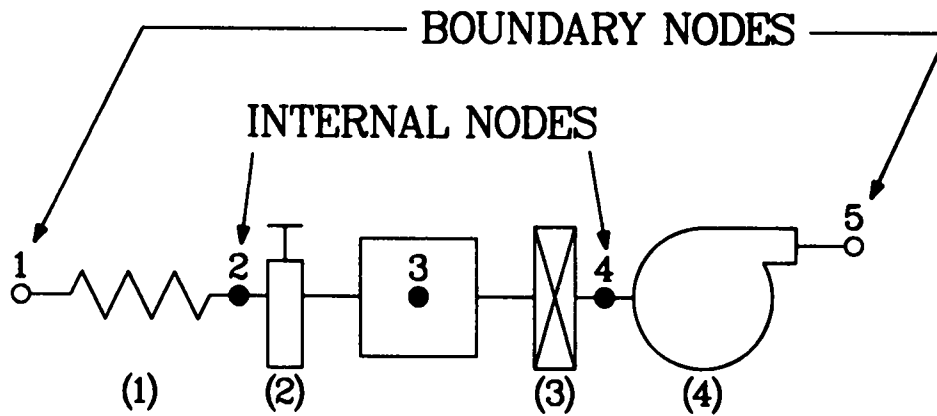


Fig. 4.  
Connection of building blocks.

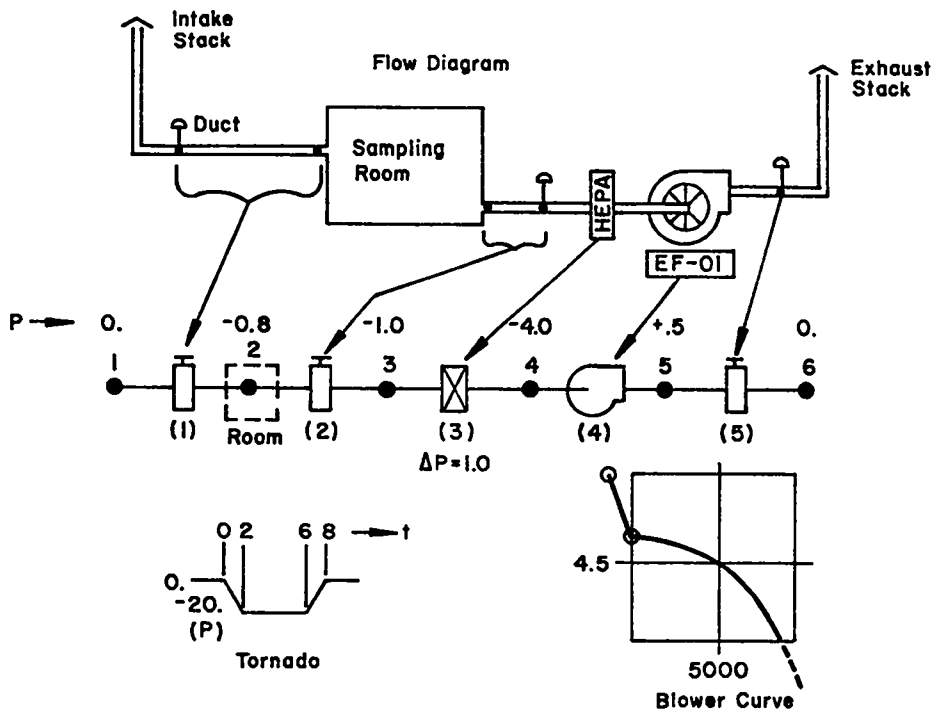


Fig. 5.  
Lumped modeling of simple system.

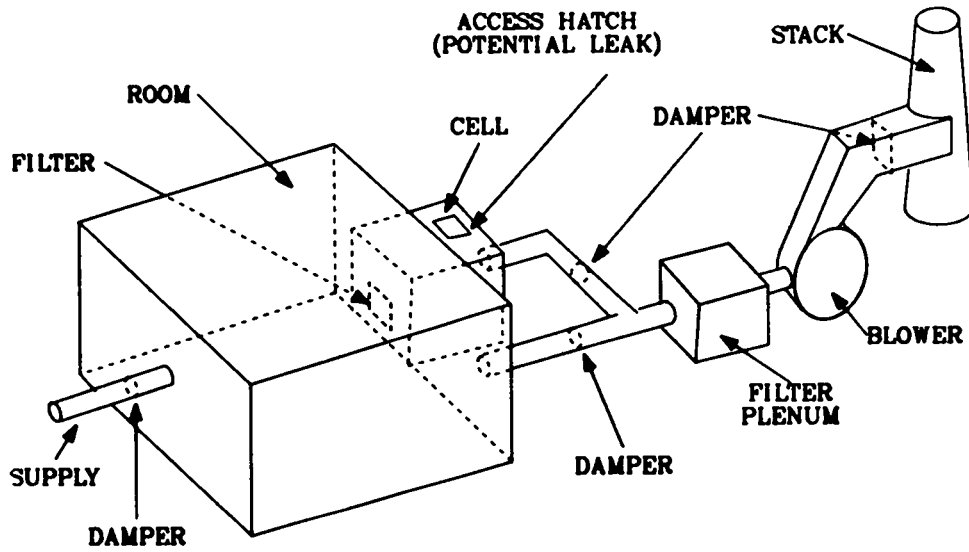


Fig. 6.  
Simple flow network.

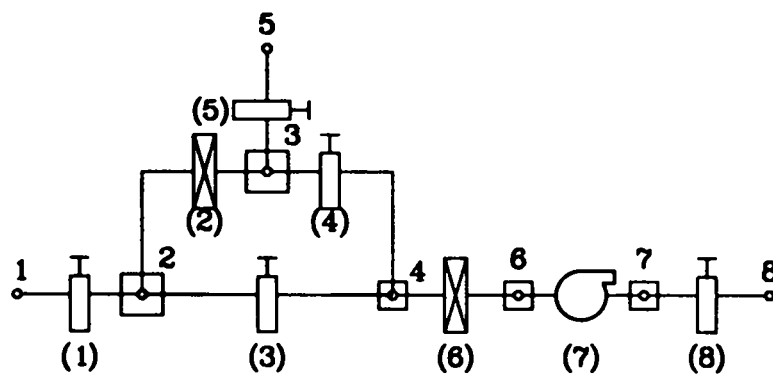


Fig. 7.  
TORAC schematic.

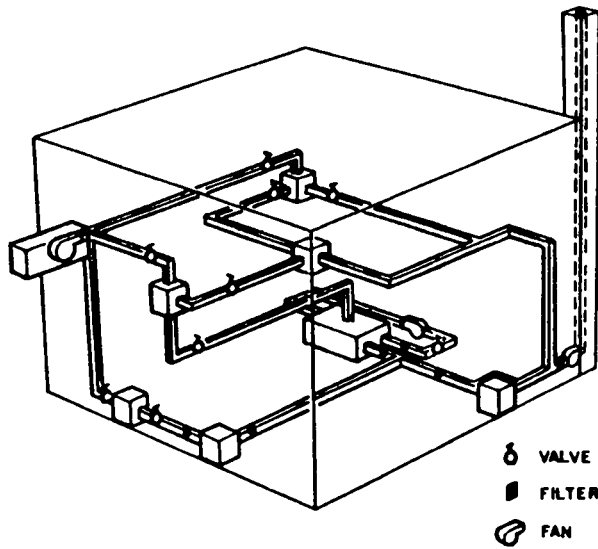


Fig. 8.  
Sample network system schematic.

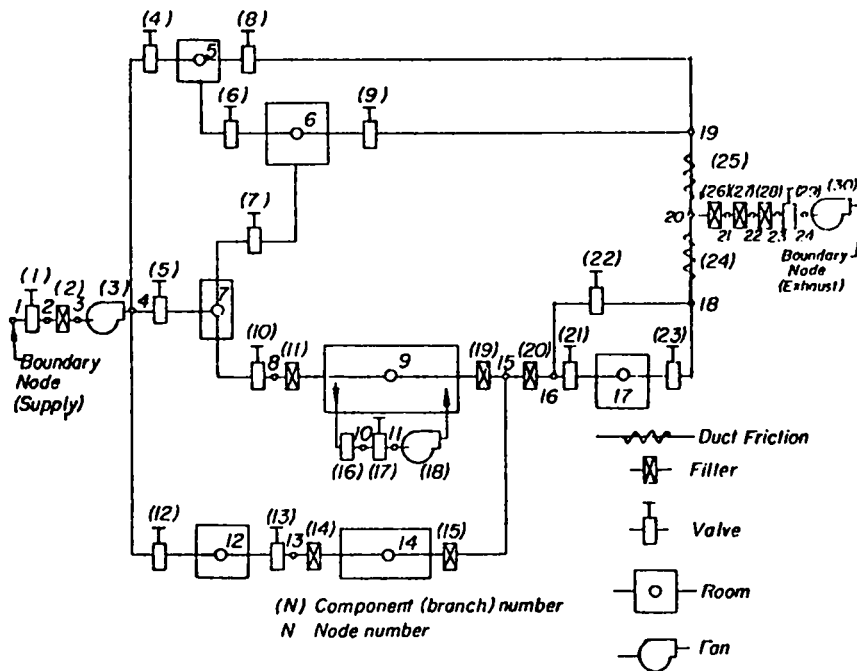


Fig. 9.  
Sample network model for TORAC.

### C. Gas Dynamics Modeling

A more detailed summary of the gas dynamics model is given in Appendix A. The modeling defines the system elements; a branch is defined as a connecting member between nodes and contains only one component. Boundary conditions (pressures as a function of time) and capacitance are prescribed at the nodal points. Following the lumped-parameter approach, all of the pressure losses for a branch are ascribed to the components contributing the largest pressure loss; thus, duct losses may be lumped with the damper loss. Similarly, the effects of components such as elbows or turning vanes are lumped with the duct losses. This is correct if the characteristic relationship between pressure drop and flow is the same (has the same exponent value). However, branches should be added when the relationship is not the same; for example, where a duct contains a filter and the duct loss is significant. A common method of representing the pressure-flow relationship<sup>1</sup> is

$$\Delta P = R Q^n \quad , \quad (1)$$

where

$\Delta P$  = pressure drop across the component,  
R = resistance coefficient,  
Q = branch volumetric flow, and  
n = flow exponent (1.0 for filters,  
2.0 for dampers and ducts).

TORAC can calculate the resistance coefficients of dampers, filters, ducts, and leakage based on Eq. (1) with the input values of pressure drop and flow. A user-supplied resistance overrides the calculated value from Eq. (1) and is particularly useful in parametric and sensitivity studies. However, any supplied R will be used with Eq. (1) in obtaining steady-state and transient results. Consequently, the supplied value must be compatible with Eq. (1).

1. Ducts. Ducts are modeled using the friction loss equation

$$P = fL/d_h(\rho u^2/2g) \quad , \quad (2)$$

where

- $f$  = nondimensional friction factor obtained from the Moody diagram,
- $d_h$  = hydraulic diameter,
- $L$  = duct length,
- $u$  = average velocity in duct,
- $g$  = acceleration of gravitational constant, and
- $\rho$  = air density.

Replacing  $u$  in Eq. (2) with its equivalent  $Q/A_c$  (volume flow divided by the cross-sectional area) gives an expression similar to Eq. (1). The friction factor varies little for transition or turbulent flow and is considered constant for transient calculations. The duct length  $L$  in Eq. (2) should include the physical length plus the summation of equivalent duct lengths because of all the minor duct losses such as elbows, bends, contraction, and expansion.

An important variation in duct modeling in TORAC is that the duct also can be treated as a capacitance or volume node with its resistive nature preserved in connection with other nodes. This representation is useful for material transport and will be discussed later.

2. Dampers and Valves. The treatment of dampers is similar to that of ducts except that the length need not be specified. The effective resistance coefficient is prescribed or calculated similar to the treatment of ducts. Ducts and dampers are nonlinear system elements. Thus, the damper or valve losses can be lumped freely with those of ducts. Control valves with variable resistance coefficients are included in this version of the TORAC code; the variable resistance coefficient option is provided to allow the user to simulate manual opening or closing of damper components. Parametric studies could be performed to determine the effects of isolating or not isolating portions of the system model at different times during the transient, but this option was not incorporated into the code.

3. Filters. The filters are considered linear elements [ $n$  in Eq. (1) equals 1]. The filter resistance coefficients can be obtained from the manufacturer, or the code will calculate them for given pressure drop and flow rate if desired. The resistance of dirty filters is usually estimated as 2 to 5 times that of clean filters.



Based on empirical evidence, the filter is no longer a linear element as the flow rate increases. In Sec. VI of Appendix B we will review the more fundamental aspects of filter behavior for a broad range of velocities from the viewpoint of flow through porous media. We then conclude that the pressure drop across a filter contains the summation of linear and quadratic dependencies on flow rate. The TORAC code contains these new features, but the option of using the quadratic portion requires additional input for the turbulence dissipation. This is done by the filter function card specification.

4. Blowers and Fans. The blower head-vs-flow characteristic curve is approximated by a series of straight-line segments (Fig. 10). The curve is valid for a given blower speed and will be shifted vertically for other blower speeds. The appropriate curve can be obtained from the blower manufacturer's literature. The blower is placed in a branch, as are filters, dampers, and ducts, and is considered an active element in the system because it supplies energy to the system. Blower branches must be assigned blower characteristics obtained from blower performance curves furnished by the manufacturer. Such curves provide data for the positive flow and head region (first quadrant data).

Tornado depressurization can produce backflow (negative flow) when applied to the supply side of a blower and outrunning flow (positive flow with negative head) when applied to the discharge side. Usually manufacturers do not have blower operating data for these regions. Los Alamos has obtained blower data

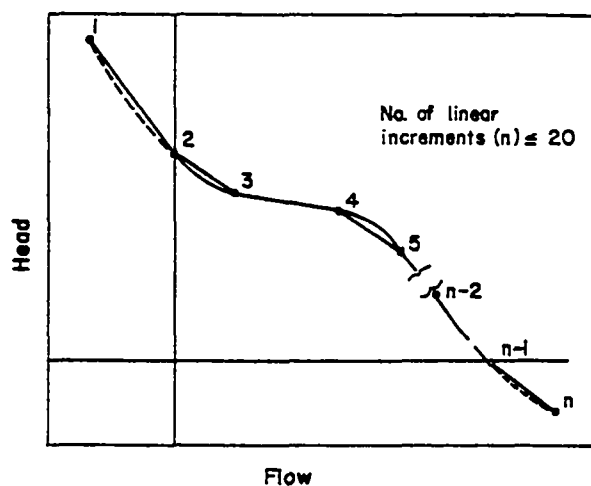


Fig. 10.  
Blower characteristics representation.

for regions of outrunning and backflow, and an example of the quasi-steady data is given in Fig. 11.

The above information is preliminary, and more data are needed (especially for dynamic testing) before the blowers can be modeled accurately in these abnormal flow regions. However, combining this information with worst-case assumptions can give a designer guidelines for determining the effects of these abnormal operating conditions on system integrity.

As an approximation, we use the same slope in the backflow quadrant as that to the right of the typical operating point in our blower models. (We feel that this practice is conservative.) Also, because blower curve data for the region of outrunning and backflow are not available from the manufacturer, the user could encounter problems when attempting to generate blower curves for TORAC. After the user has obtained the operating characteristics of the blowers to be modeled, a similar blower curve profile (slopes of the blower curve) as shown in the input deck of the sample problem can be used as a first approximation to generate the TORAC blower curve data. The user may choose to perform a series of sensitivity studies to determine the importance of the selected backflow and outrunning region data on the calculated results.

Blower oscillation has been observed for some problems. We avoid curves with local maximums or minimums. The slope of the alternate curve should be monotonically decreasing as in Fig. 10. The curve may be nearly flat; that is the slope may approach but not equal zero.

Preliminary dynamic tests indicate a band of values around the steady-state characteristic curve as shown in Fig. 12 (QSS means quasi-steady state). Further, the transient induced by a tornado does not dwell for a significant period of time in the oscillatory region of the blower curve. Therefore, the required alternate representation may not be a poor assumption.

Blower control capability has been added to TORAC. This capability includes blower curve change and turning blowers on and off during a transient. The blower is assumed to behave as a damper in the off-mode.

5. Rooms, Cells, and Plenums. Rooms, cells, and containment volumes are specified at nodal points. The capacitance coefficient is a function of room volume estimated from architectural and construction drawings. A room acts as an accumulator and provides storage for the gas; manifolds and returns also may have sufficient volume to require a capacitance node. TORAC produces a message

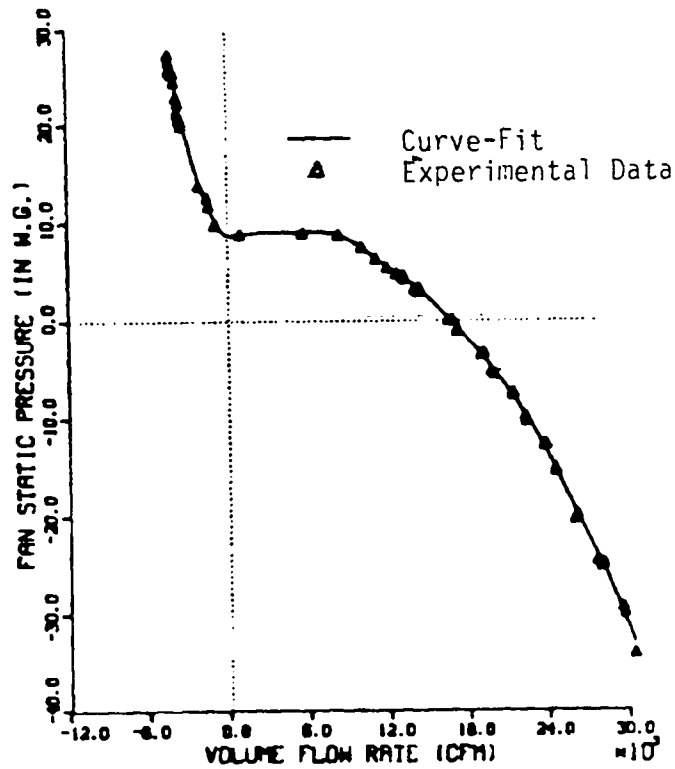


Fig. 11.  
Quasi-steady state performance results  
for a 24-in. centrifugal blower.

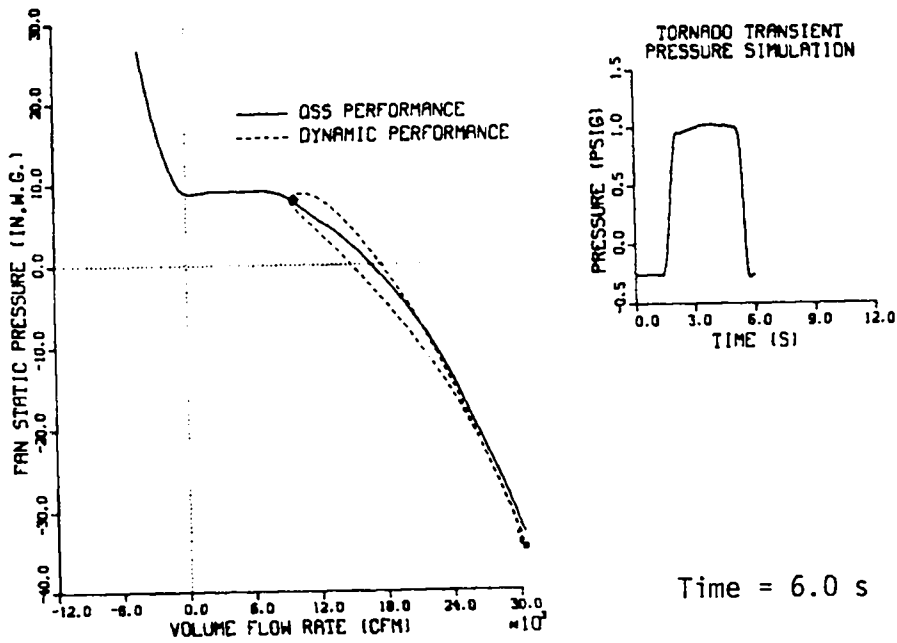


Fig. 12.  
Dynamic test result.

indicating this when it finds that the duct volume is greater than half the volume of the smallest room. The capacitance coefficient can be varied for parametric studies by adjusting the room volume. An average cross-sectional area also can be specified by the user code so that velocities through rooms can be calculated.

The capacitance of ducts is not included automatically even when duct dimensions are specified; capacitance is included only for rooms defined at nodal points. Therefore, a volume node must be given the capacitance of a duct. The material transport option requires that some of the ducts be represented as volumes, which is discussed in the material transport section. The dimensions of rooms always must be specified even though capacitance only enters into transient calculations.

6. Boundary Nodes. Any atmospheric region that has supply or exhaust openings to the ventilation system of a facility is considered to be a boundary node. This node can be held at a constant initial pressure, or pressure can be varied by specifying a time function as described in the input section. In either case, the pressure is known, and the node acts as a source or a sink to the rest of the system. The accident description for a tornado is given in greater detail in Sec. III.F.

7. Leakage. Effective leakage can be approximated in the model by using a boundary node and a fictitious duct. The leak rate is the flow rate. One could specify a filter in the leak branch and use an exponent of 1.0 in Eq. (1). However, it is usually more convenient to use the default (blank) specification on the branch description and use an exponent of 2.0 in Eq. (1) because a duct is assumed in this case.

#### D. Material Transport Models

1. Introduction. The material transport portion of TORAC estimates material transport (aerosol or gas) in an interconnected network of ventilation system components that represent a given fuel cycle facility. Using this capability, TORAC can calculate material concentrations and mass flow rates at any location in the network. Most importantly, the code will perform these transport calculations as a function of time for arbitrary user-specified pressure transients imposed on the facility boundary. There is no need to piece together a material

transport estimate based on separate steady flow calculations for rooms and duct segments. TORAC solves the entire network for actual transient flow and in doing so accounts for system interactions.

A generalized treatment of material transport under tornado-induced accident conditions could become very complex.<sup>2--4</sup> Several different types of materials could be transported, and more than one phase could be involved, including solids, liquids, and gases with phase transitions. Chemical reactions could occur during transport that lead to the formation of new species. Further, there will be a size distribution function for each type of material that varies with time and position, depending on the relative importance of effects such as homogeneous nucleation, coagulation (material interaction), diffusion (both by Brownian motion and by turbulence), and gravitational sedimentation. No current computer code can handle transient flow-induced material transport in a network system subject to the possibility of all of these complications, and the transport portion of TORAC also does not include this level of generality. (See Sec. 3 below.) However, this version of the TORAC code does provide a simple yet powerful material transport capability. TORAC's material transport components consist of the following.

- (1) Material characteristics
- (2) Transport initiation
- (3) Convective transport
- (4) Aerosol depletion
- (5) Filtration

Material characteristics and transport initiation are areas that must be considered by the user as he begins to set up the TORAC code to solve a given problem. Calculations of convective transport, aerosol depletion, and filtration are performed automatically by the code. Items 2--5 are actually separate subroutines or modules within the code. Item 3, convective transport, is a key subroutine that calls on items 2, 4, and 5 as needed during the course of the calculation. Each of the components listed above is subject to certain limitations and assumptions that will be discussed below or in Appendix B. We also will specify the required user inputs and provide appropriate references for the theory in each case.

2. Material Characteristics. The limitations of the TORAC material transport capabilities with regard to the physical and chemical characteristics of

the material are as follows. The pneumatically transportable contaminant material is restricted to a single phase of a single species. No phase transitions or chemical reactions are allowed. For example, condensation and gas-to-particle conversion are not permitted. If the contaminant is an aerosol (solid particles or liquid droplets suspended in air), it will be treated as monodisperse (equal-sized) and homogeneous (uniform density) with spherical particles or droplets during a given code run. Both size and density must be specified by the user. If the contaminant is a gas, it is assumed to be inert. Guidance in the area of aerosol and gas characteristics is provided for the user in Appendix B. (We will make some suggestions for describing fuel-grade plutonium and uranium oxide powders.)

3. Transport Initiation. To calculate material transport using TORAC, the analyst must determine or assume the location, distribution, and total quantity of contaminant material. The contaminant may be located in any or all rooms, cells, gloveboxes, corridors, or rectangular ducts. (An assumption about material distribution is necessary only when the user wishes to use the calculated aerodynamic entrainment of dry powder from thick beds option discussed below.) A total quantity (mass of material) must be known or assumed.

There are two options for material transport initiation: user-specified and calculated aerodynamic entrainment. The user-specified option gives the analyst considerable flexibility but requires engineering judgment to specify input to the code. This option involves preparing a table or graph of mass injection rate (kilograms per second) vs time. The data are supplied to the code on the input deck Material Injection Cards. The material also could be a gas. This user-specified option may be used to calculate the consequences of a hypothetical aerosol or gaseous release, and we recommend using it to handle reentrainment from thin beds (dirty cells or ductwork). The TORAC code was developed assuming that tornado-induced off-design flows are the primary cause of source-term initiation. Los Alamos is developing other codes specifically to assess the consequences of fires and explosions. For accidents that do not disrupt the normal ventilation system flow significantly (such as pressurized releases, spills, and equipment failures), a general purpose utility code may be used. Guidance for user source-term estimation is given in Appendix B.

The calculated entrainment option refers specifically to a subroutine designed to calculate aerodynamic entrainment of dry powder from thick beds. It uses a new semi-empirical analytical approach for calculating entrainment

that takes advantage of detailed flow information produced by the gas-dynamics module of TORAC. To arrive at our estimate of the mass of material entrained at each time step of calculation, this subroutine calculates when the surface particles will begin to move. Particle, surface, and flow characteristics are taken into account. It also accounts for the aerodynamic, interparticle (cohesion), and surface to particle (adhesion) forces that may be acting. This procedure was used in Ref. 5 and is discussed more fully there and in Appendix B.

This calculated entrainment option can be used whenever powder beds are known or assumed to be present in rooms, cells, gloveboxes, corridors, or rectangular ducts. The user must provide the code with particle size (microns) and density (kilograms per cubic meter) (see Appendix B), total mass of contaminant (kilograms), and the width (meters) and length (meters) of the (assumed floor) surface over which the powder is distributed uniformly. This information is fed to the code through the input deck on Control Card I, the Boundary Control Card, the Material Generation Cards (Material Function), the Room Data Cards, and the Calculated Source and Sink Cards.

If material transport is requested on Control Card I, the user must select at least one of the material transport initiation options. This may be user-specified with data on the Material Generation Cards or calculated entrainment-specified on the Calculated Source and Sink Cards. (See Sec. V.) Both options can be used simultaneously.

4. Convective Transport. The convective transport module of TORAC is the controller for material transport. This module is called only when the user requests a material transport calculation. Thus, TORAC may be run to calculate pressures and flow rates with or without material transport, depending on how the user sets a flag (a numerical value of zero or one) on Control Card I of his input deck. (See Sec. V.) For each time step of a calculation, the gas-dynamics problem is solved first for the entire network to yield pressures and flow rates independent of material transport. The gas dynamics module then can call the convective transport module to advance the material transport calculation by one time step from the last.

The mass conservation equation solved in this section and the assumptions leading up to it are given and discussed in detail in Appendix B. References for this section also are provided in Appendix B. Two-phase flow is allowed in

the sense that normal ventilation gas (usually air) is one phase and a pneumatically transportable contaminant material is the other phase. The contaminant material must be dispersed sufficiently (by volume fraction) so that equilibrium conditions exist between the air and contaminant and no material interactions occur. This assumption is discussed more fully in Appendix B, and it will be valid for most conditions of interest here.

5. Material Depletion. When the user has chosen to exercise material transport, he can calculate aerosol losses caused by gravitational sedimentation in rooms, cells, and so on and in horizontal, rectangular ducts. This module can be turned on for horizontal ducts and rooms and turned off for vertical ducts by adjusting the input flags on the Calculated Source and Sink Cards. Aerosol depletion may be calculated throughout the network during transient flow. The theory is based on quasi-steady-state settling with the terminal settling velocity corrected by the Cunningham slip factor. The flow in ducts and rooms is assumed to be well-mixed so that the aerosol concentration is uniform within the volume. More detail and references can be found in Appendix B. The user must supply only the aerosol diameter and density to this model. The aerosol may consist of solid particles or liquid droplets.

6. Filter Loading. A phenomenological approach to filter loading is presented so that the filter-gas dynamic performance can be changed by accumulation of the airborne material on the filter, which in turn causes an increase in the resistance as used in Eq. (1). A model is used in which the increase in resistance is linearly proportional to the amount of material on the filter; the proportionality constant is a function of material and filter properties. The user supplies the filter efficiency and plugging factor.

#### E. Initial Conditions

The gas dynamics require that steady-state conditions be established in the system before initiating the transient perturbation caused by the tornado.

#### F. Accident Description

A tornado can interact with a nuclear facility in several ways. In many cases, the principal concern is the potential threat of tornado-generated missiles. Our concern here is the atmospheric depressurization caused by the tornado. High airflows or large differential pressures may be generated through



plant openings to the atmosphere as a result of the tornado-induced low atmospheric pressure. (This is illustrated in Fig. 13.) The principal areas of concern are the ventilation supply and exhaust openings. Cracks in building walls or other openings also must be considered.

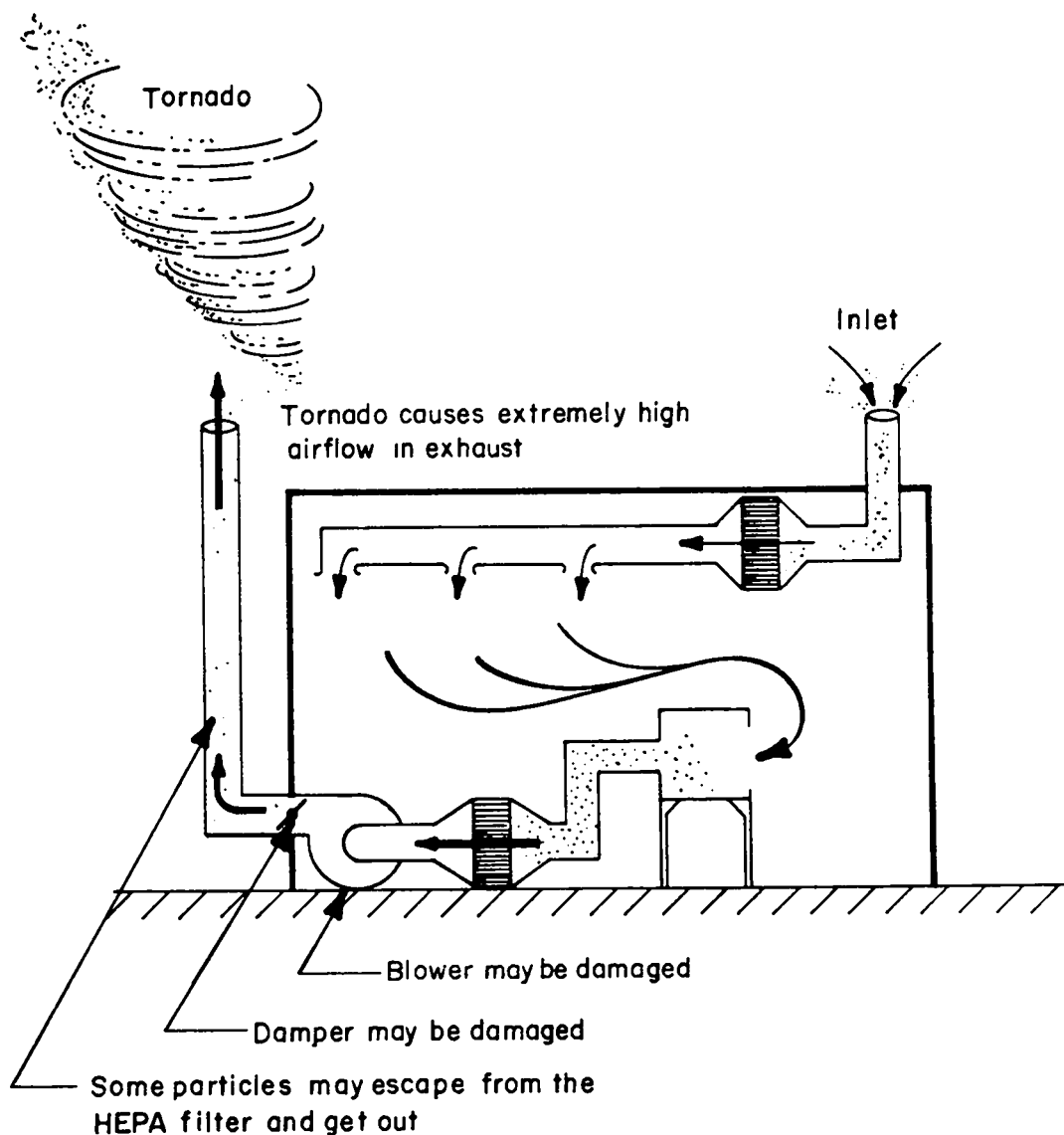


Fig. 13.  
Tornado at plant exhaust.

The transient effect of a tornado is simulated at the boundary nodes. Reference 6 provides information that allows the analyst to develop a pressure profile to simulate a tornado. Parameters that affect this profile are tornado depressurization rate, pressure drop, diameter, and translational speed.

#### G. Expected Results

Pressures, flows, material concentrations, material flow rates, and material accumulations are expected results. Pressures are calculated at nodal points, and flows are calculated in branches. Material concentrations are calculated at nodal points, and material accumulations are calculated as the amount passing through branches (ducts) and the amount remaining on filters (branches). A complete table of pressures and flows is given for the first and last calculation time step. These archival data also are broken down into component pressures and flows. Up to five special output times can be requested during the run. Filter material accumulation data are given for all filters in the system and for up to 100 times in tabular form. Material concentrations and accumulations are available in time plots if requested, as are pressures and flows.

### IV. INPUT PREPARATION

#### A. Data Deck Organization

After the TORAC model parameters have been evaluated fully, the information is placed in a file that becomes the input for the computer program. This file is based on fixed formats; that is, the location of card information is prescribed. Table I shows the organization that must be followed. Control information and data follow the title. The control information specifies the amount of data to be read, prescribes solution run options, and indicates the size of the model. Each type of information is separated from its neighbor by a blank card called a separator card that should be used to identify what follows. The separator cards must appear in the input file, but they are not read by the program. Note that if the number of data items specified on the control cards does not agree with the number of data cards provided, the program will try to read data from an adjacent category and probably will abort with a diagnostic message because the format will not be correct.

TABLE I  
TORAC INPUT FILE ORGANIZATION

<u>Order</u>	<u>Card Name</u>	<u>Note</u>
1	*Separator	1
2	TITLE	2
3	*Separator	1
4	*Separator	1
5	RUN CONTROL I	2
6	*Separator	1
7	PRINT/PLOT CONTROL	2
8	*Separator	1
9	PLOT FRAME DESCRIPTION	3
10	*Separator	2
11	RUN CONTROL II	2
12	*Separator	1
13	BOUNDARY CONTROL	2
14	*Separator	1
15	GEOMETRY AND COMPONENT CONTROL	2
16	*Separator	1
17	BRANCH DATA	2
18	*Separator	1
19	BOUNDARY NODE DATA	2
20	*Separator	1
21	CONTROL DAMPER CONTROL	3
22	CONTROL DAMPER DATA	3
23	*Separator	1
24	BLOWER CHANGE CONTROL	3
25	BLOWER CHANGE DATA	3
26	*Separator	1
27	PRESSURE FUNCTION CONTROL	3
28	PRESSURE FUNCTION DATA	3
29	*Separator	1
30	MATERIAL FUNCTION CONTROL	3
31	MATERIAL FUNCTION DATA	3
32	*Separator	1
33	RESISTANCE FUNCTION CONTROL	3
34	RESISTANCE FUNCTION DATA	3
35	*Separator	1
36	BLOWER OFF/ON CONTROL	3
37	BLOWER OFF/ON DATA	3
38	*Separator	1
39	ROOM DATA	3
40	*Separator	1
41	BLOWER CURVE CONTROL	3
42	BLOWER CURVE DESCRIPTION	3
43	*Separator	1
44	FILTER MODEL DATA (NUMBER)	3
45	FILTER MODEL DATA (EFFICIENCY)	3
46	FILTER MODEL DATA (PLUGGING FACTOR)	3
47	*Separator	1
48	PRESSURE INPUT	3
49	CALCULATED SOURCE AND SINK	3

- 
- Notes: 1. This card is required but is not read. Use it for indicating what follows. If "what follows" is not required, neither is the separator card.  
 2. Required.  
 3. Optional, depending on "control" requirements.

## B. Input Card Description

Input cards are described in the approximate order they occur in the card deck. Abbreviations used under the heading "Data Type" are A/N, for alphanumeric data (any combination of letters and numbers); FP, for floating-point data; and I, for integer data. Alphanumeric data should be left-justified with respect to the first column of the field definition. (Data should start in the first column of the field.) The filter-type field is defined as Cols. 47--50 of the branch description card. Integer data should be right-justified in the data field. (The last data character should appear in the right-most column of the field.) For example, the integer 5 placed in Col. 4 of the branch description card would be interpreted as branch 50 because the field definition encompasses Cols. 1--5. Floating-point data are also right-justified. Only large or small floating-point numbers require the format +nnnE+mm, where n and m are integers. Intermediate floating-point numbers may be specified as +nn--.nnn-- with the decimal point given or as integers with the decimal point assumed to the extreme right of the number. Values of data occurring under the heading "Default Value" are used by TORAC if the input data field is left blank.

DATA SEPARATOR CARD

Col.(s)	Data Description
1-80	These cards may be left blank or may contain alphanumeric data. They are used to separate different types of data cards. The contents of these cards are ignored by TORAC.
TITLE CARD	
Col.(s)	Data Description
1-80	Eighty columns of alphanumeric data are available to the user. These data are used for headings on output lists.

RUN CONTROL CARD I

Col.(s)	Data Description	Data Type	Default Value	Maximum Value
1-3	Not used.			
4-5	Run option. SS - steady-state solution only. ST - steady-state plus transient. RS - restart problem. TP - restart after transient. SP - restart after steady-state. RP - restart after restart.	A/N	ST	
6-10	Problem start time(s).	FP	0.0	
11-15	Transient time step size(s).	FP	1.0	
16-20	Total problem run time(s).	FP	1.0	
21-23	Not used.			
24-25	Not used.			
26-29	Not used.			
30	Number of special outputs.	I	0	5
31-35	First special output time(s).	FP	0.0	
36-40	Second special output time(s).	FP	0.0	
41-45	Third special output time(s).	FP	0.0	
46-50	Fourth special output time(s).	FP	0.0	
51-55	Fifth special output time(s).	FP	0.0	
60	Flag for material transport option.	I	0	
70	Flag for calculated source and sink option.	I	0	

Transient values are saved for listing and plotting. These values are equidistant in time between the problem start time and the total problem time. The number of output time values saved is determined by the program. Special output times (up to five) also may be requested. These special output times are not included in printer plots.

PRINT/PLOT CONTROL CARD

Col.(s)	Data Description	Data Type	Default Value	Maximum Value
1-2	Units for output lists and plots. SI specified here yields pressures (kPa) and flows (m <sup>3</sup> /s).	A/N	English Units	
3-5	Entering the letters "ALL" produces lists at every output time (including special outputs).	A/N	(blank) Lists produced only at start time, total run time, and special output times.	
6-10	Number of pressure plot frames.	I	0	25
11-15	Number of flow plot frames.	I	0	25
16-20	Number of pressure differential plot frames.	I	0	25
21-25	Number of material concentration plot frames.	I	0	25
26-30	Number of material flow plot frames.	I	0	25
31-35	Number of material accumulation on filter or amount through branches plot frames.	I	0	25

The maximum number of plot frames that can be requested is 25; therefore, the sum of any frames is 25. These entries may be left blank if printer plots are not desired.

PLOT FRAME DESCRIPTION

Col.(s)	Data Description	Data Type	Default Value	Maximum Value
1-5	Total number of curves this frame.	I	0	4
6-10	Node/branch number for first curve.	I	0	
11-15	Node/branch number for second curve.	I	0	
16-20	Node/branch number for third curve.	I	0	
21-25	Node/branch number for fourth curve.	I	0	
26-35	Scale limit for frame.	FP	Blank	

Pressures and material concentrations are calculated at nodal points (nodes). Flows, pressure differentials, material flow rates, and material accumulations on filter or through a flow pathway are calculated for branches. This card identifies how many and which nodes or branches are to appear as curves on the print/plot frame. Plot parameters cannot be mixed on the same frame. Frame description cards should appear in the order as in the PRINT/PLOT CONTROL cards. These cards may be omitted if plot frames are not requested on the print/plot control card for steady-state runs. A scale limit may be specified for the frame; otherwise, the plot routine finds the maximum and minimum values of all the variables and uses these values as 100% of full scale.



RUN CONTROL CARD II

Col.(s)	Data Description	Data Type	Default Value	Maximum Value
1-5	Maximum iterations permitted per time step. The program will abort if convergence has not been achieved for this number of iterations. Ten times this number is permitted for the steady-state calculations.	I	300	
6-15	Convergence criterion.	FP	0.0001	
21-25	Relaxation parameter. A value greater than 1.0 and less than 2.0 can be specified to reduce the number of iterations per time step. This is determined through successive runs and is different for each problem.	FP	1.0	
26-29	Not used.			
30	Pressure input option. Insert the letter "P" in this column if pressures at nodal points are to be supplied.	A/N	(Blank) no input pressures supplied	
35	Flag for blower failure option.	I	0	
40	Flag for changing blower curve.	I	0	

BOUNDARY CONTROL CARD

Col.(s)	Data Description	Data Type	Default Value	Maximum Value
1-5	Total number of pressure-time functions for all boundary nodes.	I	0	5
6-10	Total number of boundary nodes for this problem.	I	2	20
11-20	Value for atmospheric pressure (absolute, psia).	FP	14.7 psia	
21-30	Value for atmospheric temperature (absolute, R).	FP	530 R (60 <sup>0</sup> F)	
35	Number of resistance functions.	I	0	5
40	Flag for control damper option.	I	0	
45	Number of material functions.	I	0	5

GEOMETRY AND COMPONENT CONTROL CARD

Col.(s)	Data Description	Data Type	Default Value	Maximum Value
1-5	Number of branch description data cards.	I	0	500
6-10	Number of nodes defined for problem (includes boundary nodes).	I	0	400
11-15	Not used.			
16-20	Number of rooms defined for problem.	I	0	60
21-25	Total number of blower characteristic functions defined for problem.	I	0	15
30	Number of filter models.	I	0	5

Values of these parameters control the reading of input data and therefore should not exceed maximum values.

BRANCH DATA

Col.(s)	Data Description	Data Type	Default Value	Maximum Value
1-5	Branch number.	I	0	500
6-10	Upstream node number.	I	0	400
11-15	Downstream node number.	I	0	400
16-25	Initial estimate of flow (ft <sup>3</sup> /min). This value is used to calculate damper, filter, and duct resistance coefficient and to indicate the proper segment on the blower characteristic curve.	FP	0.0	
26-35	Hydraulic radius of duct (in.). Defined as the cross-sectional area divided by the wetted perimeter.	FP	0.0	
36-45	Duct length (ft). This value and the hydraulic radius are used to calculate duct volume. This volume is compared with room volumes for model consistency checks.	FP	0.0	
46	Component type V ..... Damper F ..... Filter B ..... Blower D ..... Duct	A/N	D	
51-60	Branch pressure differential (in. w.g.).	FP	0.0	

BRANCH DATA (CONT)

Col.(s)	Data Description	Data Type	Default Value	Maximum Value
61-70	Resistance coefficient for branch. This value (if greater than zero) overrides that calculated by TORAC from pressure differential and initial flow.	FP	TORAC-calculated value	
71-72	Blower curve identification. Identifies which blower curve to use for component type B.	I		
73-75	Filter model identification number.	I	0	20

The branch pressure differential is used with the initial estimate of branch flow to calculate a resistance coefficient using Eq. (1). The differential pressures also are used to calculate initial estimates of system pressures if these pressures are not input separately.

The BRANCH DESCRIPTION cards need not be ordered in the input deck (branch 10 might precede branch 5). However, the number of cards should agree with that specified in Cols. 1-5 of the GEOMETRY AND COMPONENT CONTROL CARD.

BOUNDARY NODE DATA CARD

Col.(s)	Data Description	Data Type	Default Value	Maximum Value
1-5	Boundary node number.	I	0	400
6	Not used.			
7-16	Initial value of pressure at node (in. w.g.).	FP	0.0	
17-20	Identification number of time function at this boundary node. (See time function data card.)	I	0 (Steady value of pressure)	5

All nodes that are problem boundaries must be listed on the BOUNDARY NODE DATA CARD. Furthermore, the total number of these nodes must agree with the number of boundary nodes previously specified on the BOUNDARY CONTROL CARD.

CONTROL DAMPER CONTROL CARD

Col.(s)	Data Description	Data Type	Default Value	Maximum Value
1-5	Total number of control dampers.	I	0	5

This card tells the program how many cards of control-damper data to read.

CONTROL DAMPER DATA CARD

Col.(s)	Data Description	Data Type	Default Value	Maximum Value
1-5	Branch number.	I	0	500
6-10	Resistance function I.D. number.	I	0	5
11-22	Initial value of resistance.	FP	Steady-state	

One CONTROL DAMPER DATA CARD is needed for each branch with a control damper. A control damper can be any damper in the system. Its initial value for a resistance coefficient can be obtained from a steady-state (SS) run.

BLOWER CHANGE CONTROL CARD

Col.(s)	Data Description	Data Type	Default Value	Maximum Value
1-5	Total number of blowers involved.	I	0	5

The number given on this card tells the program how many blowers (branches) are subject to a blower curve change during the run.

BLOWER CHANGE DATA CARD

Col.(s)	Data Description	Data Type	Default Value	Maximum Value
1-5	Branch number.	I	0	500
6-10	New blower function I.D. number.	I	0	5
11-20	Time that change occurs.	FD	0.0	

One BLOWER CHANGE DATA CARD is needed for each blower involved.

PRESSURE FUNCTION CONTROL CARD

Col.(s)	Data Description	Data Type	Default Value	Maximum Value
1-5	Pressure function I.D. number.	I	0	5
6-10	Number of data points in pressure function definition. A data point is defined as an ordered pair of values of time and pressure.	I	0	20

This card controls the reading of subsequent PRESSURE FUNCTION DATA cards and should precede each time function definition. The PRESSURE FUNCTION CONTROL card is followed by one or more PRESSURE FUNCTION DATA data cards. This set of cards may be present, but it is not required for steady-state runs.

PRESSURE FUNCTION DATA CARD

Col.(s)	Data Description	Data Type	Default Value	Maximum Value
1-10	Value of time(s) at first time function data point.	FP	0.0	
11-20	Value of pressure (in. w.g.) at first time function data point.	FP	0.0	
21-30	Value of time for second time function data point.		FP	0.0
31-40	Value of pressure at second data point.		FP	0.0
41-50	Value of time at third data point.	FP	0.0	
51-60	Value of pressure at third data point.		FP	0.0

Insert as many PRESSURE FUNCTION DATA cards as needed to define all the data points.



### MATERIAL FUNCTION CONTROL CARD

Col.(s)	Data Description	Data Type	Default Value	Maximum Value
1-5	Function I.D. number (n).	I	0	5
6-10	Number of points.	I	0	20
11-20	Total amount of material (kg).	FP	0.0	

These cards control the reading of subsequent MATERIAL FUNCTION DATA cards and should precede each time function definition. This function is called by the ROOM cards.

### MATERIAL FUNCTION DATA CARD

Col.(s)	Data Description	Data Type	Default Value	Maximum Value
1-10	Value of time(s) at first point of function.	FP	0.0	
11-20	Value of material generation (kg/s) at first point of function.	FP	0.0	
21-30	Value of time at second point.	FP	0.0	
31-40	Value of material generation at second point.	FP	0.0	
41-50	Value of time at third point.	FP	0.0	
51-60	Value of material generation at third point.	FP	0.0	

Insert as many MATERIAL FUNCTION DATA Cards as needed to define all the data.

### RESISTANCE FUNCTION CONTROL CARD

Col.(s)	Data Description	Data Type	Default Value	Maximum Value
1-5	Resistance function I.D. number.	I	0	5
6-10	Number of points.	I	0	20

This card controls the reading of subsequent RESISTANCE FUNCTION DATA cards and should precede each time function definition. This function is called by the CONTROL DAMPER DATA card.

### RESISTANCE FUNCTION DATA CARD

Col.(s)	Data Description	Data Type	Default Value	Maximum Value
1-10	Value of time(s) at first point.	FP	0.0	
11-25	Value of resistance at first point.	FP	0.0	
26-35	Value of time at second point.	FP	0.0	
36-50	Value of resistance at second point.	FP	0.0	
51-60	Value of time at third point.	FP	0.0	
61-75	Value of resistance at third point.	FP	0.0	

Insert as many RESISTANCE FUNCTION DATA cards as needed to define all the data.

BLOWER ON/OFF DATA CONTROL CARD

Col.(s)	Data Description	Data Type	Default Value	Maximum Value
1-5	Total number of blower branches involved.	I	0	5

This card controls the reading of subsequent BLOWER ON/OFF DATA. A blower branch is changed to a damper branch with a specified resistance coefficient.

BLOWER ON/OFF DATA CARD

Col.(s)	Data Description	Data Type	Default Value	Maximum Value
1-5	Blower branch number.	I	0	500
6-15	"OFF" time(s).	FP	0.0	
16-25	Value of branch resistance in blower-off position.	FP	0.0	
26-35	"ON" time(s).	FP	0.0	

One DATA card is needed for each blower branch.

ROOM DATA CARD

Col.(s)	Data Description	Data Type	Default Value	Maximum Value
1-5	Node number for room.	I	0	400
6-15	Room width (ft).	FP	0.0	
16-25	Room height (ft).	FP	0.0	
26-35	Room length (ft).	FP	0.0	
36-40	Material generation identification number	I	0	

One card is required per room. The dimensions are used in the calculation of capacitance coefficients, and zero volume is not permitted. Room volumes are required input for steady-state runs, but they are not used. Duct volume, if significant, must be input as a pseudo-room, which requires an additional node. Rooms cannot be located at boundary nodes. The ROOM DATA cards need not be in numerical order.

## BLOWER CURVE CONTROL CARD

Col.(s)	Data Description	Data Type	Default Value	Maximum Value
1-5	Blower curve number identifier.	I	0	15
6-10	Number of points defining this blower curve. A point is defined as an ordered pair of values of flow (ft <sup>3</sup> /min) and head (in. w.g.).	I	0	20

The blower curve data are ordered in the same way as time function data—a curve input control card is followed by one or more curve description cards. One curve control card is required for each blower type. The order of the blower curve is unimportant (curve 3 might precede curve 1); however, this card is used in reading the following blower curve data points and must appear just before the appropriate curve description card(s).

### BLOWER CURVE DATA CARD

Col.(s)	Data Description	Data Type	Default Value	Maximum Value
1-10	Flow (cfm) for the first point.	FP	0.0	
11-20	Blower head (in. w.g.) for the first point.	FP	0.0	
21-30	Flow for the second point.	FP	0.0	
31-40	Blower head for the second point.	FP	0.0	
41-50	Flow for the third point.	FP		
51-60	Blower head for the third point.	FP	0.0	

Figure 10 illustrates a sample blower characteristic curve that contains back-flow (negative flow), normal flow, and outrunning flow (negative head for positive flow). The points that define the linear segments of the blower curve should be ordered algebraically in flow (- to +). A card can accommodate three pairs for values of flow and blower head. Values for curves containing more than three points would appear on successive cards.

### FILTER MODEL CONTROL CARD

Col.(s)	Data Description	Data Type	Default Value	Maximum Value
1-5	Filter-model identification number.	I	0	20
6-10	Number of species.	I	0	1
11-20	Turbulent coefficient.	FP	0	0.0
21-30	Laminar coefficient.	FP	0	

One CONTROL card is needed for each filter model and each is immediately followed by its model data cards. This card contains the laminar and turbulent coefficients plus the number of material types. For now we limit the number to just 1. To use this filter model, a branch must call the filter identification number in the BRANCH card.

### FILTER MODEL DATA CARDS (First Card)

Col.(s)	Data Description	Data Type	Default Value	Maximum Value
1-15	Filter efficiency.	FP	0.0	

(Second Card)

Col.(s)	Data Description	Data Type	Default Value	Maximum Value
1-15	Filter plugging factor ( $\text{kg}^{-1}$ ).	FP	0.0	

The filter efficiency and plugging factor are specified here.

PRESSURE INPUT CARD

Col.(s)	Data Description	Data Type	Default Value	Maximum Value
1-15	Pressure (in. w.g.) at the first node.	FP	0.0	
16-30	Pressure at the second node.	FP	0.0	
31-45	Pressure at the third node.	FP	0.0	
46-60	Pressure at the fourth node.	FP	0.0	
61-75	Pressure at the fifth node.	FP	0.0	

One data separator card precedes the PRESSURE INPUT data cards. These cards are required only if column 30 of the RUN CONTROL CARD II is set to P. The values of pressure for boundary nodes may be left blank because these values are supplied on the BOUNDARY NODE DATA cards. Use as many cards as required to define all the system pressures.



CALCULATED SOURCE AND SINK  
(First Card)

Col.(s)	Data Description	Data Type	Default Value	Maximum Value
1-10	Material density (kg/m <sup>3</sup> ).	FP	0.0	
11-20	Material diameter (m).	FP	0.0	

(Second Card)

Col.(s)	Data Description	Data Type	Default Value	Maximum Value
1-5	Room entrainment flag.	I	0.0	
6-10	Room deposition flag.	I	0.0	
11-15	Duct entrainment flag.	I	0.0	
16-20	Duct deposition flag.	I	0.0	
21-30	Material mass available for entrainment (kg).	FP	0.0	

There must be as many second-card types as there are rooms, and they must be in the same order. This is not read unless the IMAT flag is greater than zero. (See CONTROL CARD I.)

### C. Restart Procedure

The restart option permits the continuation of a solution starting from the last calculated time of the previous solution. This restart capability is useful in debugging large problems before committing to runs that require large amounts of computer time.

RUN CONTROL CARD I is used to specify the restart option. The run option (Cols. 4--5) is set to the value RS if restart of a previous problem is desired. Restart is valid only if the run option for the previous problem was selected as TP or SP (transient calculation plus punch, or steady-state calculation plus punch respectively). The parameters on RUN CONTROL CARD I should be altered for restart. Columns 4--5 should be set to RS, Cols. 6--10 (problem start time) should be set to the total problem time of the previous problem, and Cols. 16--20 should be set to the new total problem time.

A restart file called RESTT is generated automatically. After the total run time has been set, this file is renamed "INPUT" and becomes the new input file for TORAC.

## V. CODE OUTPUT

### A. Input Return

The input return consists of two parts. The first category of input return is an echo of the input data card images with the card column heading across the top of the list and the card number to the left of the card image. The second part of input return consists of edited lists of input after the input has been converted to a form usable by the systems solver algorithm. This output expands the abbreviated input and gives default values that are not specified on the input cards. The card image list always appears regardless of the occurrence of errors in the input data.

### B. Output Lists and Summaries

Flows, pressures, differential pressures, material concentrations, material flows, material accumulations, and extreme values are written to a scratch file during the transient calculation for editing or plotting by the output processor. Lists for each output time requested consist of tables of archival data showing (1) pressures and flows, (2) differential pressures and flows by component type (filters and dampers), (3) a table of differential pressures

between rooms, and (4) a summary of extreme values for a specified output time. A summary of extreme values spanning the entire period of the problem is produced at the end of the problem. Pressures and flows are inspected each time step during the calculation in compiling data for this list so that extreme values are not missed by poor selection of output frequency. Frequently, one might wish output lists for a specific point in time not covered in the selection of output frequency. A maximum of five special output times may be selected arbitrarily. These special output times do not appear in the printer plots.

### C. Printer Plots

Line-printer plots may be requested on the PRINT/PLOT CONTROL card and the PLOT FRAME DESCRIPTION cards. A maximum of 10 frames can be requested, and a maximum of four curves can be put on a single frame. Each curve is identified by an alphabetic character A through D; overlapping curves are shown by the character X at the point of overlap. The first and last archival lists and summaries are produced automatically when plots are requested. Intermediate lists are suppressed because the volume of output data can be quite large. The intermediate lists can be requested with a nonblank specification in Cols. 3-5 of the PRINT/PLOT CONTROL card.

The program attempts to fill the plot frame page when the number of output times is sparse by spacing with blank lines between points. The extreme value summaries can serve as valuable guides in selecting node or branch candidates for plotting. Further, the final extreme value summary can be checked for missing extrema on the plots. By their nature, printer-plots are not precise; however, they can give the analyst a good picture of how the system behaves.

### D. Diagnostic Messages

Diagnostic (warning or error) messages are provided to help the user isolate possible input data or modeling errors. In most cases, the error is easily discerned from the message. However, out-of-order or missing cards tend to produce messages that may confound the reader. In these cases, a careful check of the input return list and a review of input preparation usually can isolate the problem.

Diagnostic messages are produced during input processing or the system solver calculations, and thus, there is not a set pattern to their location in the output. \*\*\*DIAGNOSTIC MESSAGES always precede these messages, and if the

error is fatal, either ERROR WITH INPUT CAN'T CONTINUE or \*\*\*\*FATAL ERROR\*\*\*\* SEE PREVIOUS MESSAGES is printed following the message. See Fig. 14 for an illustration of the mixture of informative (nonfatal) messages and fatal error messages that can occur.

## VI. SAMPLE PROBLEMS

A single file containing the input for all the sample problems appears as a subroutine at the end of the TORAC source program. Executing of this file "as is" results in a simulation of the "Tornado at Exhaust" condition. Nine other sample problems can be run from this same file by following the instructions given in comment statements at the end of it. The hypothetical ventilation system for these problems is shown in Fig. 15 and consists of a supply and exhaust blower, a large room, dampers, a filter plenum, a long duct, and an exhaust stack. The corresponding computer model is shown schematically in Fig. 16. The purpose of these sample problems is to demonstrate the capabilities of the various program features. The problems do not necessarily reflect a realistic situation.

### \*\*DIAGNOSTIC MESSAGES

```
BRANCH 6 FLOW NEGATIVE, UP AND DOWN-STREAM NODES 6 5 REVERSED BY PROGRAM
-----PRESSURES READ IN (NOT CALC, FROM DP)
      INPUT RESISTANCE          1.00000E-04   USED FOR BRANCH      4
      INPUT RESISTANCE          6.94400E-07   USED FOR BRANCH      5
CAN'T CALC. RESISTANCE (SET TO MIN. VALUE) FOR BRANCH      6
      INPUT RESISTANCE          6.94400E-07   USED FOR BRANCH     13
      INPUT RESISTANCE          1.42800E-03   USED FOR BRANCH     14
      INPUT RESISTANCE          6.94400E-07   USED FOR BRANCH     23
      INPUT RESISTANCE          3.08600E-07   USED FOR BRANCH     24
BRANCH COUNT IMPOSSIBLE FOR NODE 1  COUNT = 1
BRANCH COUNT IMPOSSIBLE FOR NODE 25  COUNT = 1
*****FATAL ERROR*****SEE PREVIOUS MESSAGES
```

Fig. 14.  
Multiple diagnostic list.

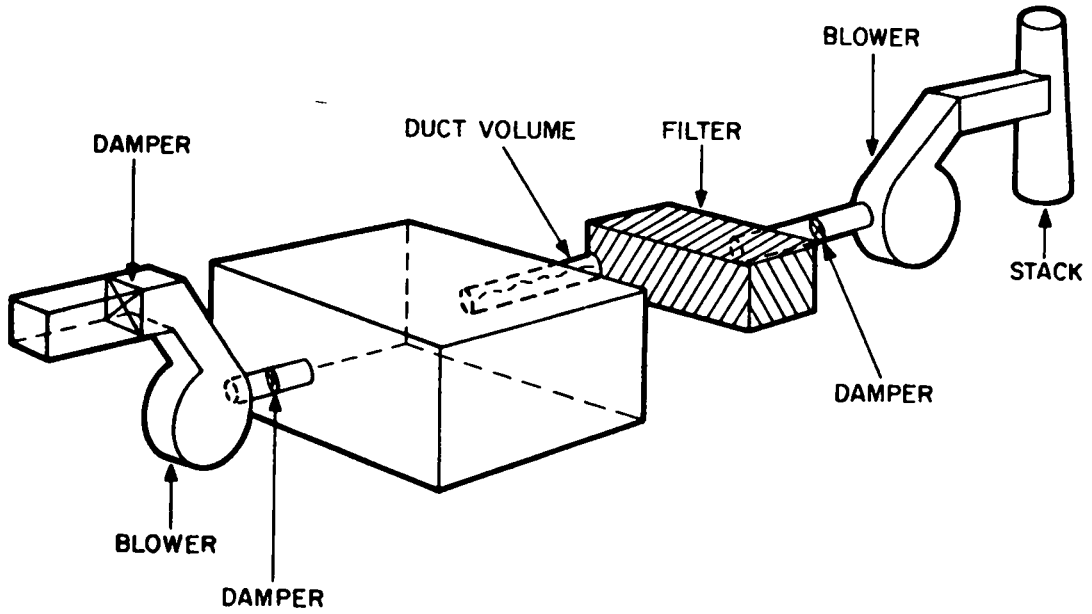


Fig. 15.  
Sample system for TORAC.

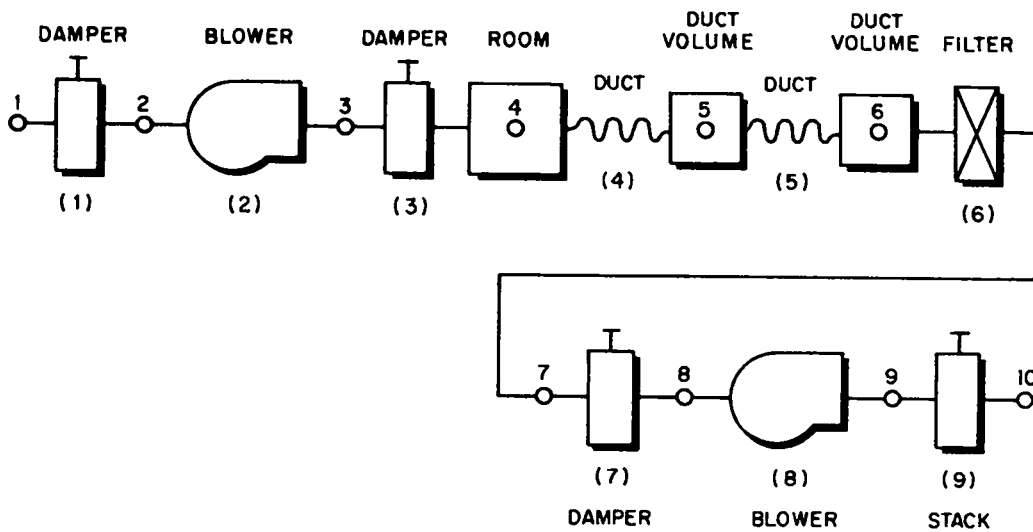


Fig. 16.  
Sample system for TORAC.

The input file (Fig. 17) at the end of the program is written to a file called "INPUT" if TORAC is executed without the existence of a file called "INPUT." The test for this file is made automatically if the file-search utility is available. If this is not the case, the user must change the source program for the initial run only to write the input file rather than reading from one in the local file space. The sample problems demonstrate the following program features.

- A tornado
- Turning a blower off and then on
- Changing blower characteristics during a run
- Closing a damper
- Combining features
- Material transport
- Filter plugging

A tornado is imposed on the system by specifying a pressure-time function at one or both boundary nodes. The sample problem input file shown in Fig. 17 initiates the tornado transient after 10 s of normal operation. Because the code determines a steady-state solution before time = 0.5, the user could initiate the transient at time = 0.5. If the user desired to rerun the sample problem with the tornado transient starting at time = 0.5, to the pressure time function data would have to be modified. Up to 20 points can be used to define the assumed fluctuations in pressure that simulate the passing of a tornado. A blower is turned off by replacing it with a damper having a known resistance characteristic. Blower characteristics are changed during a run by substituting another blower curve at the time the change occurs. A damper is closed or opened according to a given resistance coefficient time function for that branch. These features can be made to occur at different intervals during a run to depict a sequence of events. Material can be injected into any room and will be transported to the boundaries by the flow. Filter plugging will occur if the filter model used is assigned a plugging coefficient.

```

1 *
2 example problems (e.g. tornado at exhaust)
3 *
4 * run control 1
5   st 0.0 .01 030.
6 * print/plot control
7   3 1 1
8 * frame descriptions
9   4 2 3 4 5
10  4 6 7 8 9
11  2 10 1
12  4 2 4 6 8
13  3 2 6 8
14 * run control 2
15  500 p 1 1
16 * boundary control
17  1 2 1 1 1
18 * geometry and component control
19  9 10 3 3 1
20 * branch data
21  1 1 2 1000. v
22  2 2 3 1000. b 1
23  3 3 4 1000. v
24  4 4 5 1000. v
25  5 5 6 1000. v
26  6 6 7 1000. f 0
27  7 7 8 1000. v
28  8 8 9 1000. b 2
29  9 9 10 1000. v
30 * boundary data
31  1 0
32  10 1
33 * control damper instructions
34  1
35  0 1 4.000e-07 9
36 * blower curve change instructions
37  1
38  0 3 50. 2
39 * tornado pressure function
40  1 5
41 0.0 0.0 10. 0.0 12. -25.
42 16. -25. 18. 0.0
43 * particulate function
44  1 6 0.35
45 0.0 0.0 10. 0.0 12. 0.1
46 14. 0.1 16. 0.0 60. 00
47 * control damper function
48  1 4
49 0.0 4.000e-07 80. 4.000e-07 100. 1.000e-06
50 150. 1.000e-06
51 * blower turned off/on instructions
52  1
53  0 50. 1.000e-09 150. 2
54 * room data
55  4 10. 10. 10. 0
56  5 2. 2. 50.
57  6 2. 2. 50.
58 * blower curves
59  1 6

```

Fig. 17.  
Input file for sample problems.

```

60 -100.      2.7      0.0      1.9      800.      1.8
61 1000.     1.6      1300.     0.8      1400.     0.0
62      2      6
63 -200.     1.4      0.0      1.0      700.     0.9
64 1000.     0.7      1400.     0.4      1600.     0.0
65      3      6
66 -100.     2.3      0.0      1.6      770.     1.5
67 940.     1.3      1100.     0.8      1200.     0.0
68 * filter model data
69      1      1
70      .8
71      0.0
72 * pressures
73      0.0      -0.5      +1.1      1.0      0.9
74      0.8      -0.2      -0.3      0.4      0.0
75 * calc. source/sink coefficients
76
77      0      0      0      0      0.0
78      0      0      0      0      0.0
79      0      0      0      0      0.0
80 end of input file. anything written beyond this point will be ignored
81 when this file is read.
82
83 replace lines 6 thru 13 with one of the following options
84
85 * print/plot control      plot option no. 1
86      2      1      1      0      0      0      "      "      "      1
87 * frame descriptions      "      "      "      1
88      4      2      3      4      5      "      "      "      1
89      4      6      7      8      9      "      "      "      1
90      4      2      4      6      8      "      "      "      1
91      3      2      6      8      "      "      "      1
92
93 * print/plot control      plot option no. 2
94      3      1      1      0      0      0      "      "      "      2
95 * frame descriptions      "      "      "      2
96      4      2      3      4      5      "      "      "      2
97      4      6      7      8      9      "      "      "      2
98      2      10      1      "      "      "      "      2
99      4      2      4      6      8      "      "      "      2
100     3      2      6      8      "      "      "      2
101
102 * print/plot control      plot option no. 3
103     0      0      1      1      1      1      "      "      "      3
104 * frame descriptions      "      "      "      3
105     1      6      "      "      "      "      3
106     3      3      4      5      "      "      "      3
107     4      4      5      6      7      "      "      "      3
108     4      4      5      6      7      "      "      "      3
109
110
111 * print/plot control      plot option no. 4
112     0      1      0      1      1      1      "      "      "      4
113 * frame descriptions      "      "      "      4
114     4      2      4      5      8      "      "      "      4
115     4      4      5      6      7      "      "      "      4
116     4      4      5      6      7      "      "      "      4
117     4      4      5      6      7      "      "      "      4

```

the following r  
uns can be made from the above input file by making the  
118 changes indicated

Fig. 17. (Cont.)  
Input file for sample problems.



```

119
120 run          changes to "combined input file"
121 ----          -----
122
123 tornado at exhaust (plot option no. 2)
124     "as is"
125
126 tornado at intake (plot option no. 2)
127     line 32 - 1 to 0
128     line 31 - 0 to 1
129
130 supply blower turned off and on (plot option no. 1)
131     line 5 - 030. to 200.
132     line 32 - 1 to 0
133     line 53 - 0 to 2
134
135 supply blower speed reduced (plot option no. 1)
136     line 5 - 030. to 200.
137     line 32 = 1 to 0
138     line 38 - 0 to 2
139
140 control damper closing (branch 9) (plot option no. 1)
141     line 5 - 030. to 200.
142     line 32 = 1 to 0
143     line 35 - 0 to 9
144
145 blower speed reduced & damper closing (plot option no. 1)
146     line 5 - 030. to 200.
147     line 32 = 1 to 0
148     line 35 - 0 to 9
149     line 38 - 0 to 2
150
151 material transport (plot option no. 3)
152     line 5 - 030. to 200.
153     line 5 - 0    0    0 to 1    0    0
154     line 32 = 1 to 0
155     line 26 - 0 to 1
156     line 55 - 0 to 1
157
158 filter plugging (plot option no. 3)
159     line 5 - 030. to 200.
160     line 5 - 0    0    0 to 1    0    0
161     line 26 - 0 to 1
162     line 32 - 1 to 0
163     line 55 - 0 to 1
164     line 71 - 0.0 to 30.
165
166 entrainment (plot option no. 4)
167     line 5 - 0    0    0 to 1    0    1
168     line 26 - 0 to 1
169     line 41 - -25. to -50.
170     line 42 - -25. to -50.
171     line 76 - add 3000.      1.0e-05
172     line 78 - 0    0    0    0 to 0    0    1    0
173     line 78 - 0.0 to 1.0
174
175 deposition (plot option no. 4)
176     line 5 - 0    0    0 to 1    0    1
177     line 26 - 0 to 1
178     line 41 - -25. to -50.
179     line 42 - -25. to -50.
180     line 55 - 0 to 1
181     line 76 - add 3000.      1.0e-05
182     line 78 - 0    0    0    0 to 0    0    0    1
183     line 79 - 0    0    0    0 to 0    0    0    1

```

Fig. 17. (Cont.)  
Input file for sample problems.

The Sample Problems appearing in this combined input file are (1) Tornado at Exhaust, (2) Tornado at Intake, (3) Supply Blower Turned Off and On, (4) Supply Blower Speed Reduced, (5) Control Damper Closing, Blower Speed Reduced, and Damper Closing, (6) Material Transport (No Filter Plugging), and (7) Material Transport (Filter Plugging).

#### Problem No. 1 – Tornado at Exhaust

A pressure-time function dropping to -25 in. w.g. (about 1 psi or 6200 Pa) is placed at the exhaust boundary, node No. 10. (Figs. 18--22)

#### Problem No. 2 – Tornado at Intake

The same pressure-time function used in Problem No. 1 is reassigned to the system intake boundary, node No. 1. (Figs. 23--27)

#### Problem No. 3 – Supply Blower Turned Off and On

The branch containing the supply blower is replaced by a damper with a resistance coefficient of 1.000E-09 at 50 s. This branch is returned to a blower again at 150 s. (Figs. 28--31)

#### Problem 4 – Supply Blower Speed Reduced

The supply blower normally identifies with blower curve No. 1 as specified on the branch 2 input card. This changes to Curve No. 3 at 50 s. Curve No 3 reflects a speed reduction. (Figs. 32--35)

#### Problem 5 – Control Damper Closing

The damper in branch No. 9 is assigned Control Damper Function 1, which is a resistance coefficient time function showing an increase in resistance to simulate a closing damper. (Figs. 36--39)

#### Problem 6 – Blower Speed Reduced and Damper Closing

This is an example of how features can be combined to depict a scenario from a series of events. In this case, reducing the speed of the supply blower has made the pressure in the room more negative. Closing a control damper located in branch 9 is an attempt to restore the pressure in the room to its original value. (Figs. 40--43)

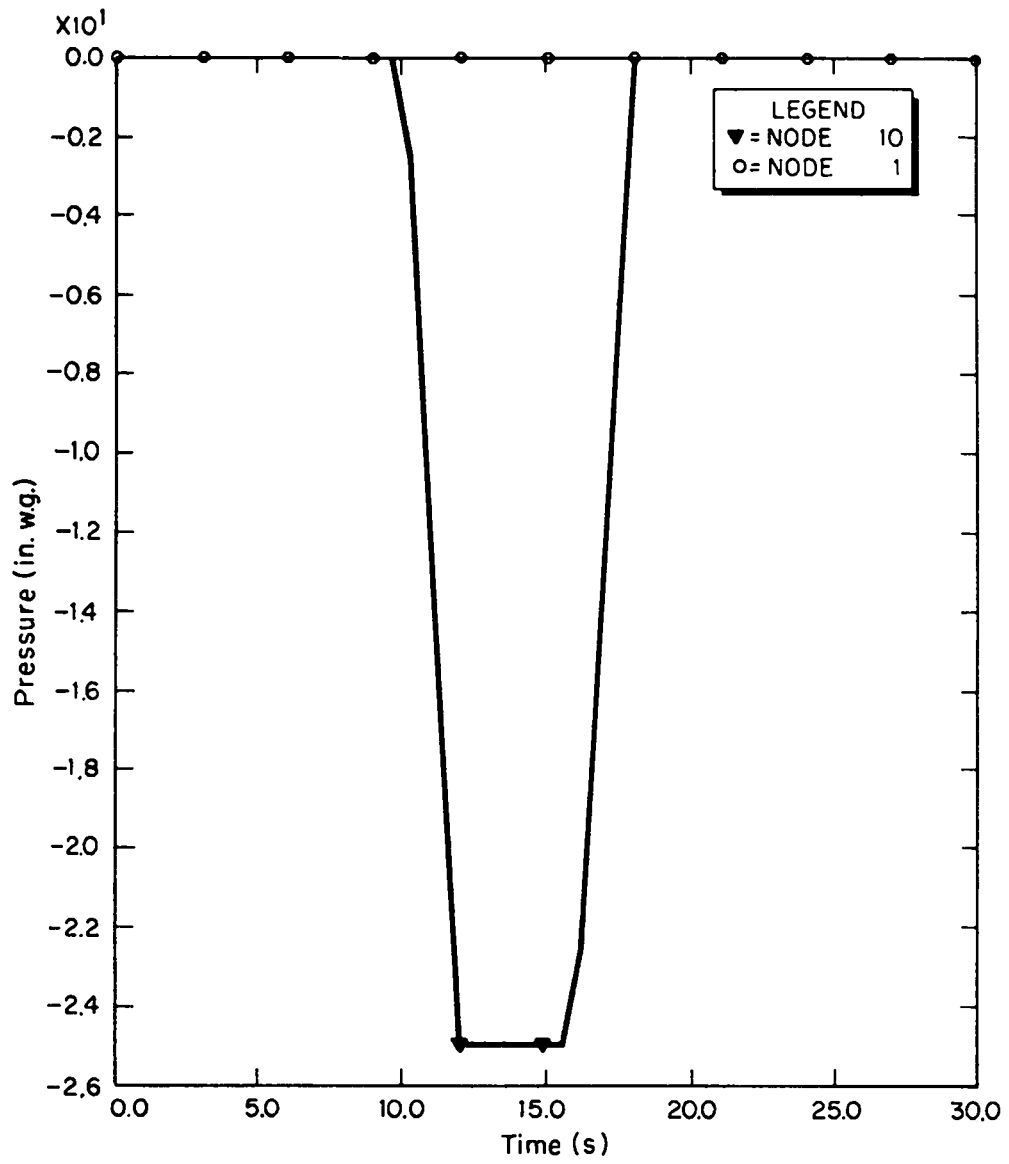


Fig. 18.  
Tornado at exhaust.

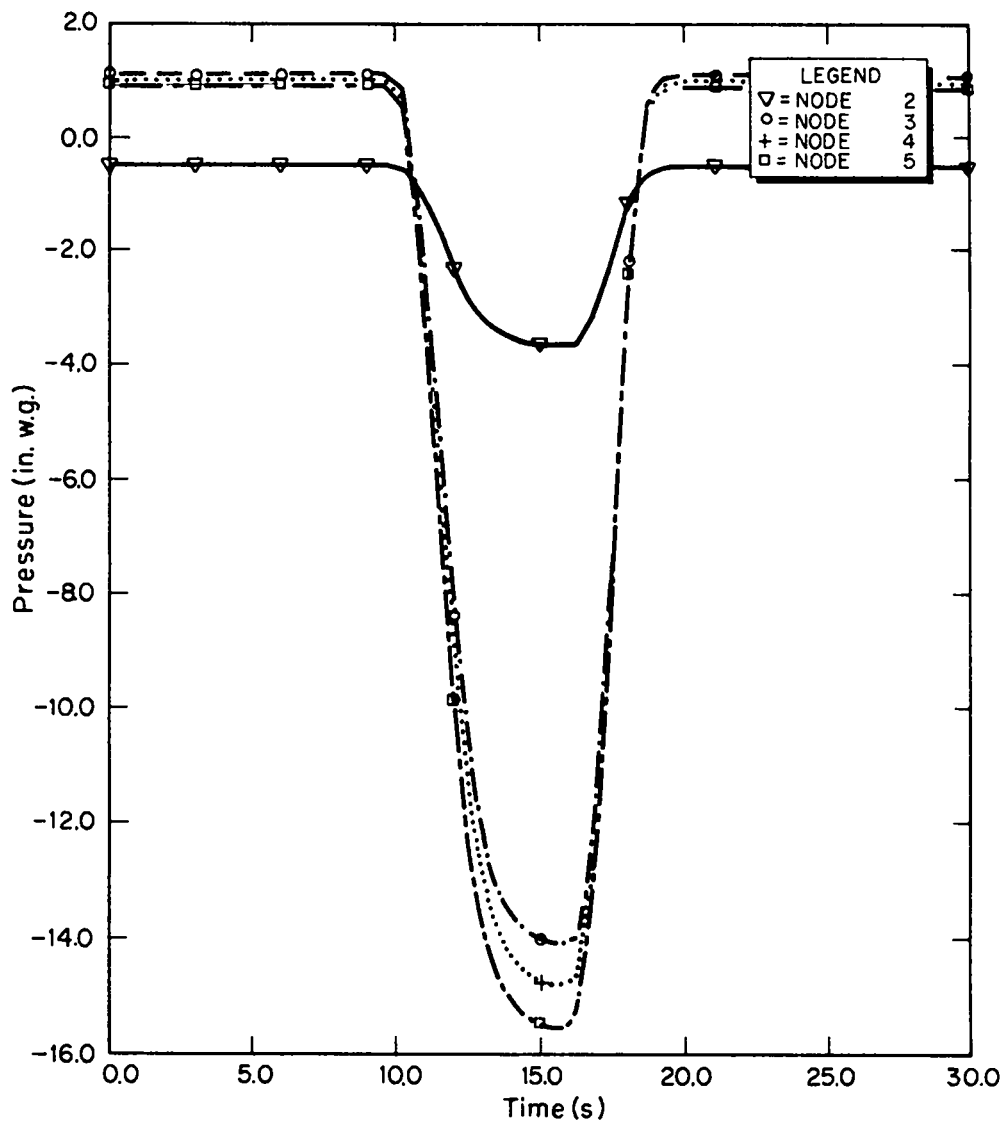


Fig. 19.  
Tornado at exhaust.

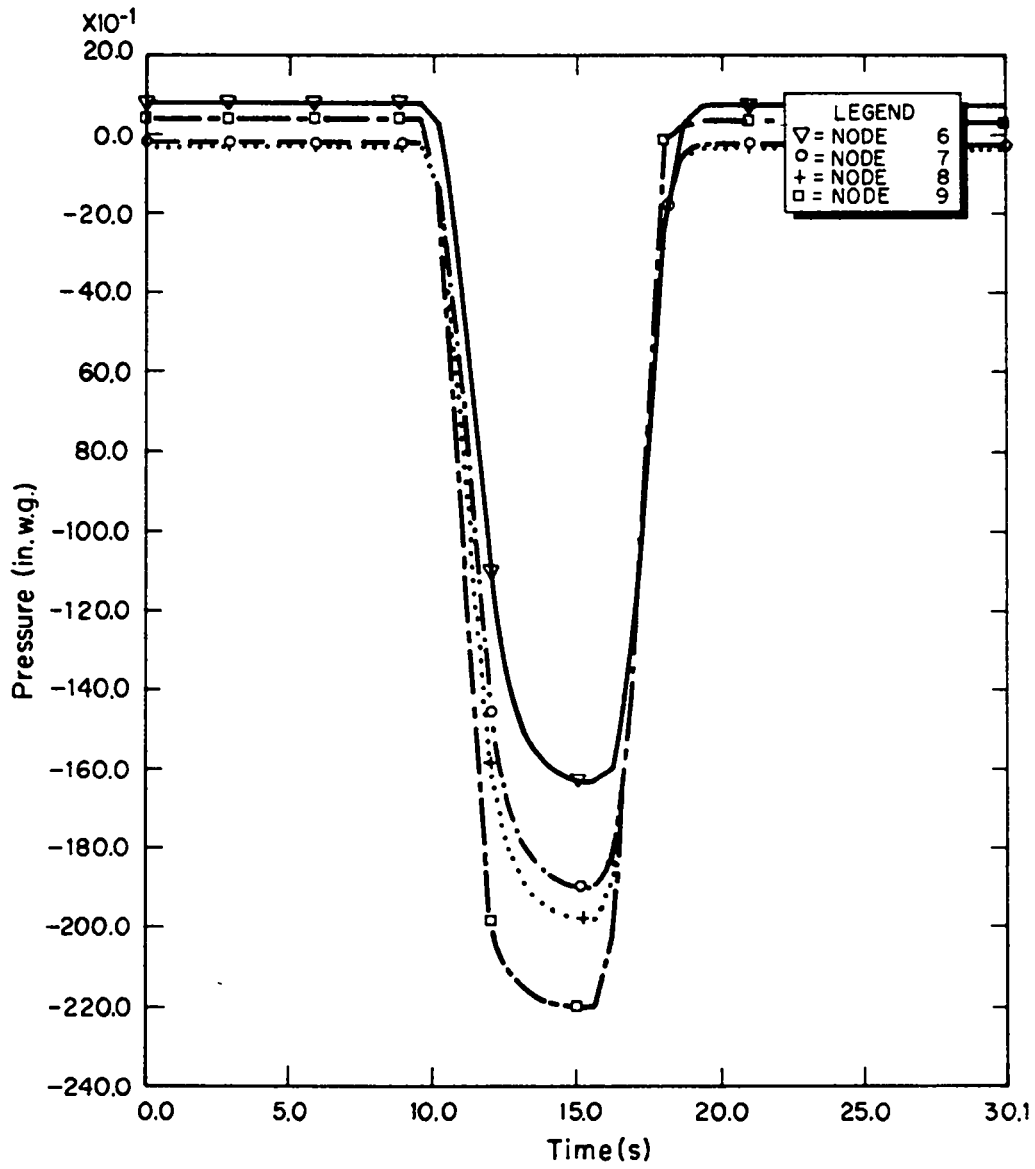


Fig. 20.  
Tornado at exhaust.

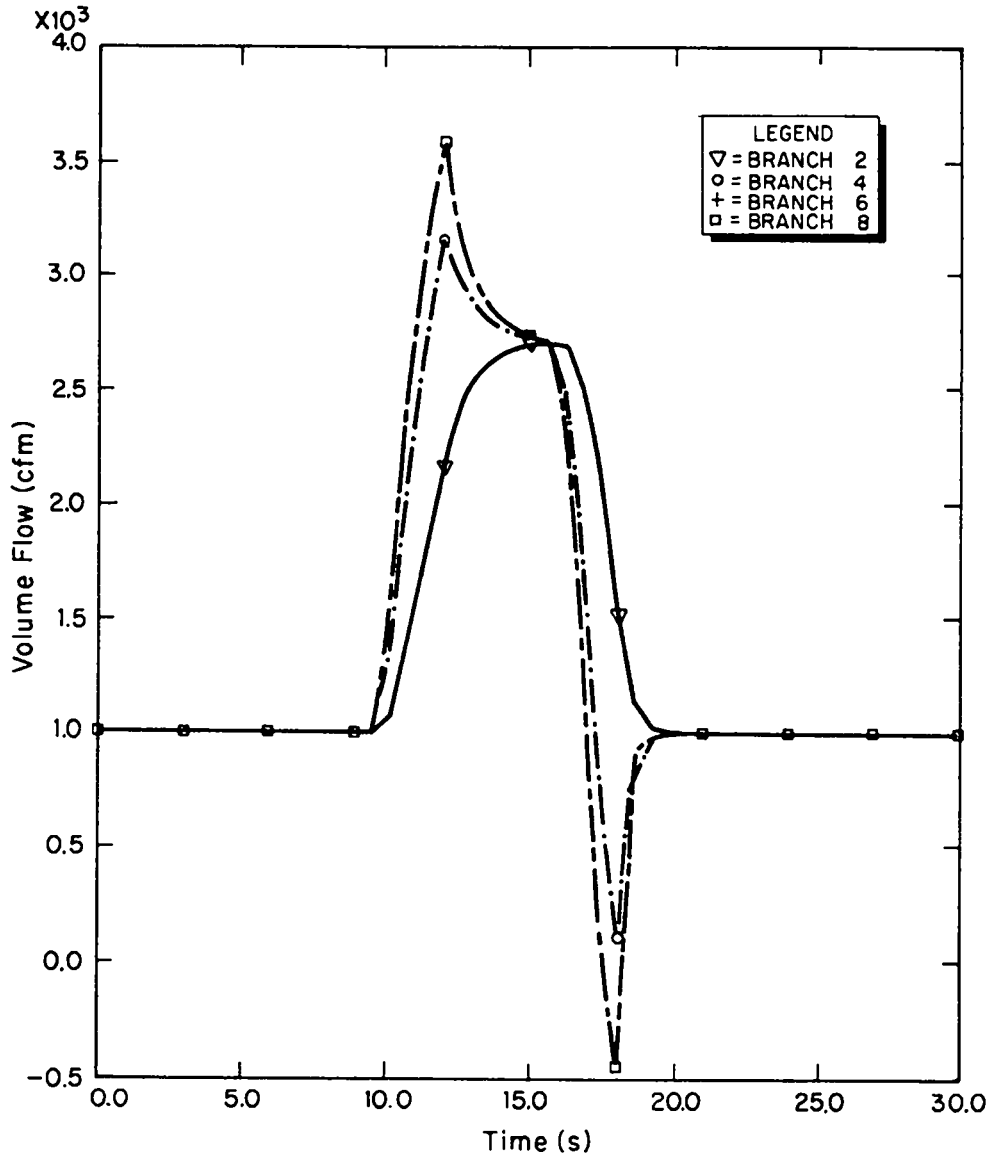


Fig. 21.  
Tornado at exhaust.

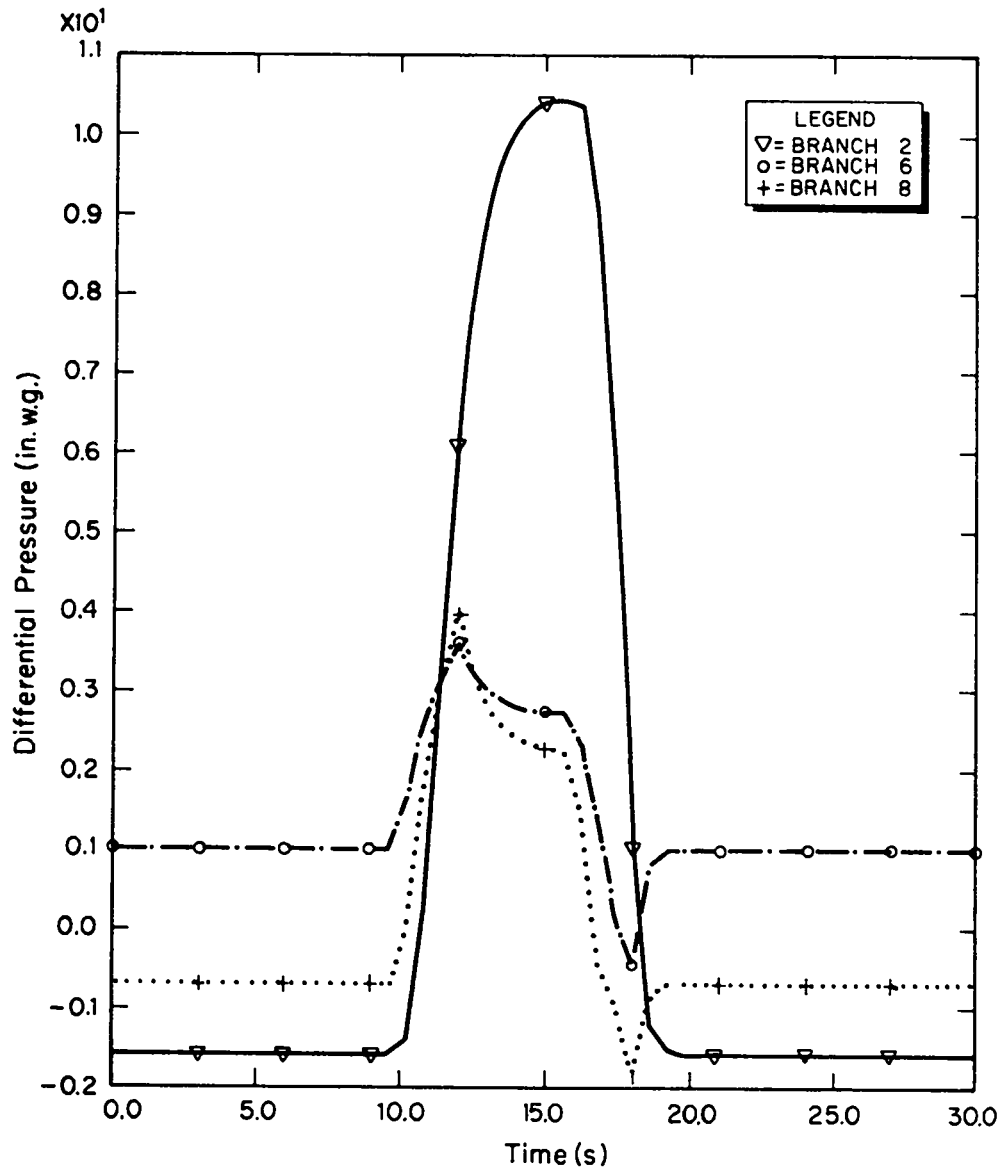


Fig. 22.  
Tornado at exhaust.

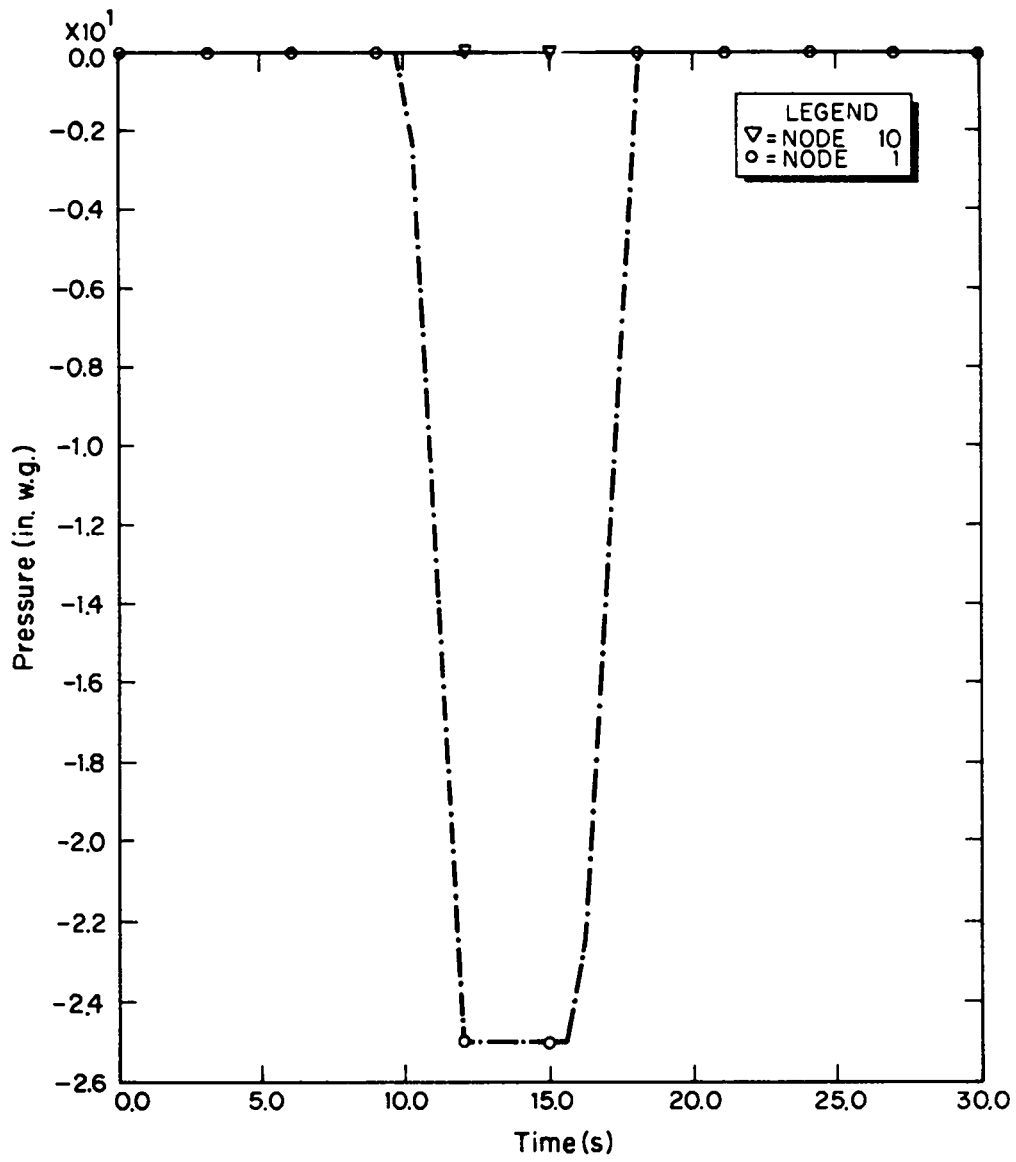


Fig. 23.  
Tornado at intake.



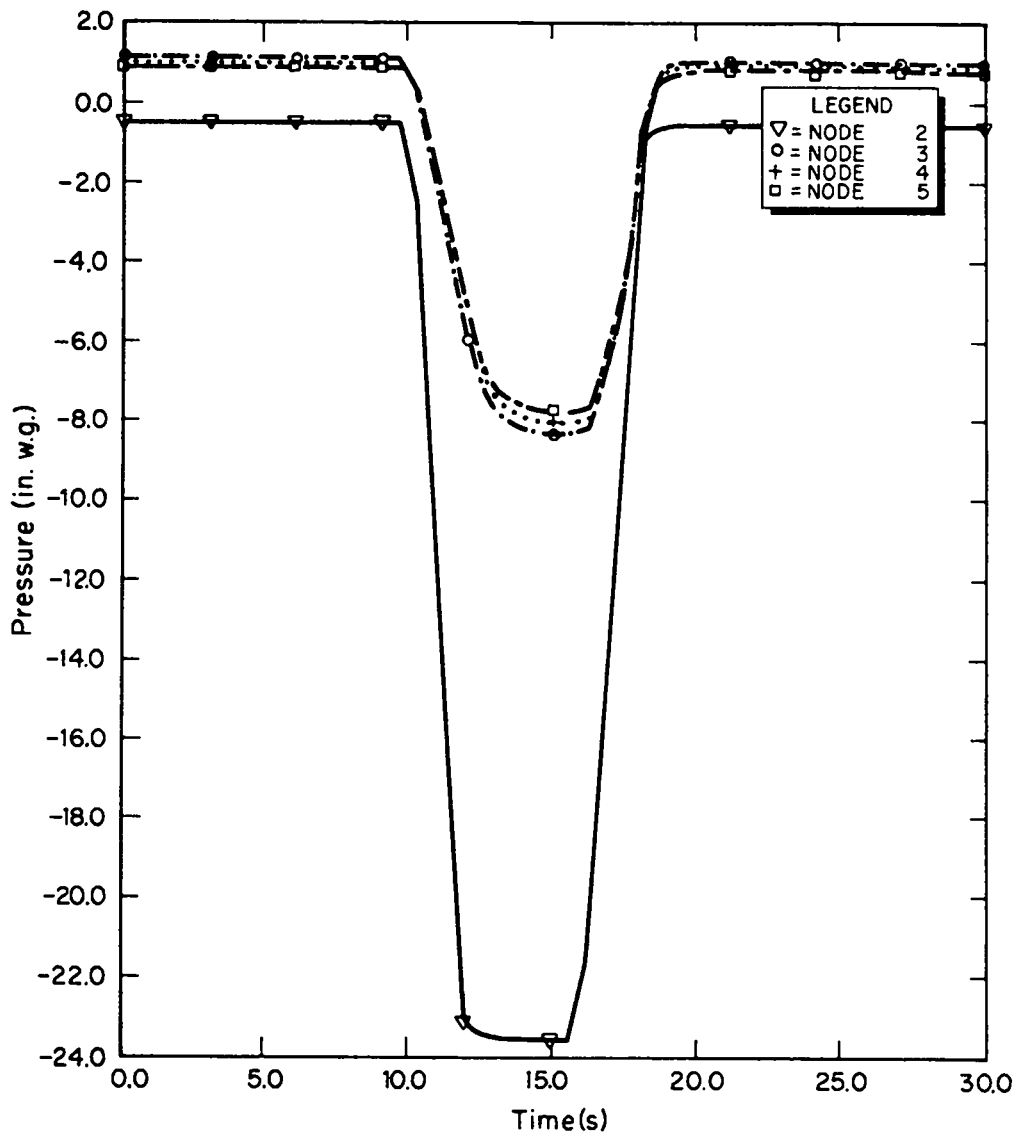


Fig. 24.  
Tornado at intake.

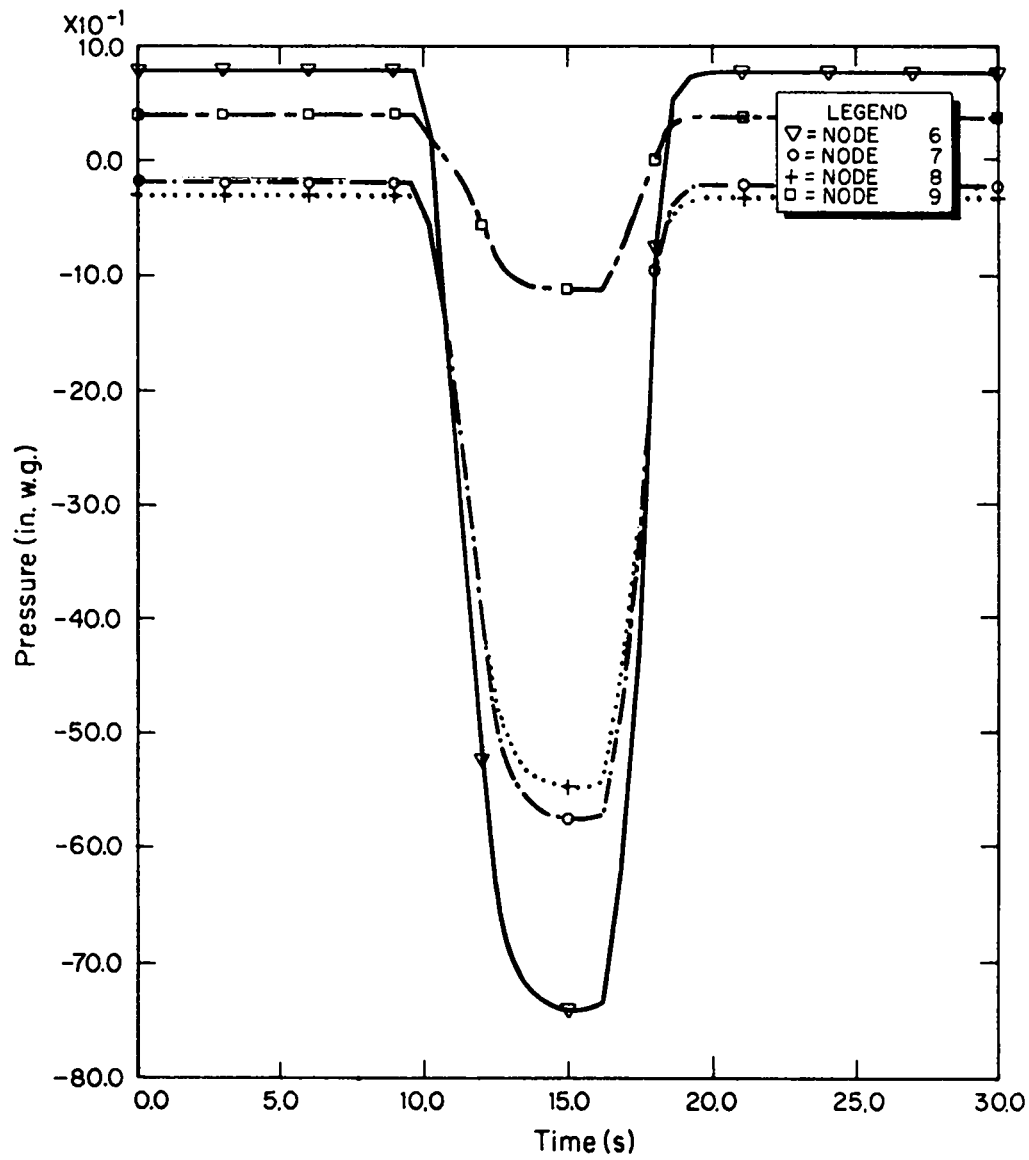


Fig. 25.  
Tornado at intake.

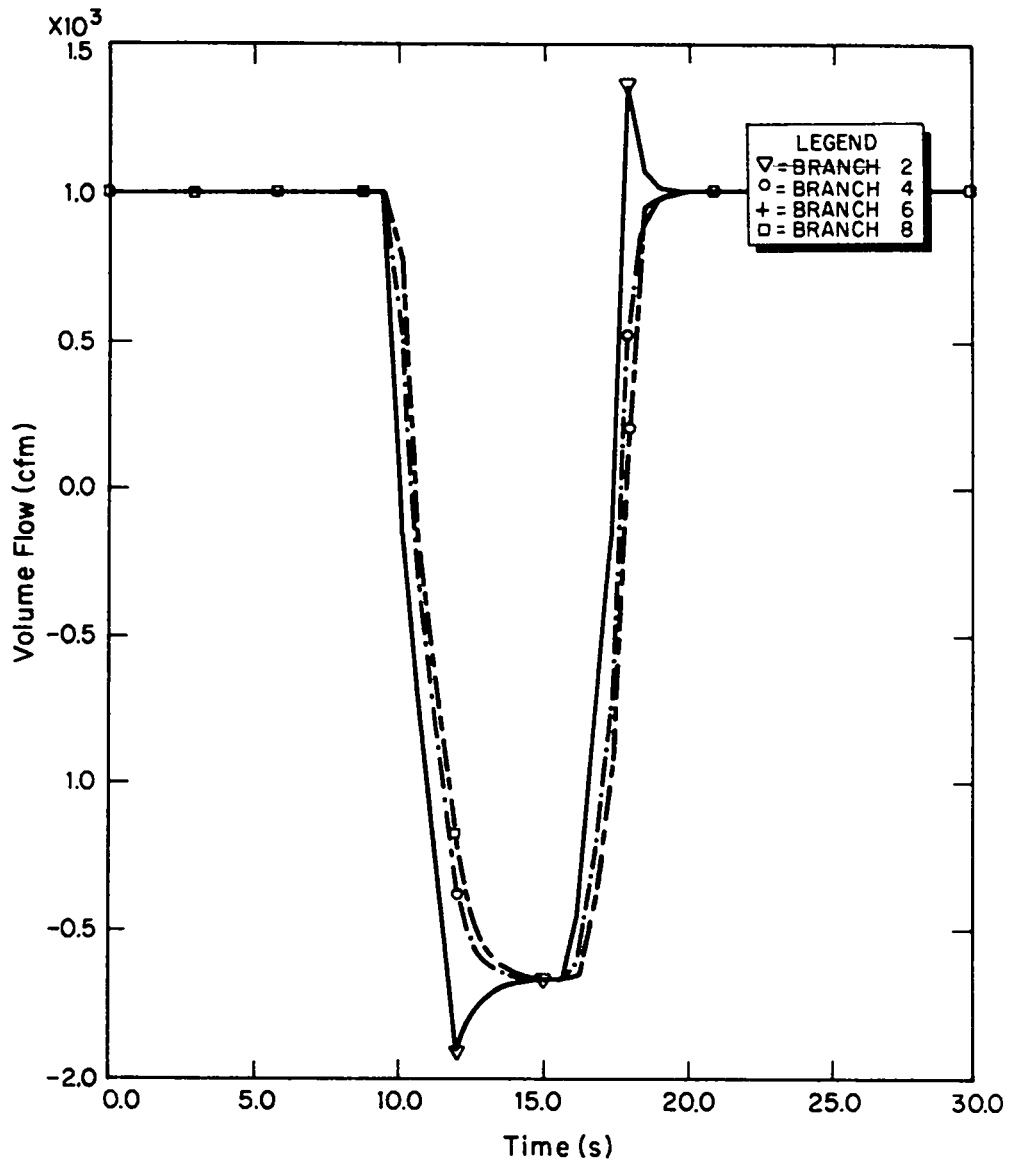


Fig. 26.  
Tornado at intake.

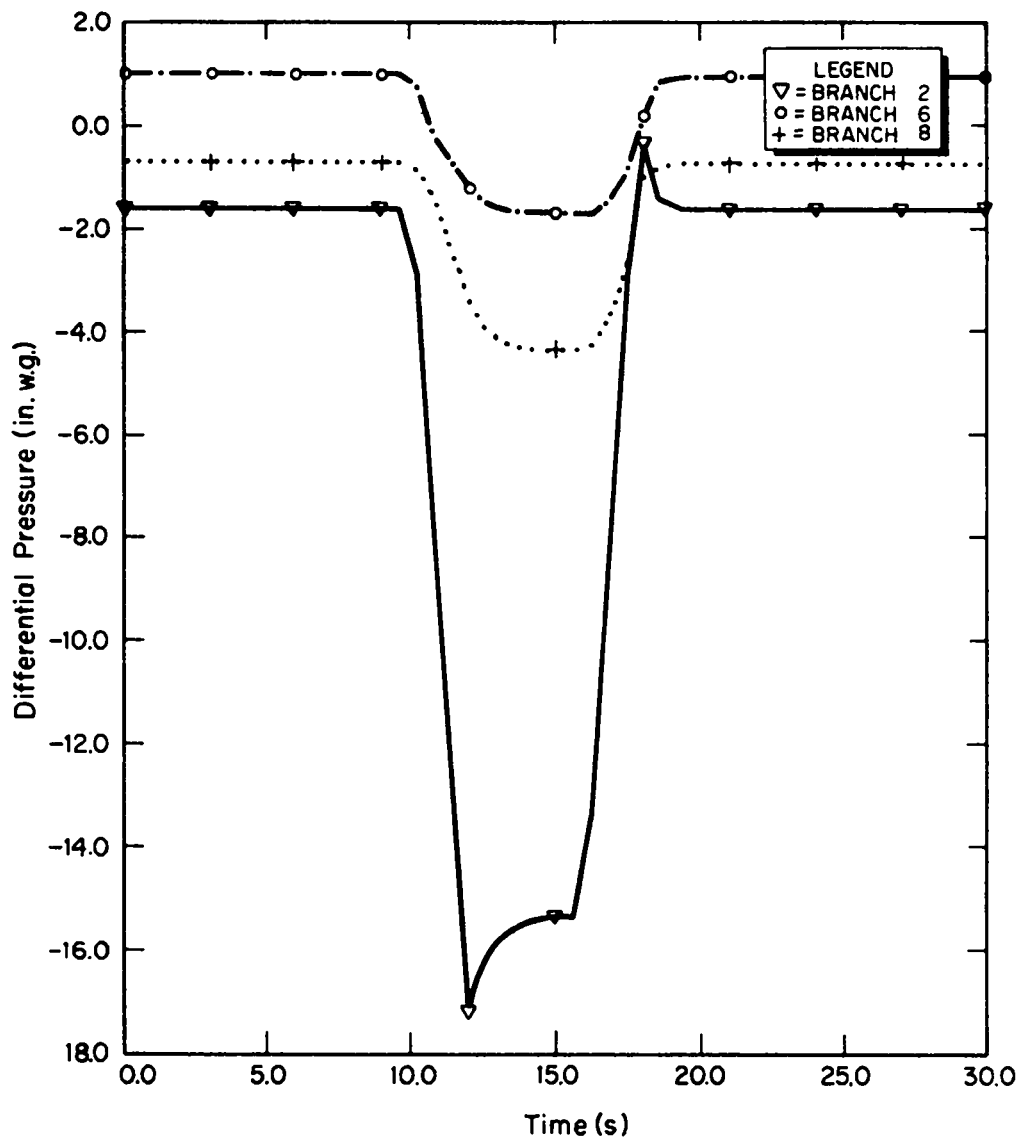


Fig. 27.  
Tornado at intake.

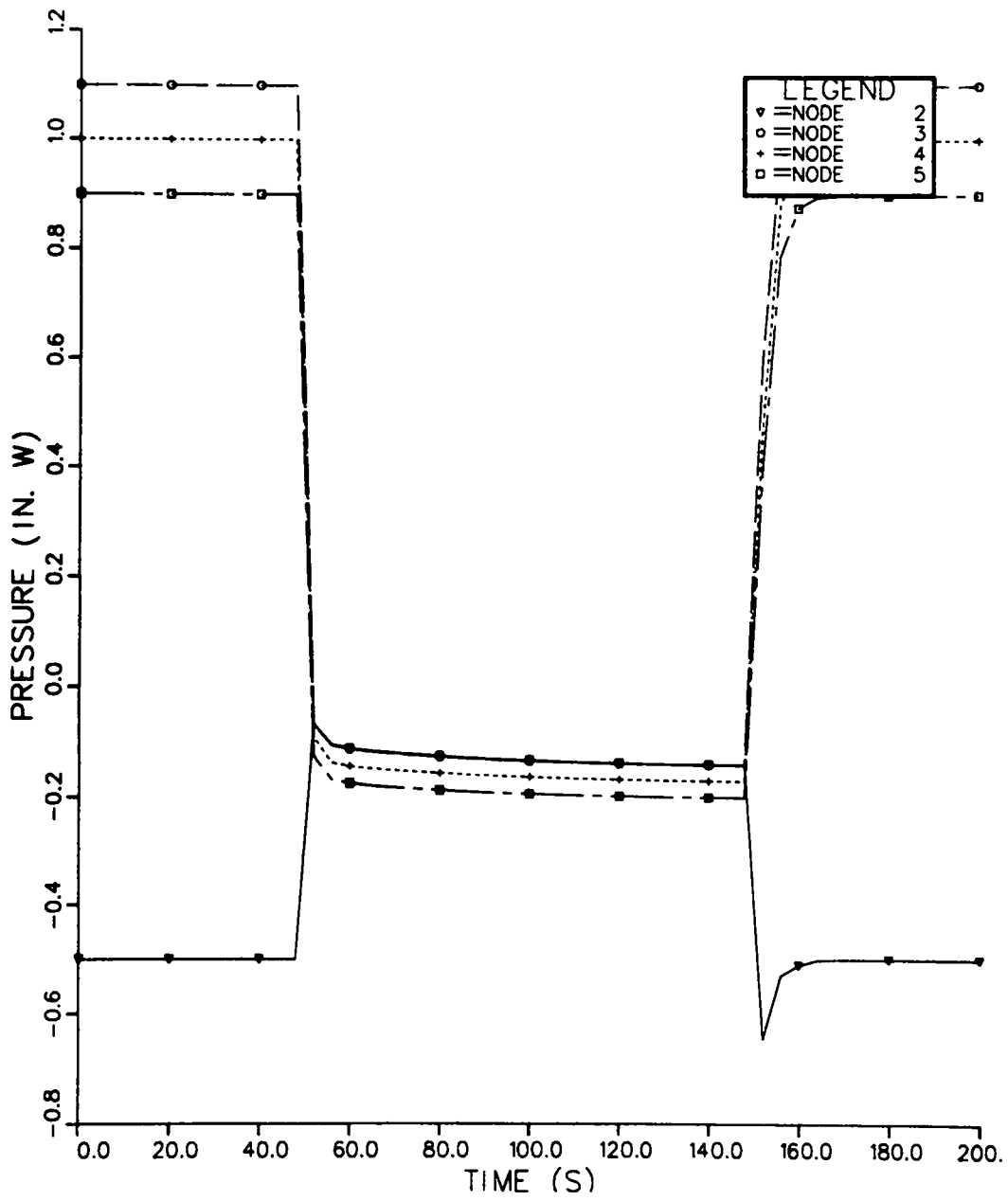


Fig. 28.  
Supply blower turned off and on.

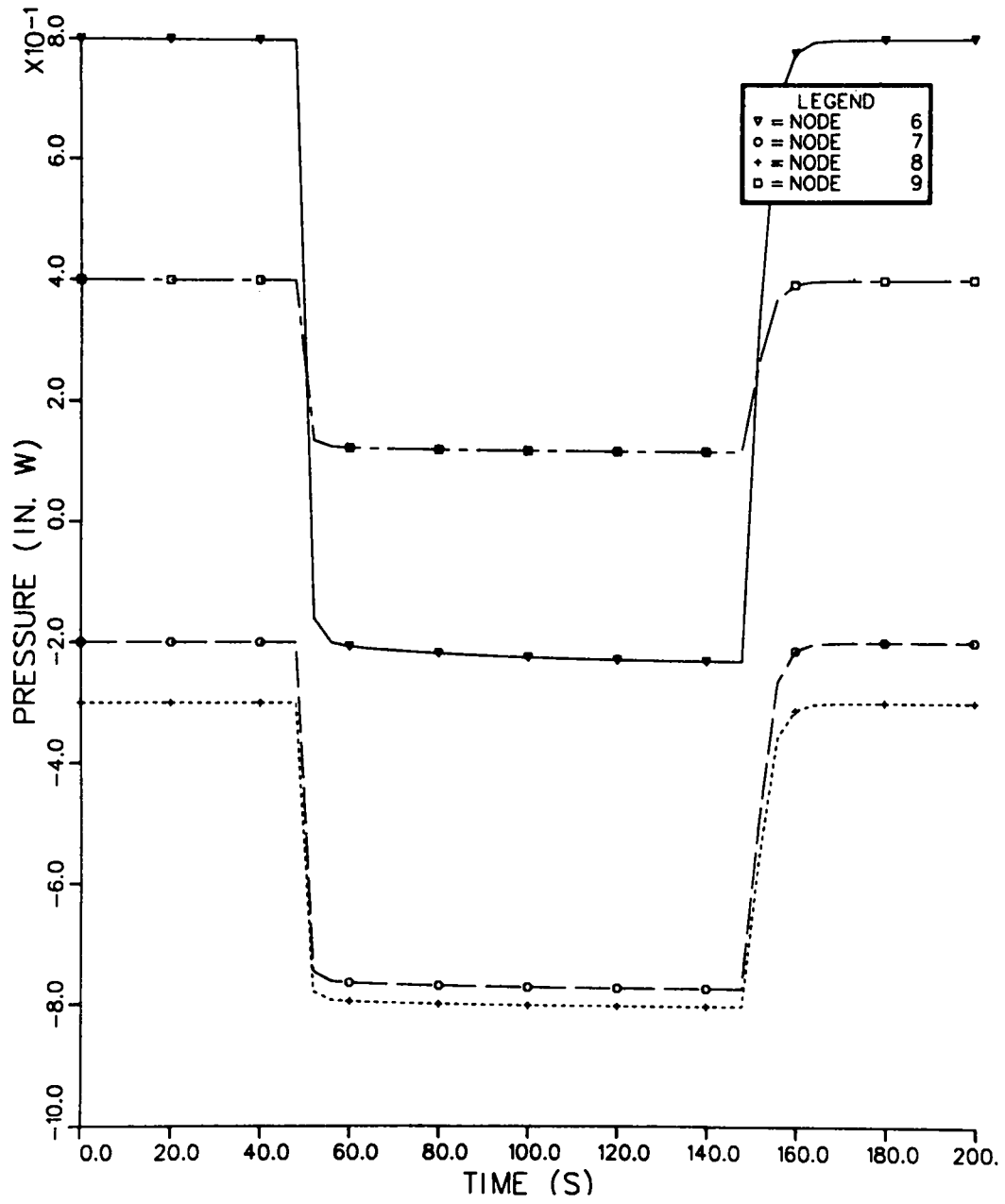


Fig. 29.  
Supply blower turned off and on.

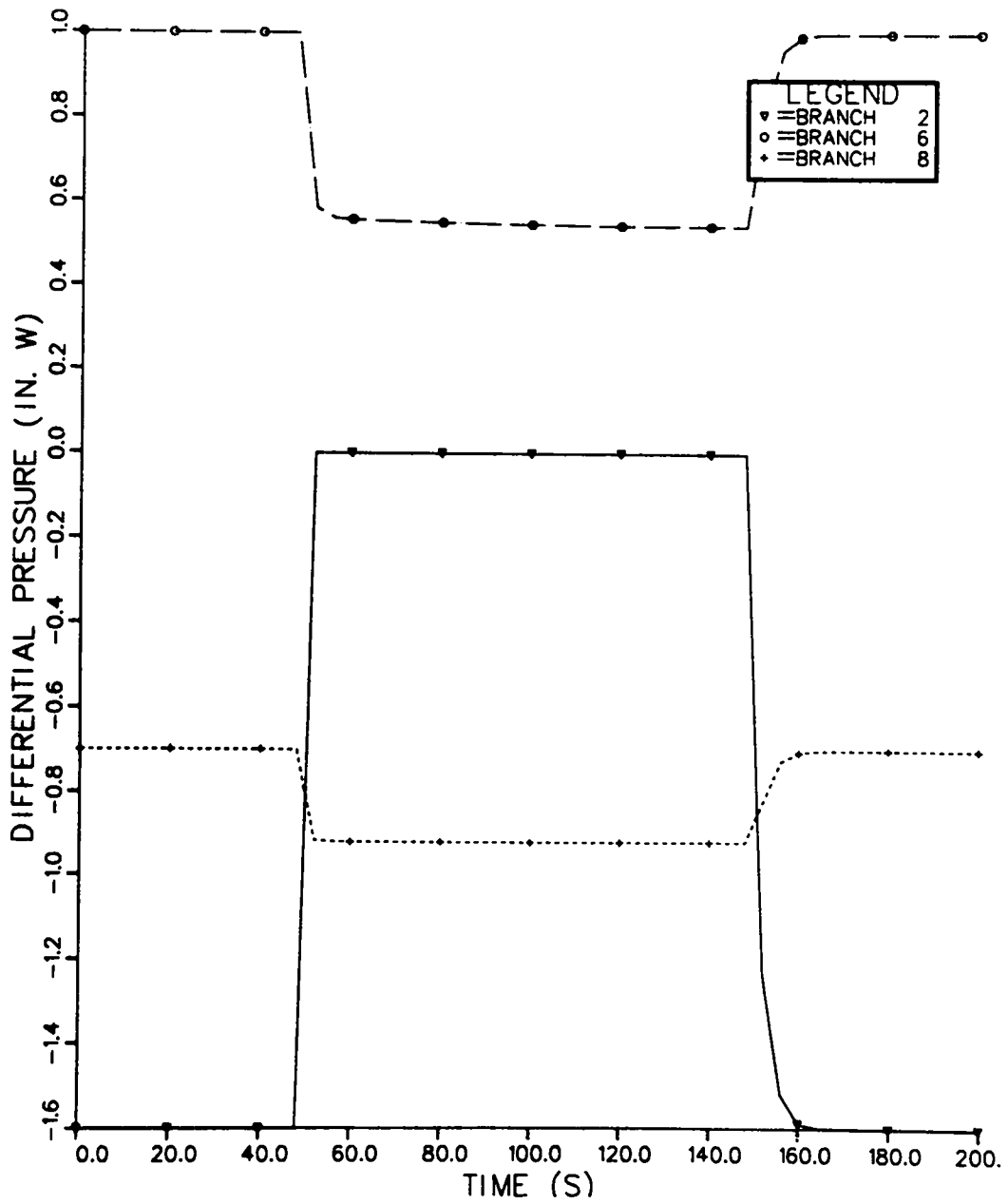


Fig. 30.  
Supply blower turned off and on.

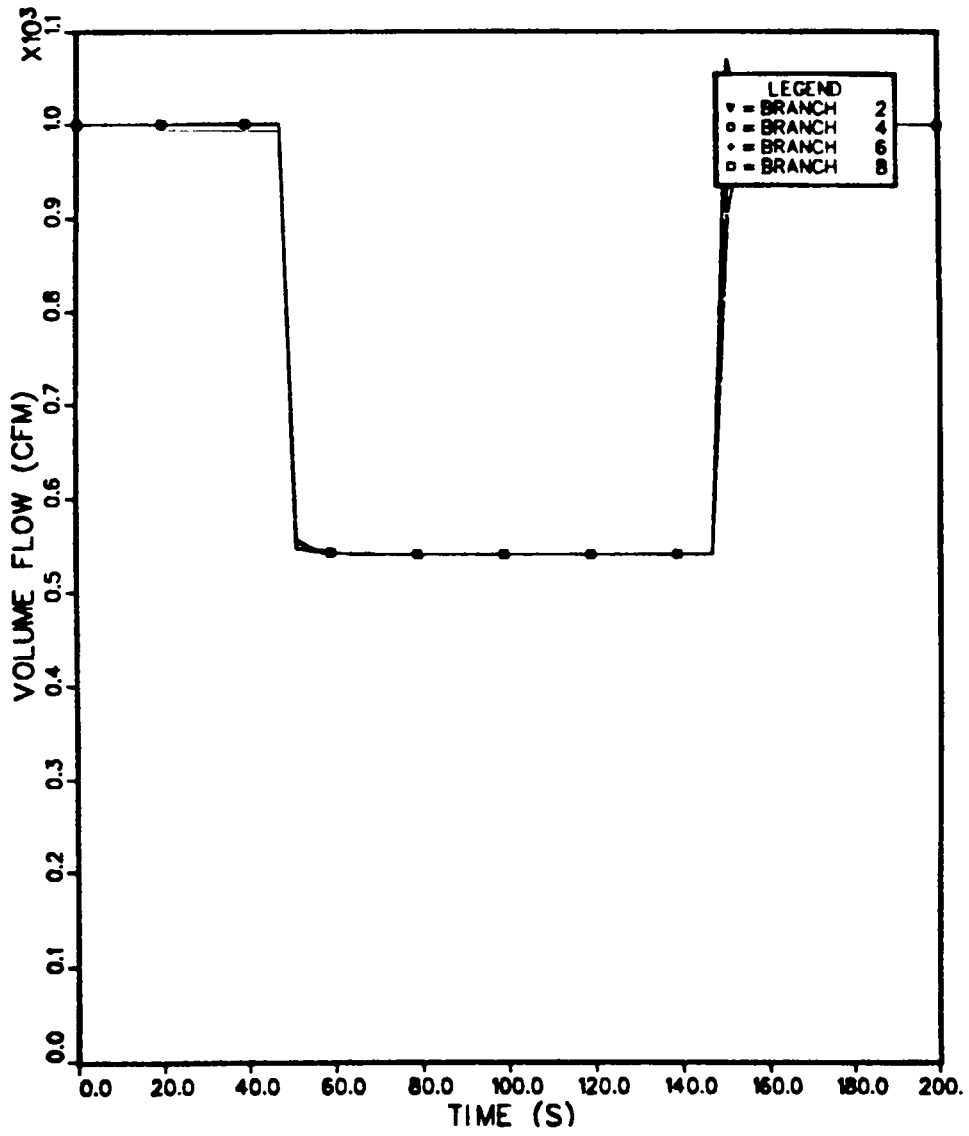


Fig. 31.  
Supply blower turned off and on.



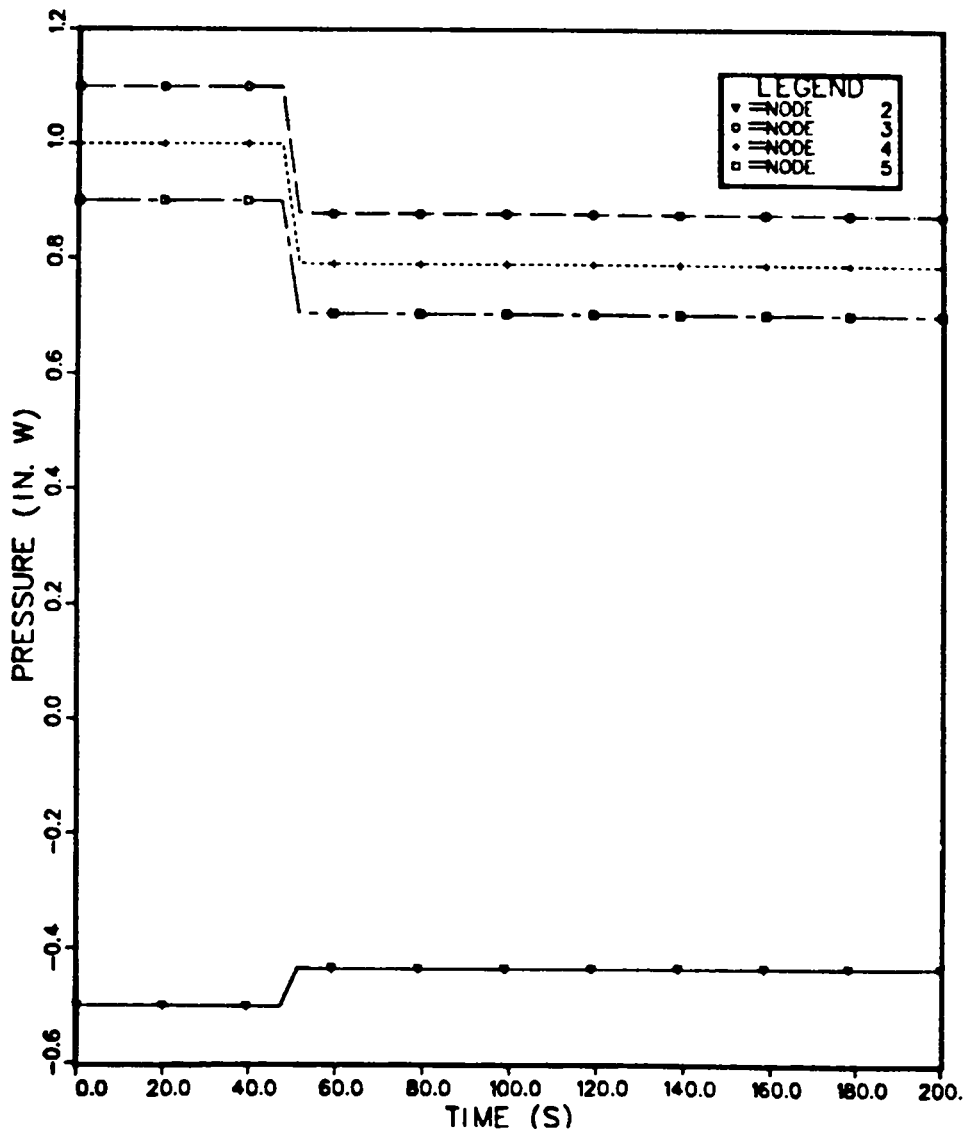


Fig. 32.  
Supply blower speed reduced.

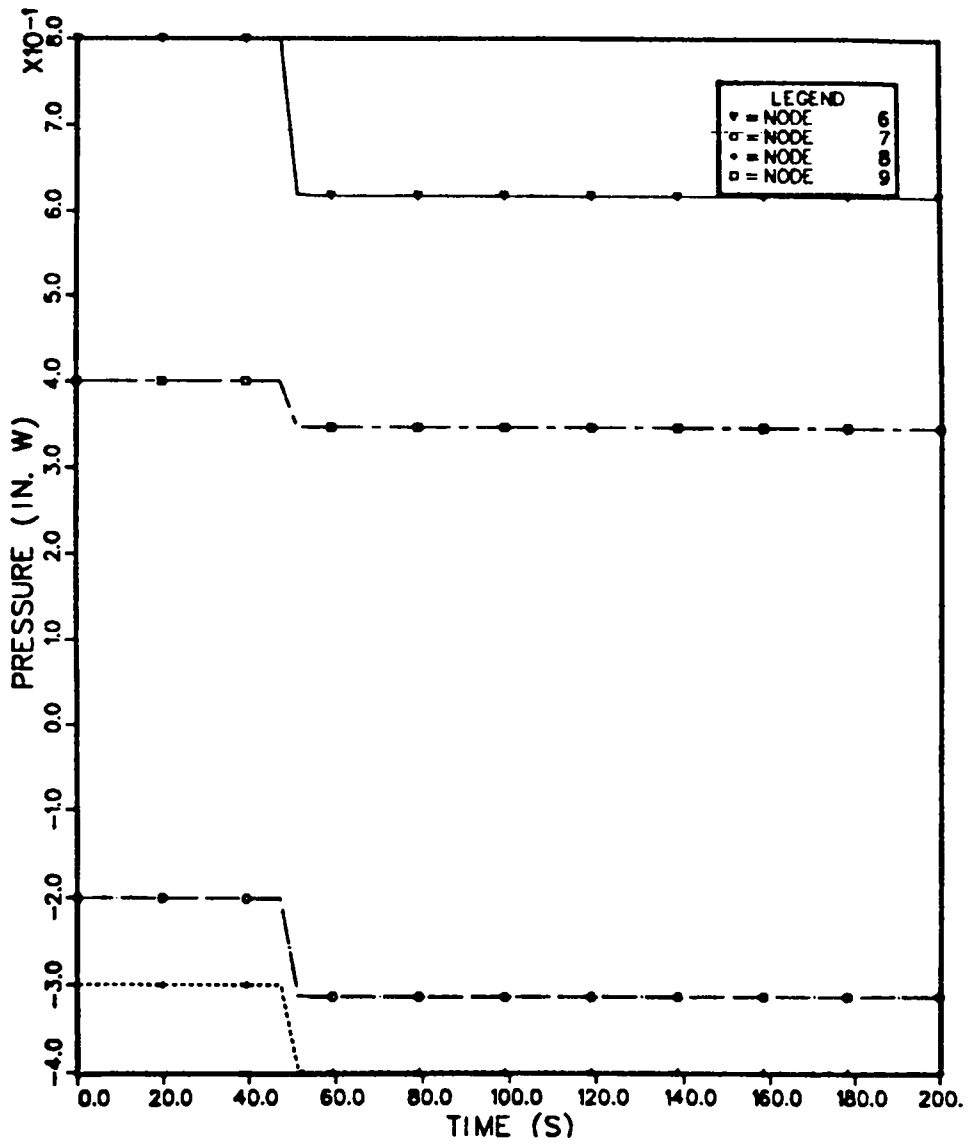


Fig. 33.  
Supply blower speed reduced.

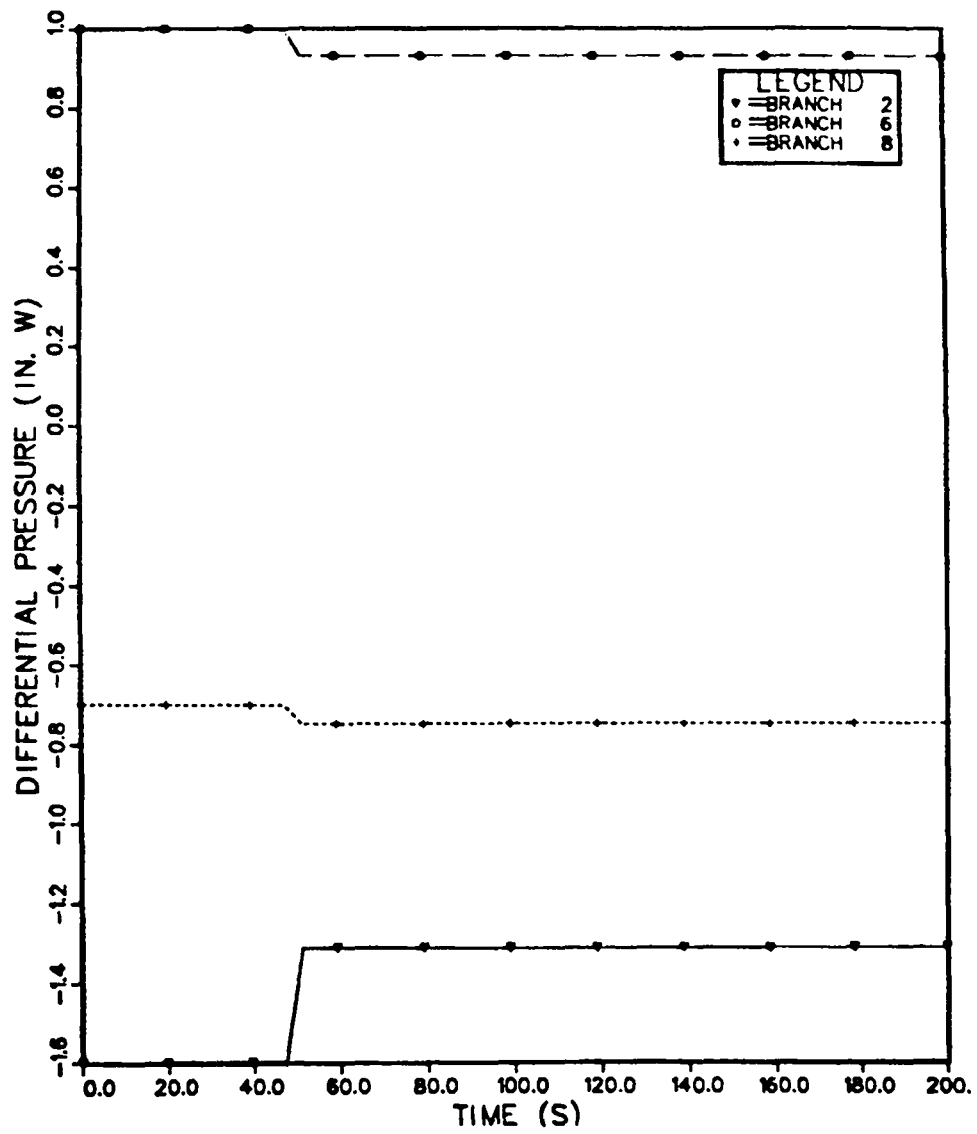


Fig. 34.  
Supply blower speed reduced.

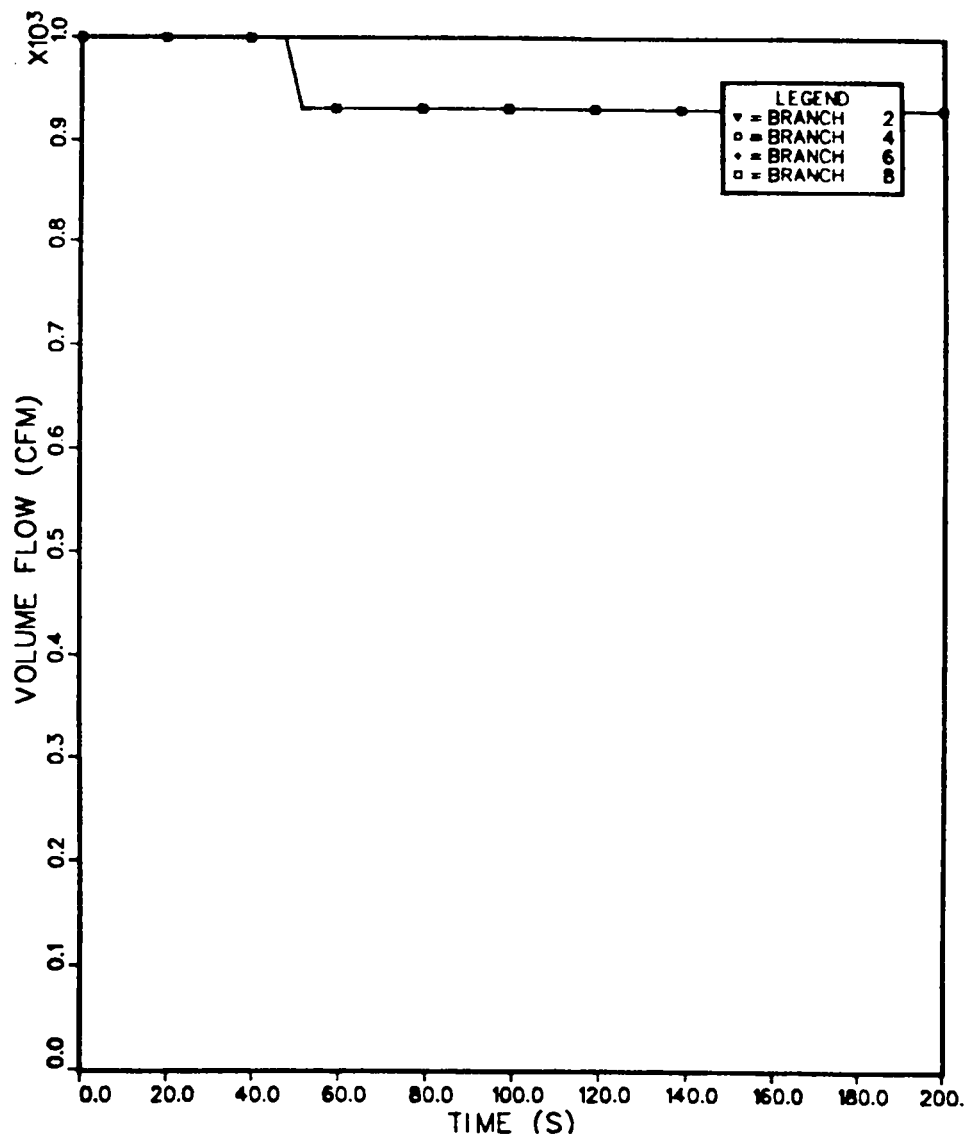


Fig. 35.  
Supply blower speed reduced.

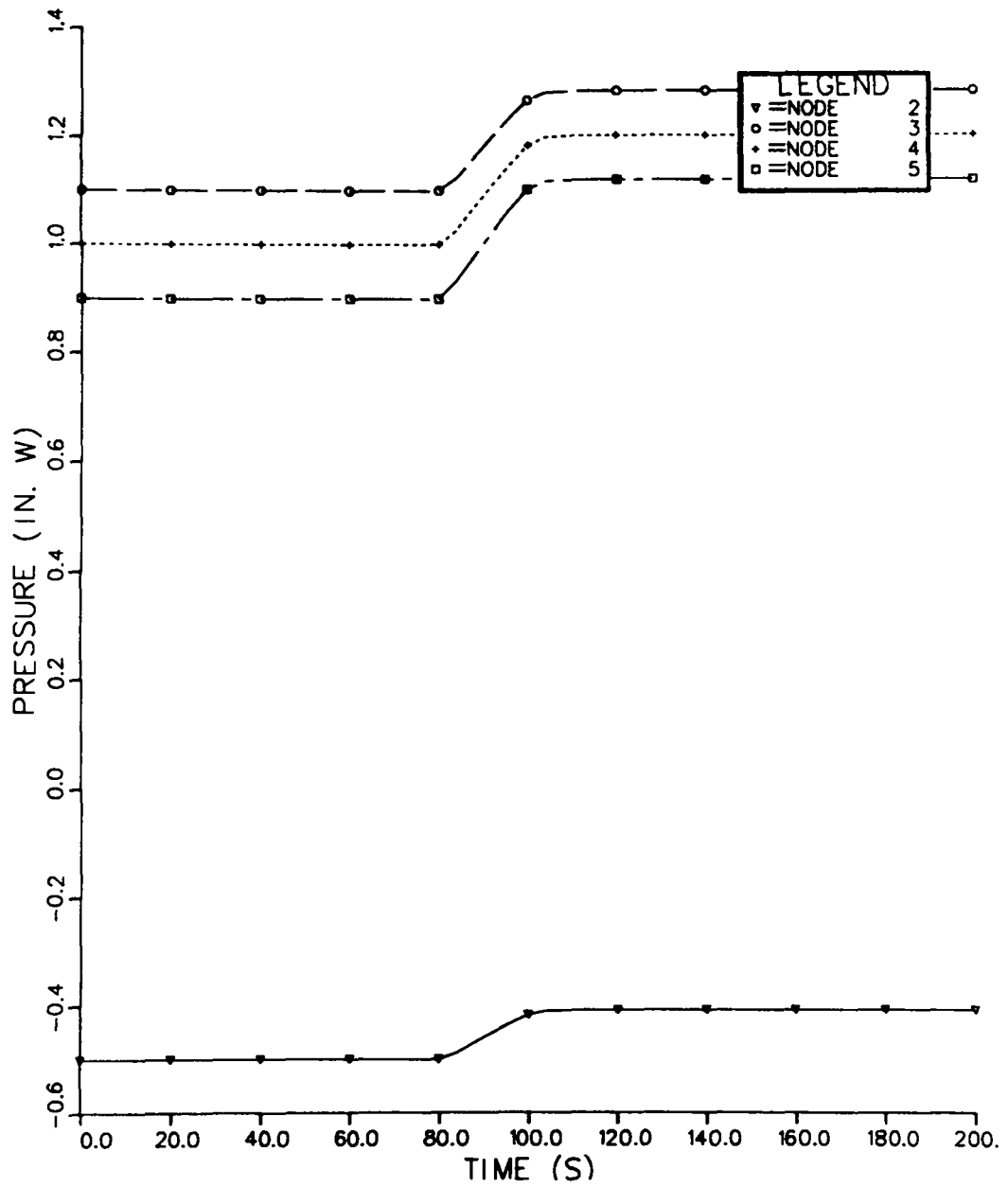


Fig. 36.  
Control damper closing.

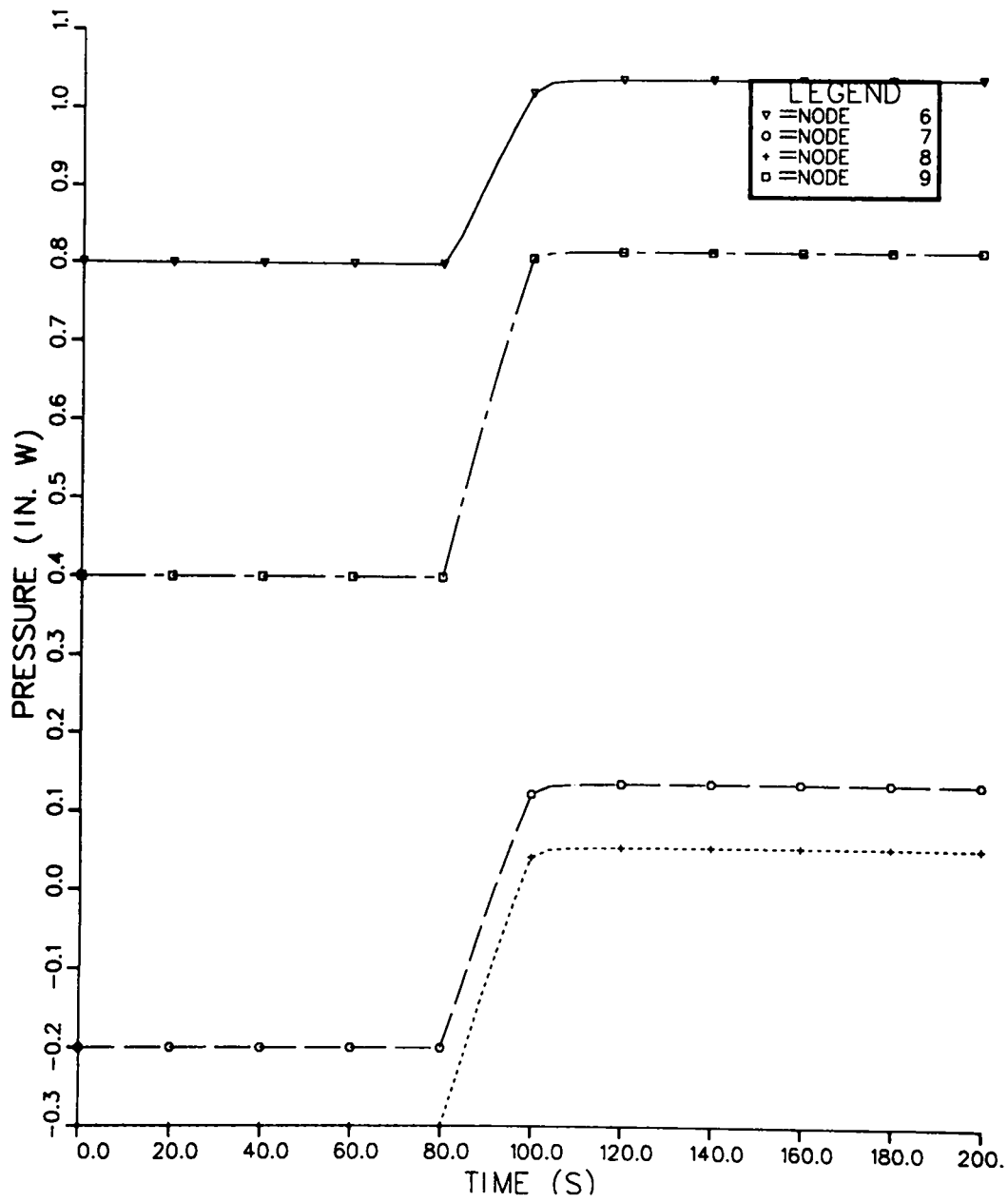


Fig. 37.  
Control damper closing.

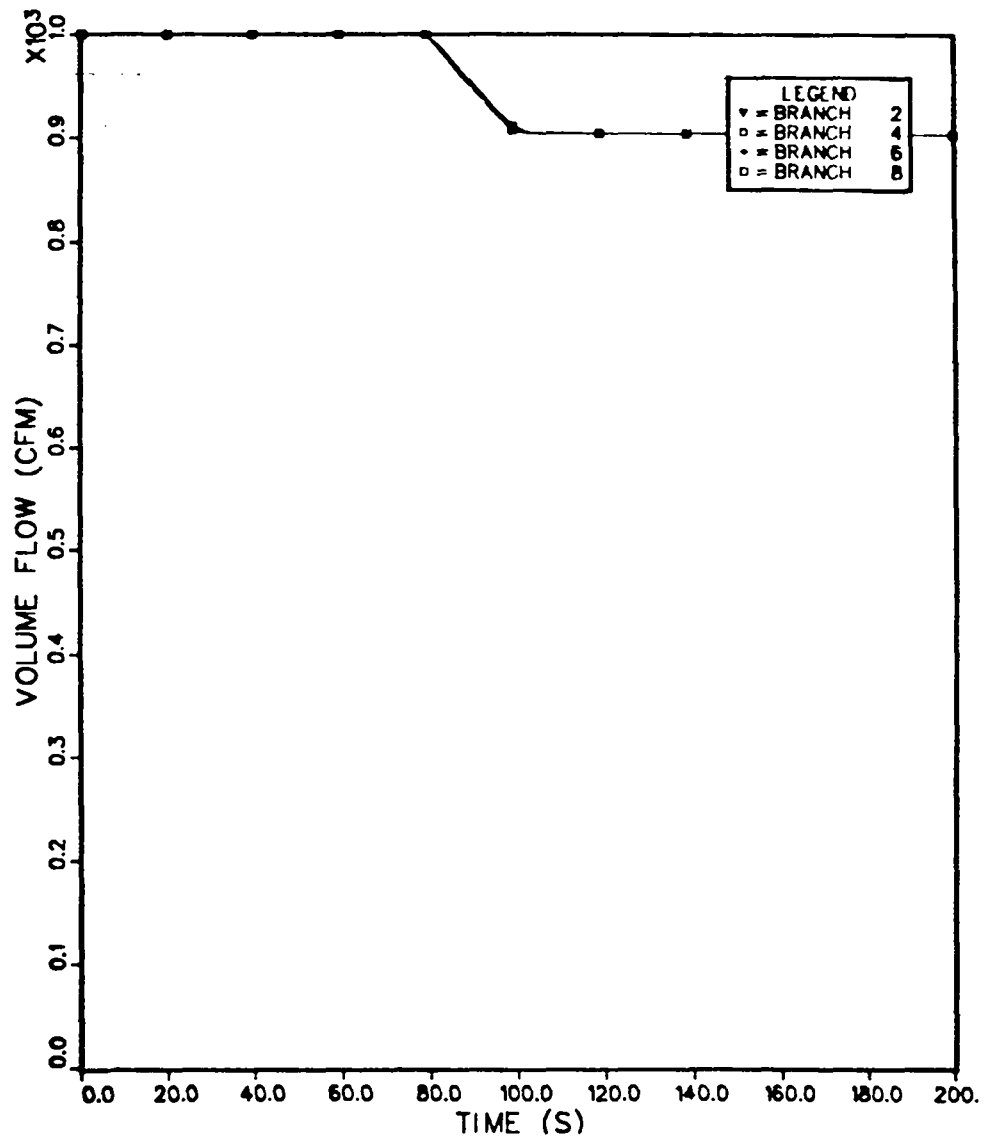


Fig. 38.  
Control damper closing.

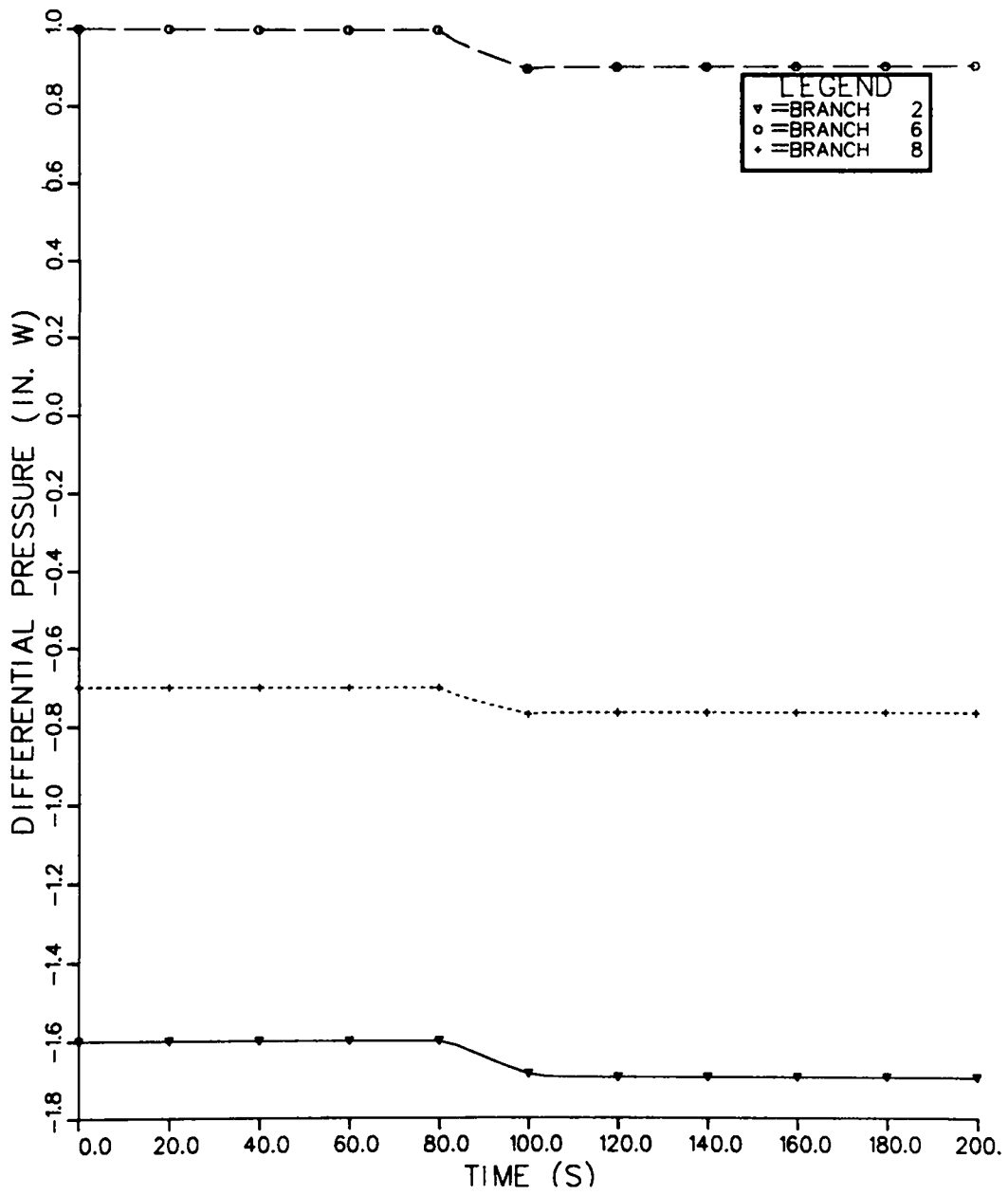


Fig. 39.  
Control damper closing.



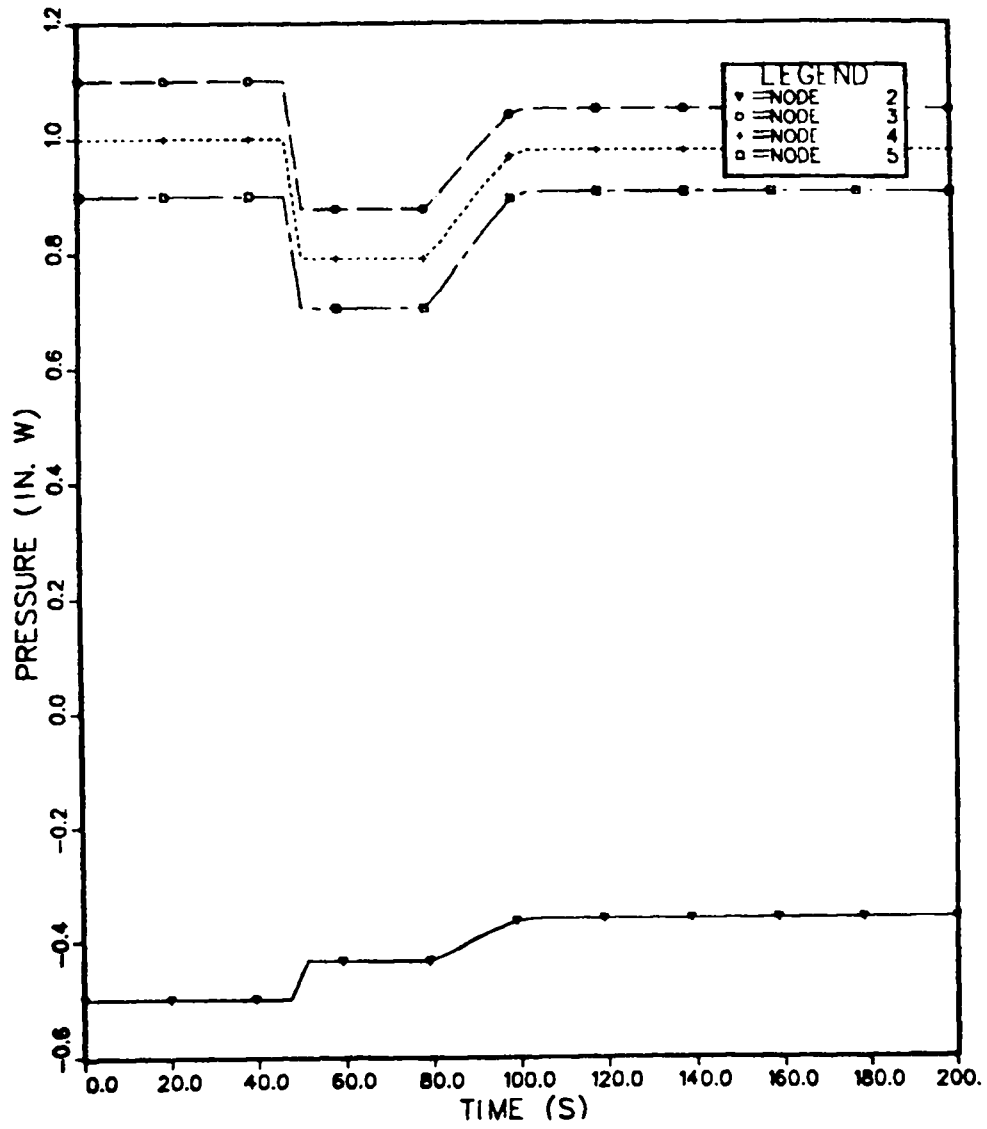


Fig. 40.  
Blower speed reduced and damper closing.

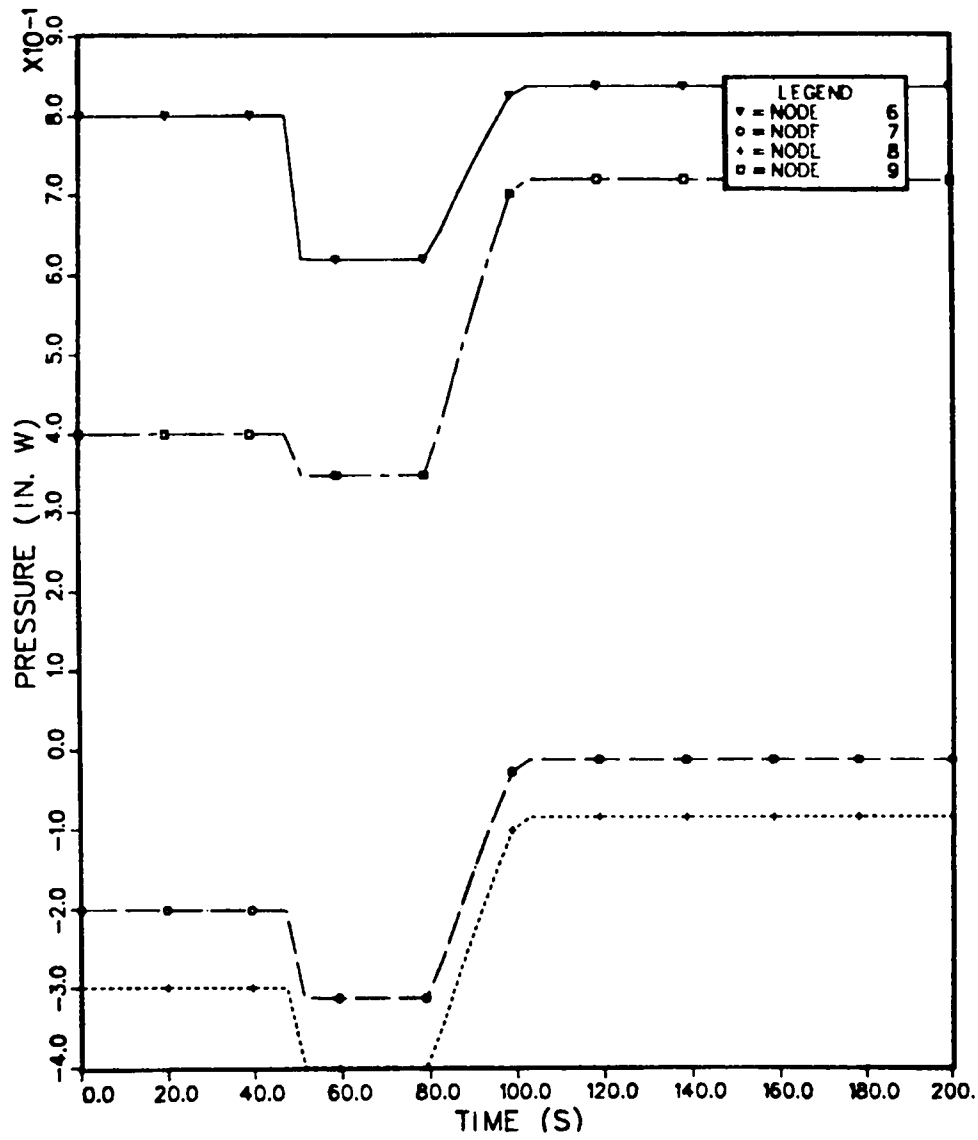


Fig. 41.  
Blower speed reduced and damper closing.

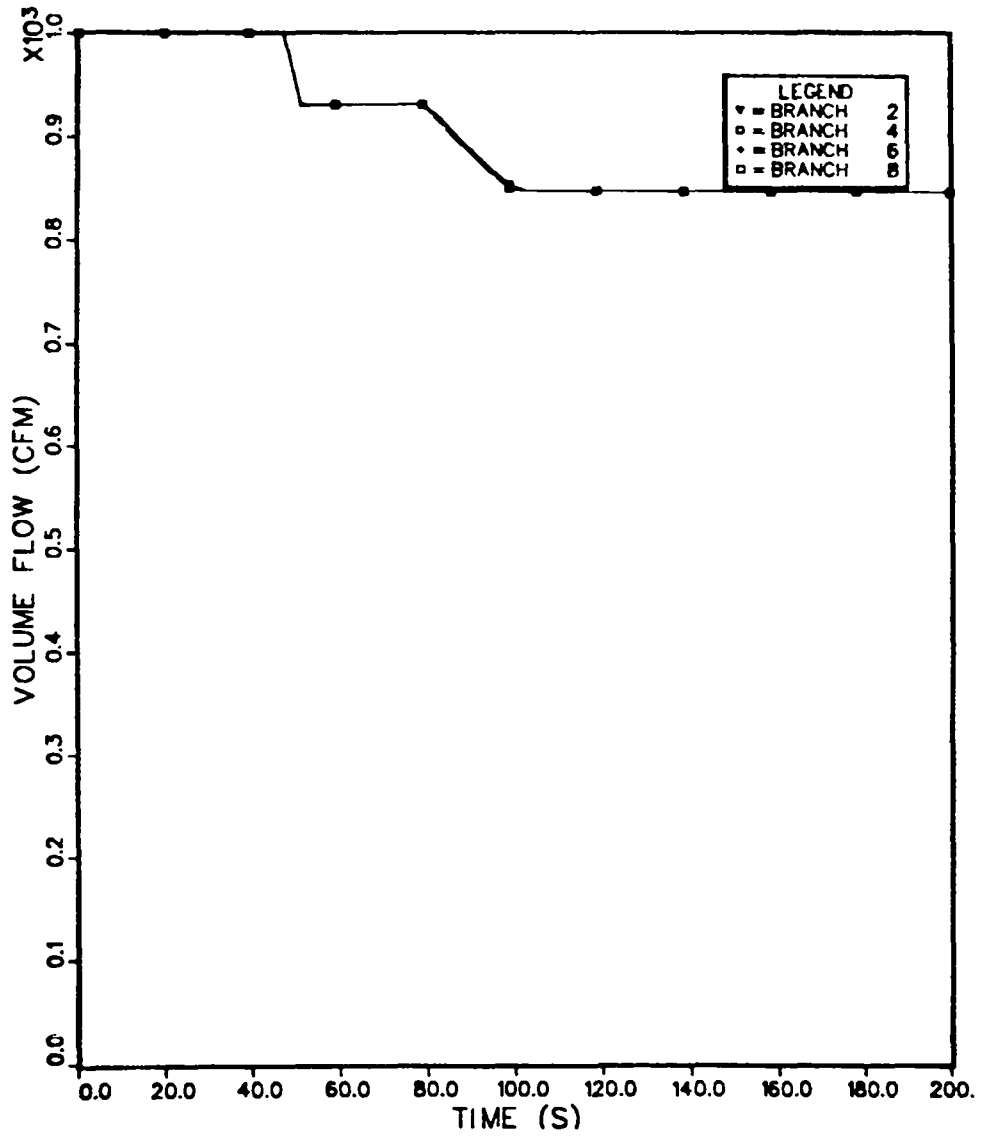


Fig. 42.  
Blower speed reduced and damper closing.

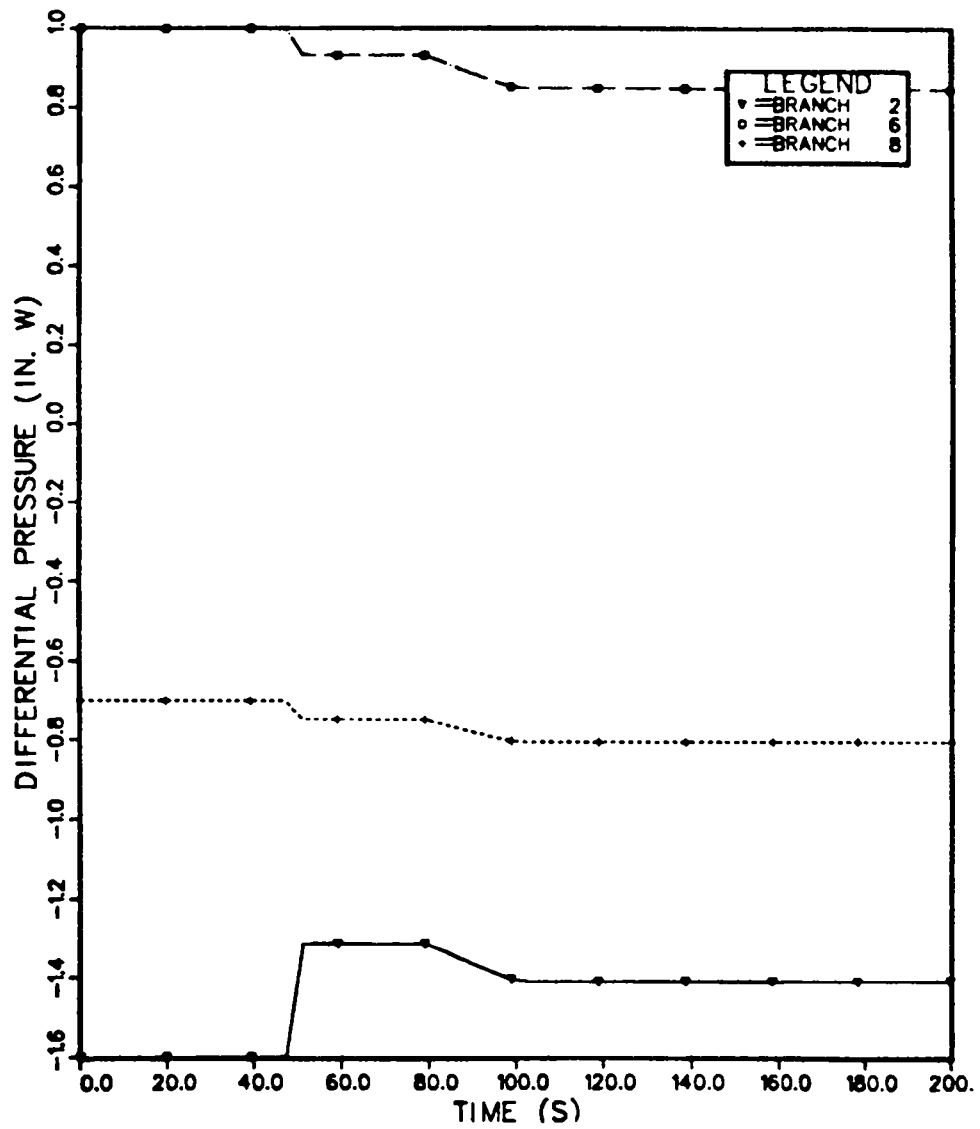


Fig. 43.  
Blower speed reduced and damper closing.

### Problem 7 - Material Transport (No Filter Plugging)

Runs 7 and 8 involve the transportation of material injected in the room at node 4 and carried downstream by the normal operating flow of  $0.5 \text{ m}^3/\text{S}$  ( $1000 \text{ ft}^3/\text{min}$ ). Most of this material is trapped on the filter. (Figs. 44--47)

### Problem 8 - Material Transport (Filter Plugging)

This is the same condition as in problem No. 7, but the filter has been assigned a plugging factor of 30. (Figs. 48--51)

### Problem 9 - Calculated Aerodynamic Entrainment

This sample problem illustrates use of the calculated aerodynamic entrainment option for material transport initiation in a duct. The user requirements and theory for this option are discussed in Sec. III.D.3. and in Appendix B, Sec. IV. For convenience, we used the same system shown in Figs. 15 and 16. The 30.48-m (100-ft)-long duct connecting the room at node 4 to the filter in branch 6 was modeled using two segments. Each segment contained a resistance lumped in a branch and a volume lumped at a node. Duct entrainment should be specified at the latter nodes. More segments should be used for more accurate results. In this version of TORAC, entrainment of beds of material in rooms or cells is treated in the same way as illustrated here. The following conditions were assumed and set up in the master input file of TORAC. (See Fig. 17.)

1. A tornado of strength 127 cm w.g. (50 in. w.g.) applied at exhaust node 10.
2. No material injection (transport initiation) occurs in room 4 or elsewhere using the user-specification option.
3. A total of 1 kg of contaminant material is subjected to entrainment in the duct volume represented by node 5.
4. The contaminant material is assumed to consist of homogeneous, monodisperse, spherical particles with aerodynamic diameter  $D_p = 100 \text{ }\mu\text{m}$  and bulk density  $\rho_p = 3 \text{ g/cm}^3$  ( $0.11 \text{ lb/in.}^3$ ).
5. The contaminant material is distributed uniformly over the 0.6-m by 15.24-m (2-ft by 50-ft) floor area of duct volume 5.
6. No deposition occurs in duct branches 4 or 5.
7. The filter efficiency was set at 0.8.

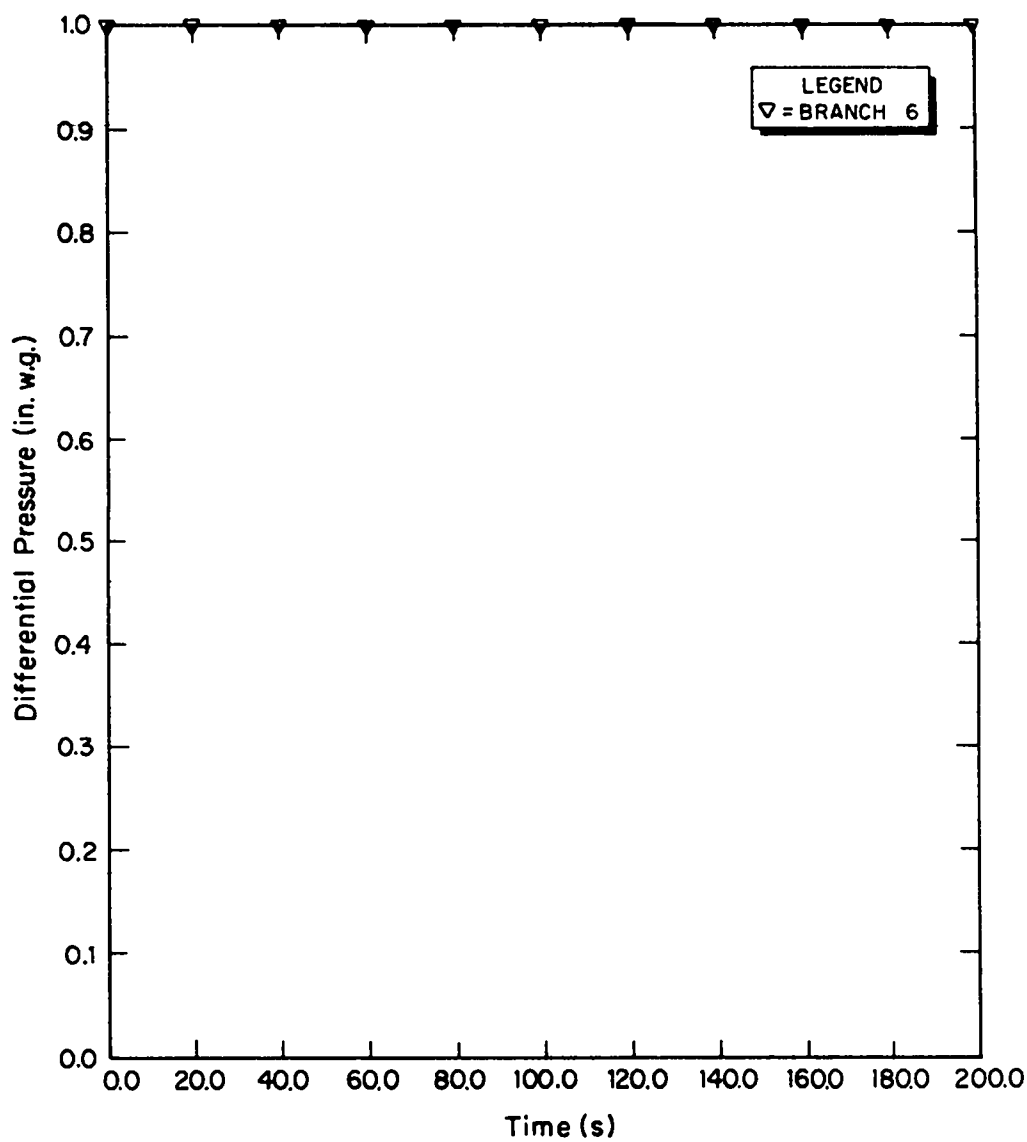


Fig. 44.  
Material transport (no filter plugging).

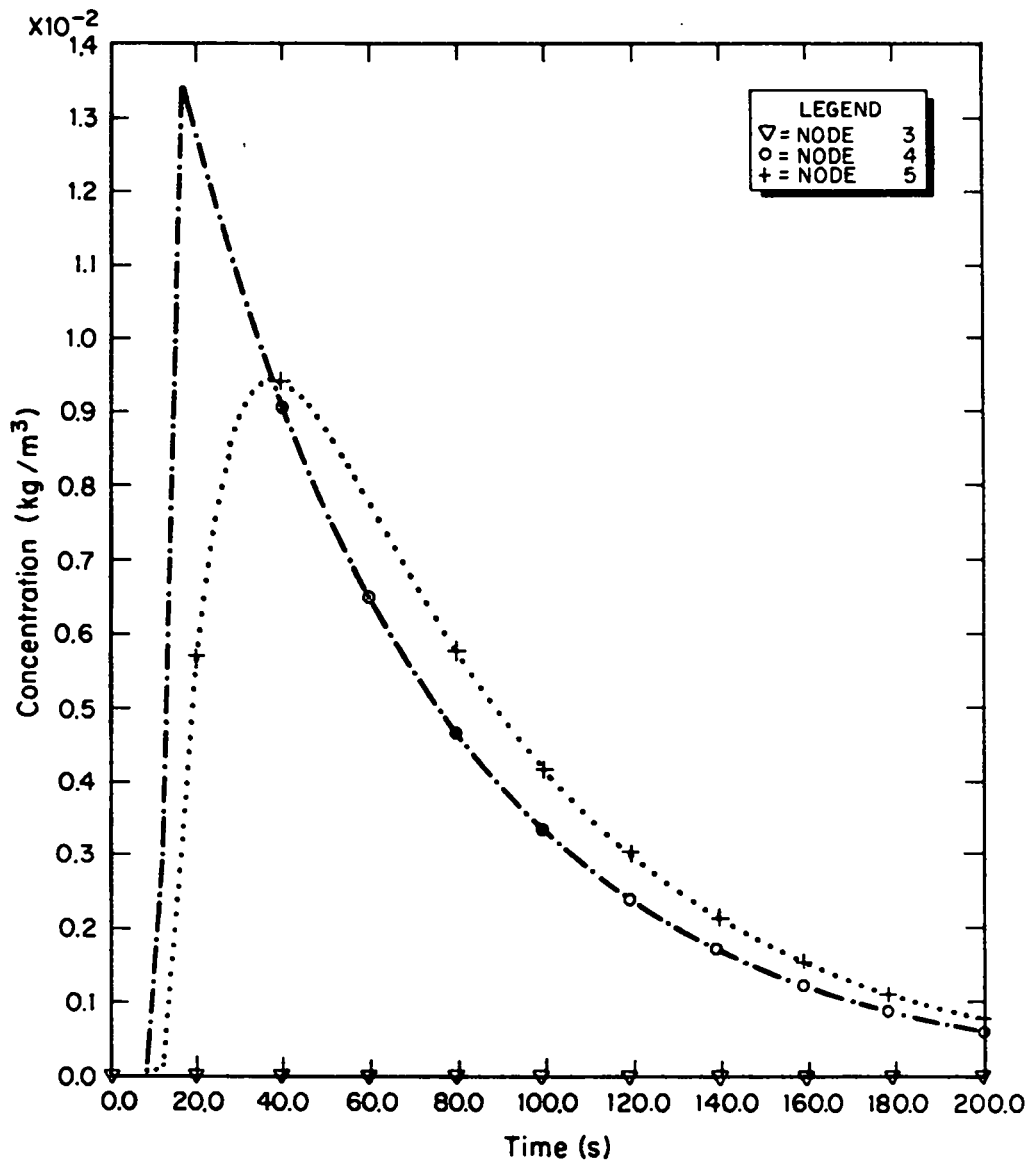


Fig. 45.  
Material transport (no filter plugging).

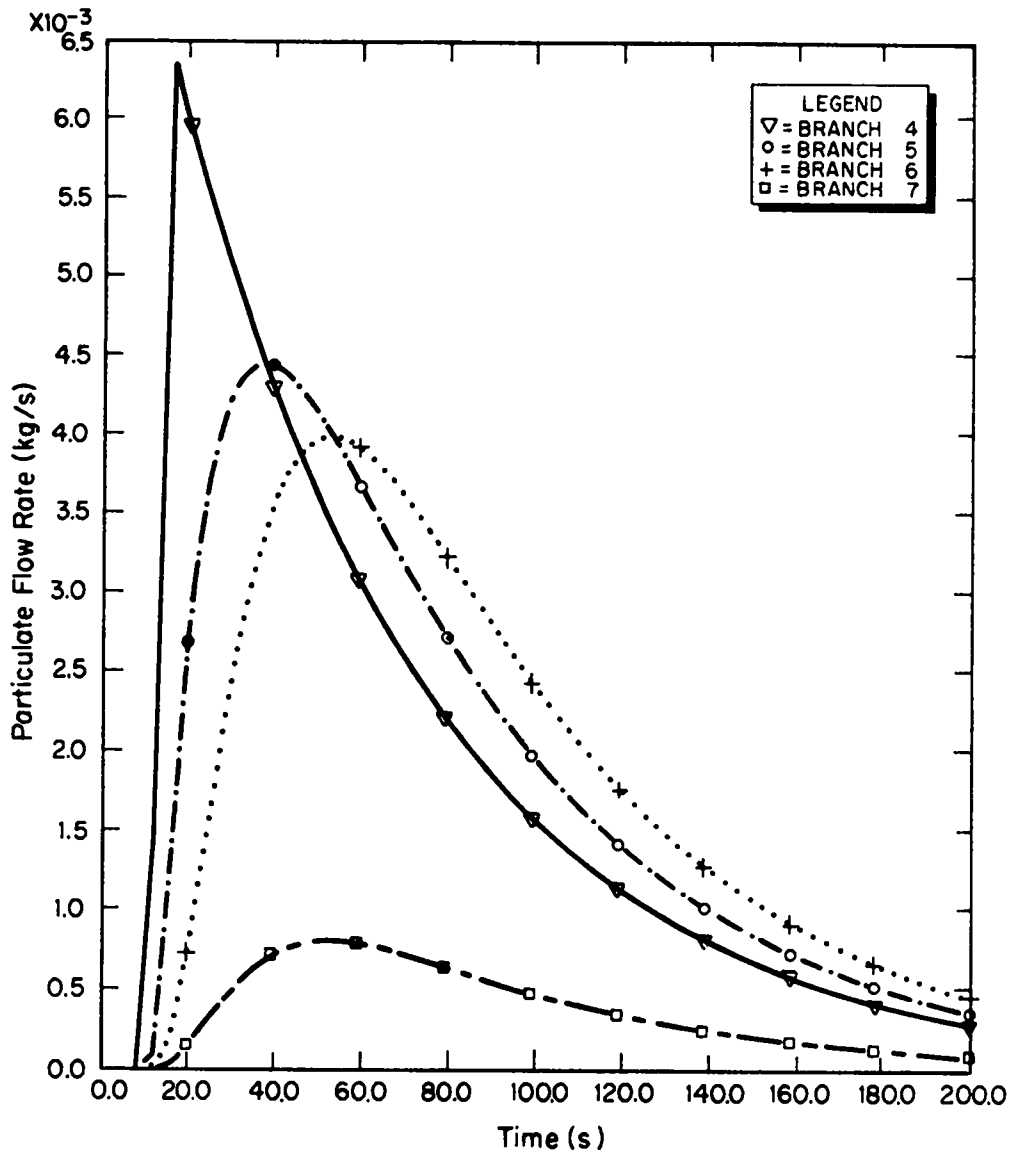


Fig. 46.  
Material transport (no filter plugging).



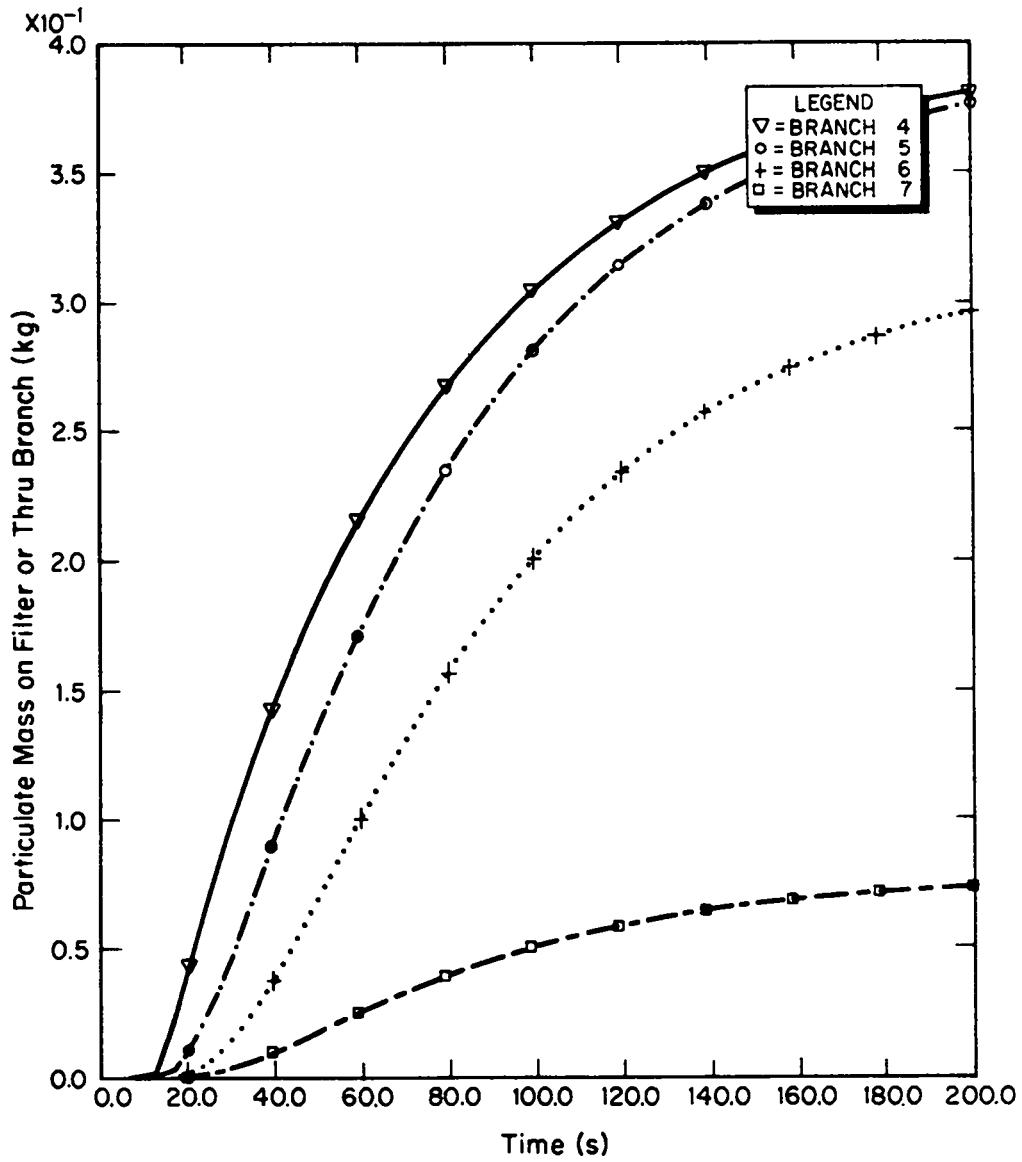


Fig. 47.  
Material transport (no filter plugging).

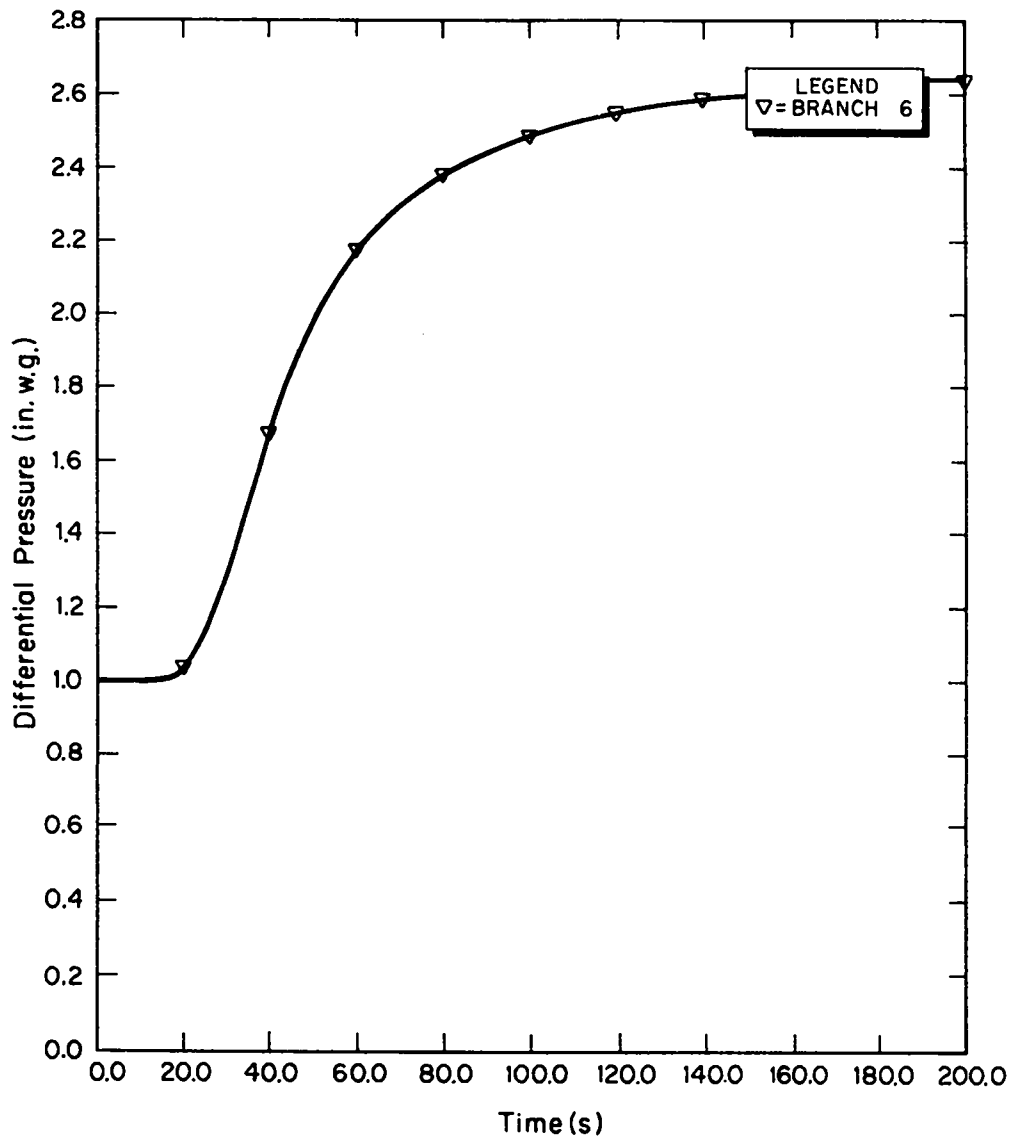


Fig. 48.  
Material transport (filter plugging).

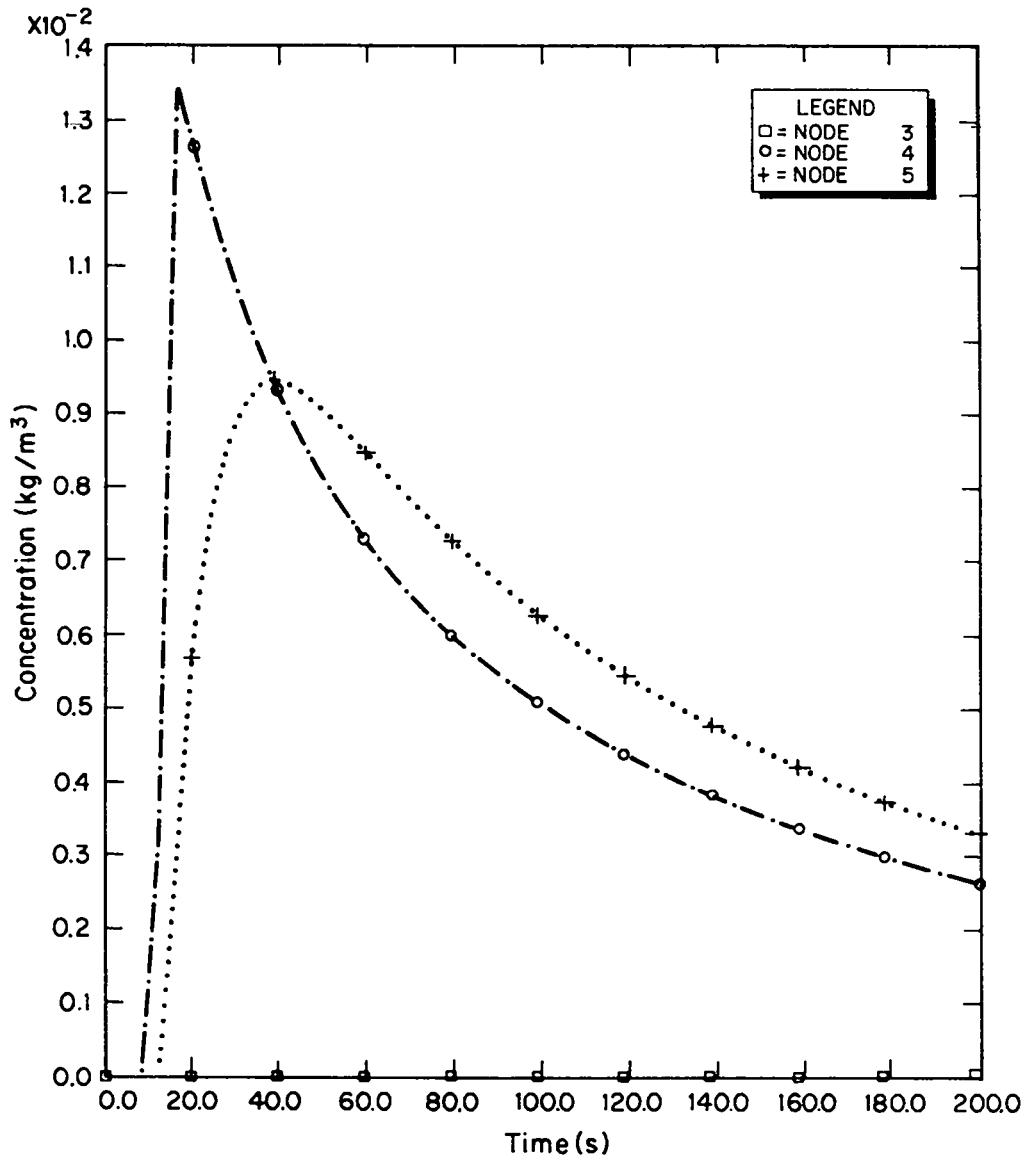


Fig. 49.  
Material transport (filter plugging).

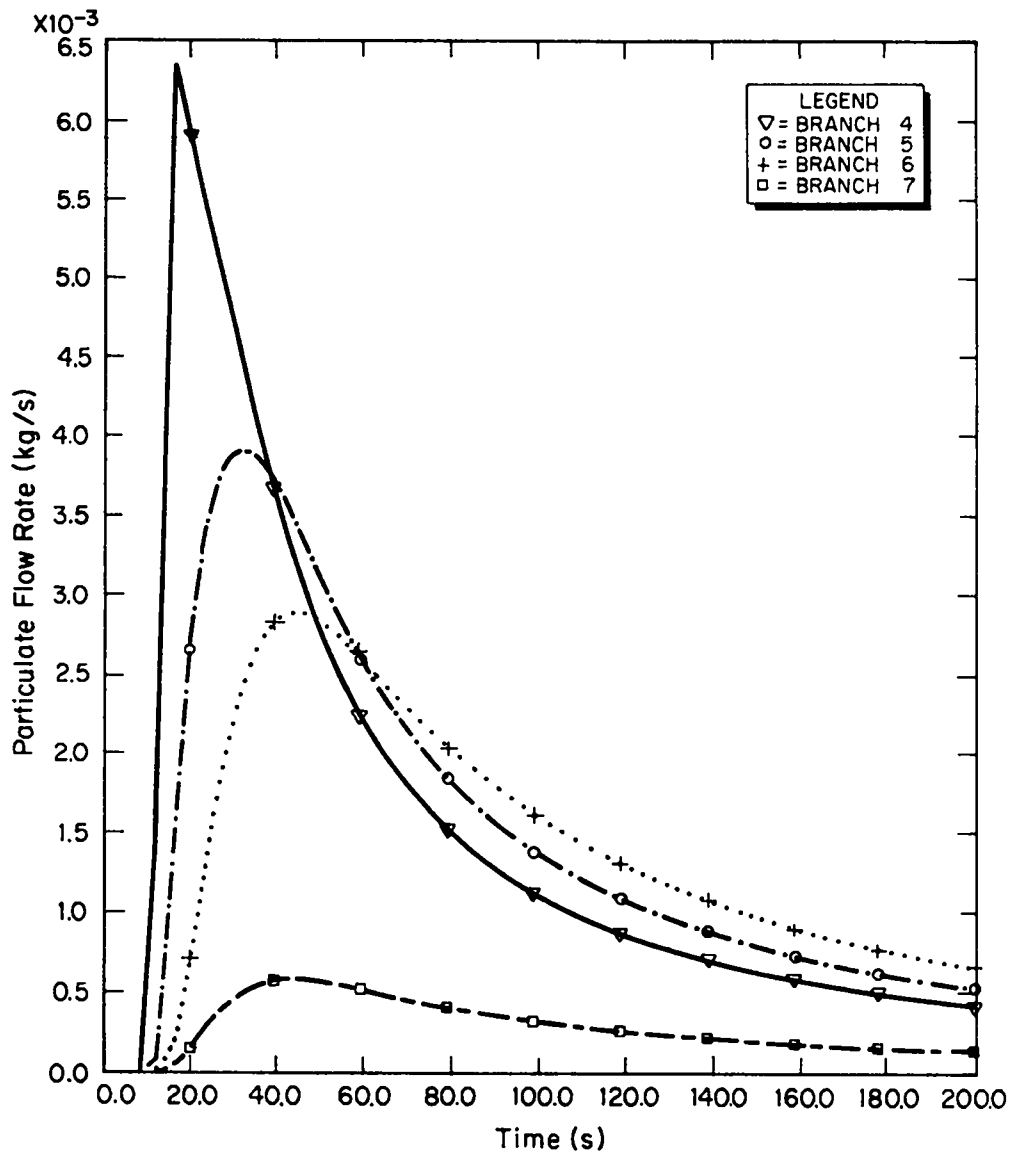


Fig. 50.  
Material transport (filter plugging).

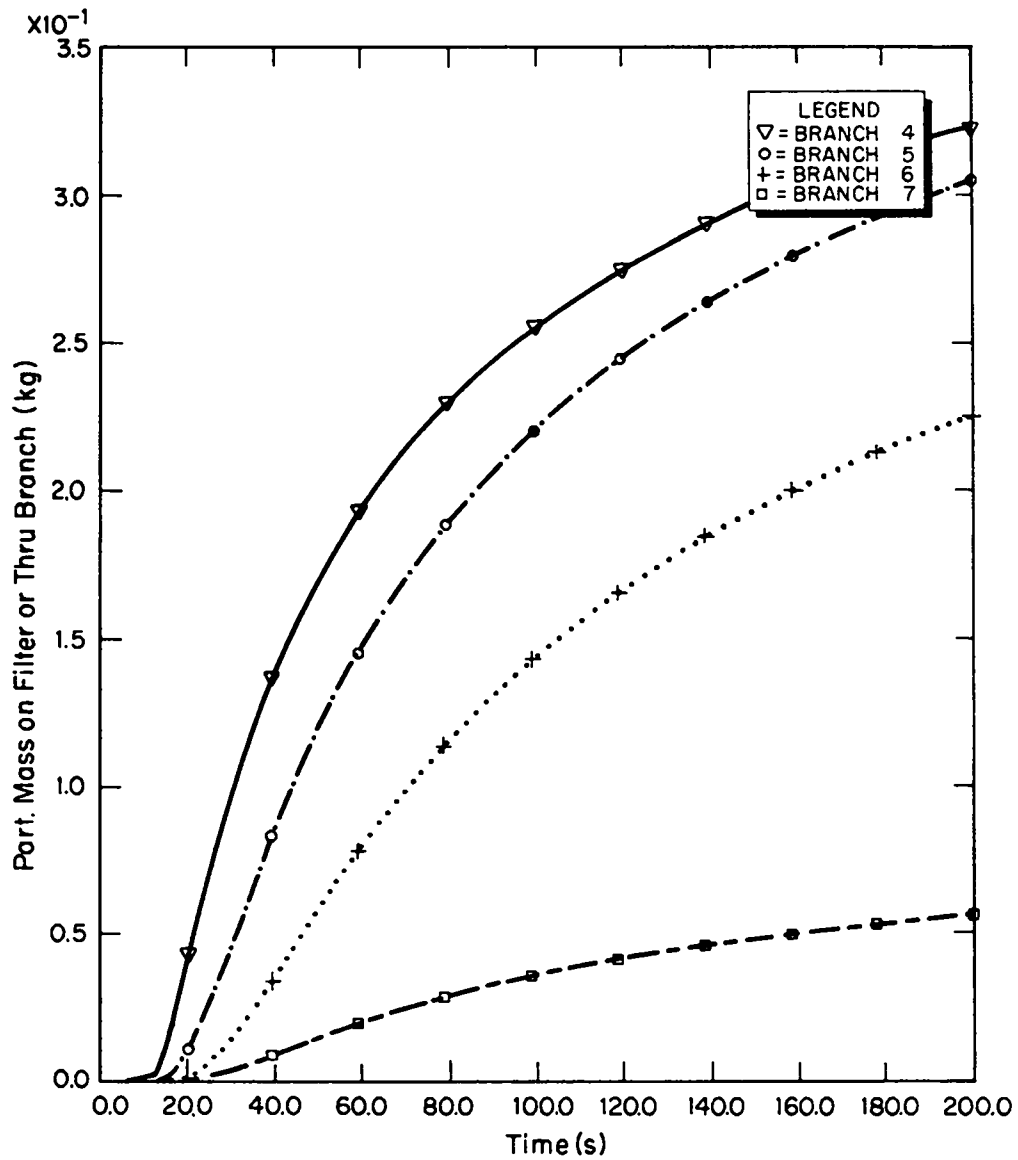


Fig. 51.  
Material transport (filter plugging).

Our choice of material and surface loading for this example were somewhat arbitrary. Specific values are presented for illustrative purposes only. Based on data referenced in Appendix B Sec. IV, for mixed-oxide fuel  $\text{PuO}_2$  powder size, a more realistic choice may be mass median aerodynamic diameter equals  $20 \mu\text{m}$  and density equals  $10 \text{ g/cm}^3$  ( $0.36 \text{ lb/in.}^3$ ). The theoretical density of  $\text{PuO}_2$  is about  $11.5 \text{ g/cm}^3$  ( $0.42 \text{ lb/in.}^3$ ). The values used here may be representative of a more agglomerated material. The material loading of  $27 \text{ g/m}^2$  ( $0.000038 \text{ lb/in.}^2$ ) (based on four surfaces) for duct volume 5 is about four times  $7 \text{ g/m}^2$  ( $0.00001 \text{ lb/in.}^2$ ), which is for a very dusty surface. The latter material loading value is reported in Ref. 13.

The tornado-induced nodal pressure time histories for this example are similar in shape to those shown in Figs. 18--20 except that they show more negative peaks in gauge pressure because the tornado is more severe in the current example. The peak negative gauge pressure for node 10 is  $-127 \text{ cm w.g.}$  ( $-50 \text{ in. w.g.}$ ) compared with  $-63.50 \text{ cm w.g.}$  ( $-25 \text{ in. w.g.}$ ) shown in Fig. 18.

The results of sample Problem 9 are shown in Figs. 52--55. The volume flow rates in four selected branches are shown in Fig. 52. These flows were induced by a tornado depressurization from 0 to  $-127 \text{ cm w.g.}$  (0 to  $-50 \text{ in. w.g.}$ ) between times 10 and 12 s, constant at  $-50 \text{ in. w.g.}$  from times 12 s to 16 s, and back up to  $0 \text{ cm w.g.}$  ( $0 \text{ in. w.g.}$ ) at time  $t = 18 \text{ s}$ . A flow reversal occurs in branches 4, 5, and 8 at about  $t = 18 \text{ s}$ . The material concentration time histories for four selected nodes are shown in Fig. 53. Aerodynamic entrainment of powder with  $D_p = 100 \mu\text{m}$  and  $\rho_p = 3 \text{ g/cm}^3$  ( $0.11 \text{ lb/in.}^3$ ) from thick beds may be expected for surface friction velocities exceeding a threshold value of about  $u_{*t} = 21.7 \text{ cm/s}$  ( $42.7 \text{ ft/min}$ ). This corresponds to an air velocity of about  $U = 374 \text{ cm/s}$  ( $12.3 \text{ ft/s}$ ) and an airflow rate of about  $Q = 1.42 \text{ m}^3/\text{s}$  ( $3000 \text{ ft}^3/\text{min}$ ) through a duct with a cross section of  $0.37 \text{ m}^2$  ( $4 \text{ ft}^2$ ). In Fig. 52 for branch 4,  $Q = 1.42 \text{ m}^3/\text{s}$  ( $3000 \text{ ft}^3/\text{min}$ ) is induced by the tornado at about  $t = 12 \text{ s}$ . At about this time the aerosol concentration at node 5 jumps as a spike to over  $0.16 \text{ kg/m}^3$  ( $0.01 \text{ lb/F}^3$ ) in Fig. 53. If 1 kg of material were injected instantly into the  $5.66\text{-m}^3$  ( $200\text{-ft}^3$ ) volume of the duct segment represented by node 5, we would expect an instantaneous spike in concentration to  $0.18 \text{ kg/m}^3$  ( $0.011 \text{ lb/ft}^3$ ). The airborne material is convected into node 6 and partially collected on the 80 filter in branch 6. Particulate flow rate is presented in Fig. 54. Figure 55 gives the cumulative particulate mass on a filter or through each branch. The

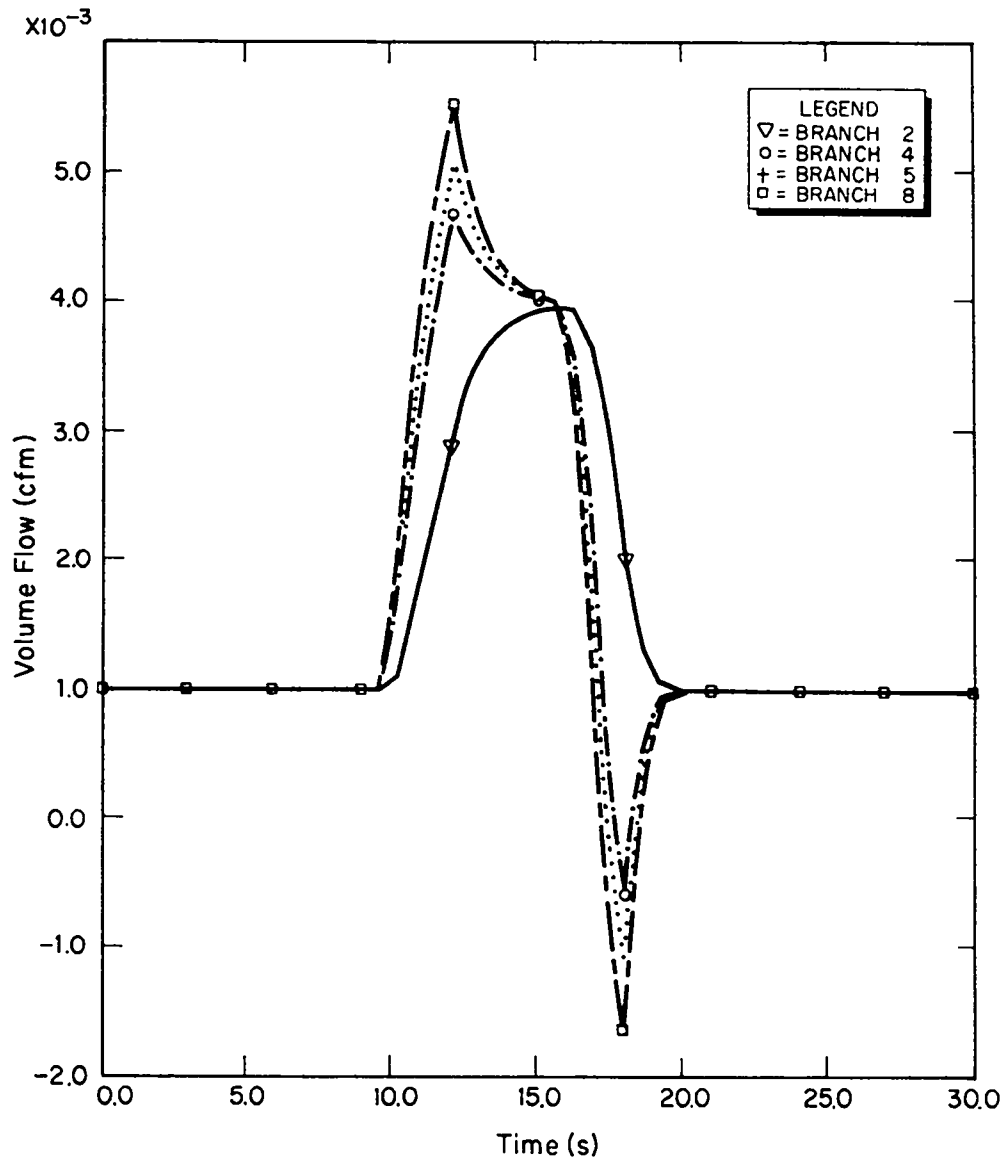


Fig. 52.  
Entrainment T(50) D(100).

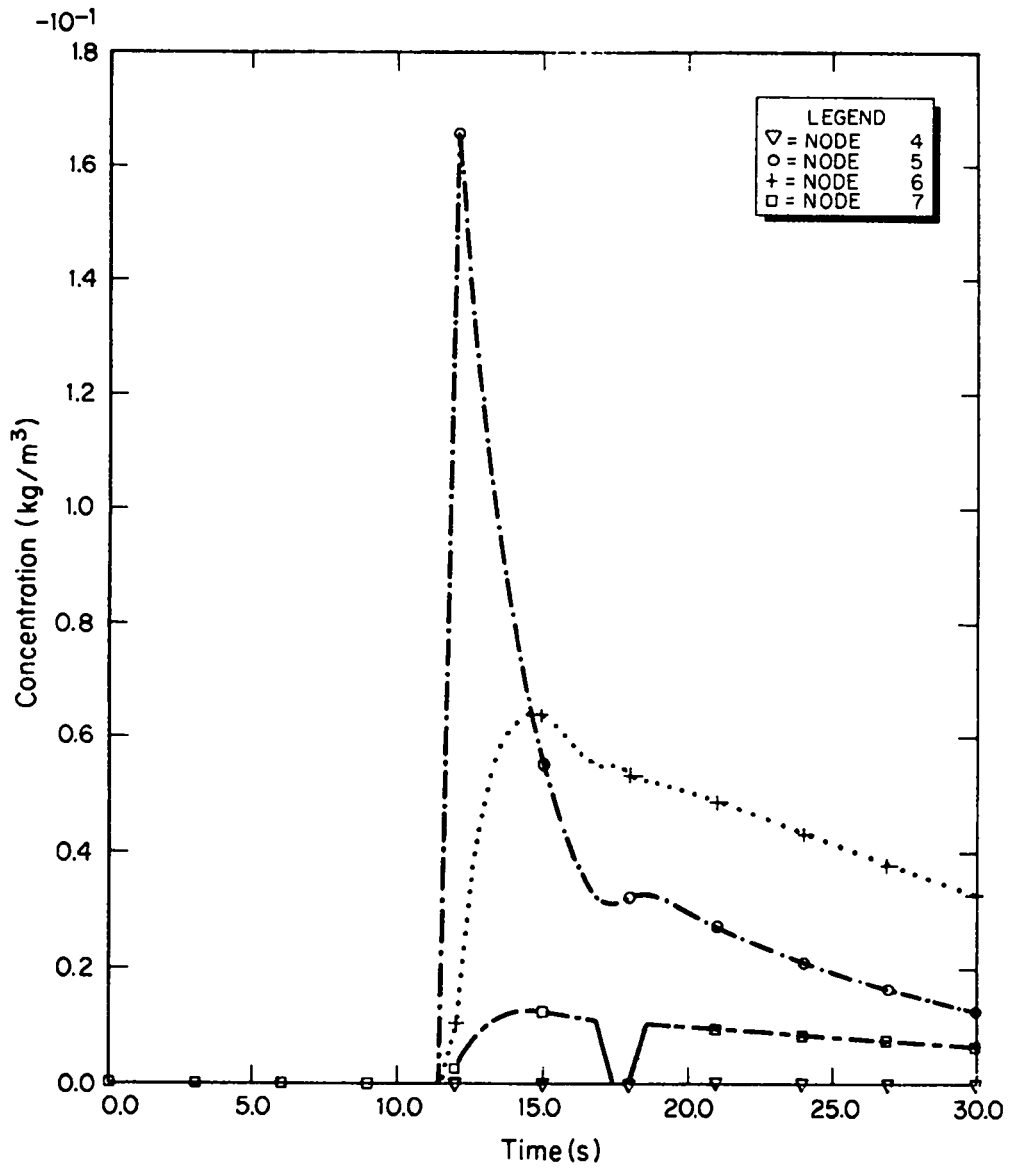


Fig. 53.  
Entrainment T(50) D(100).



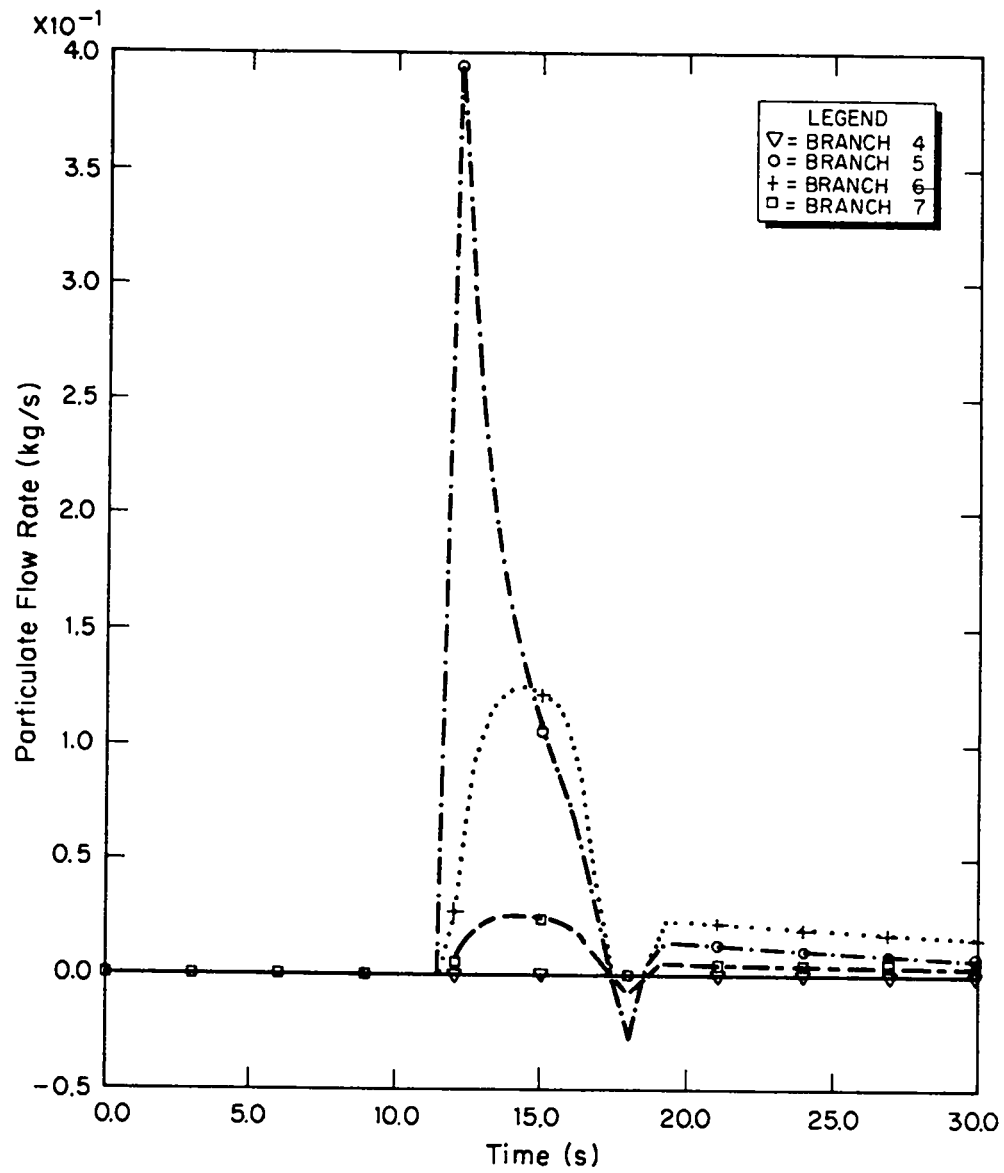


Fig. 54.  
Entrainment T(50) (D100).

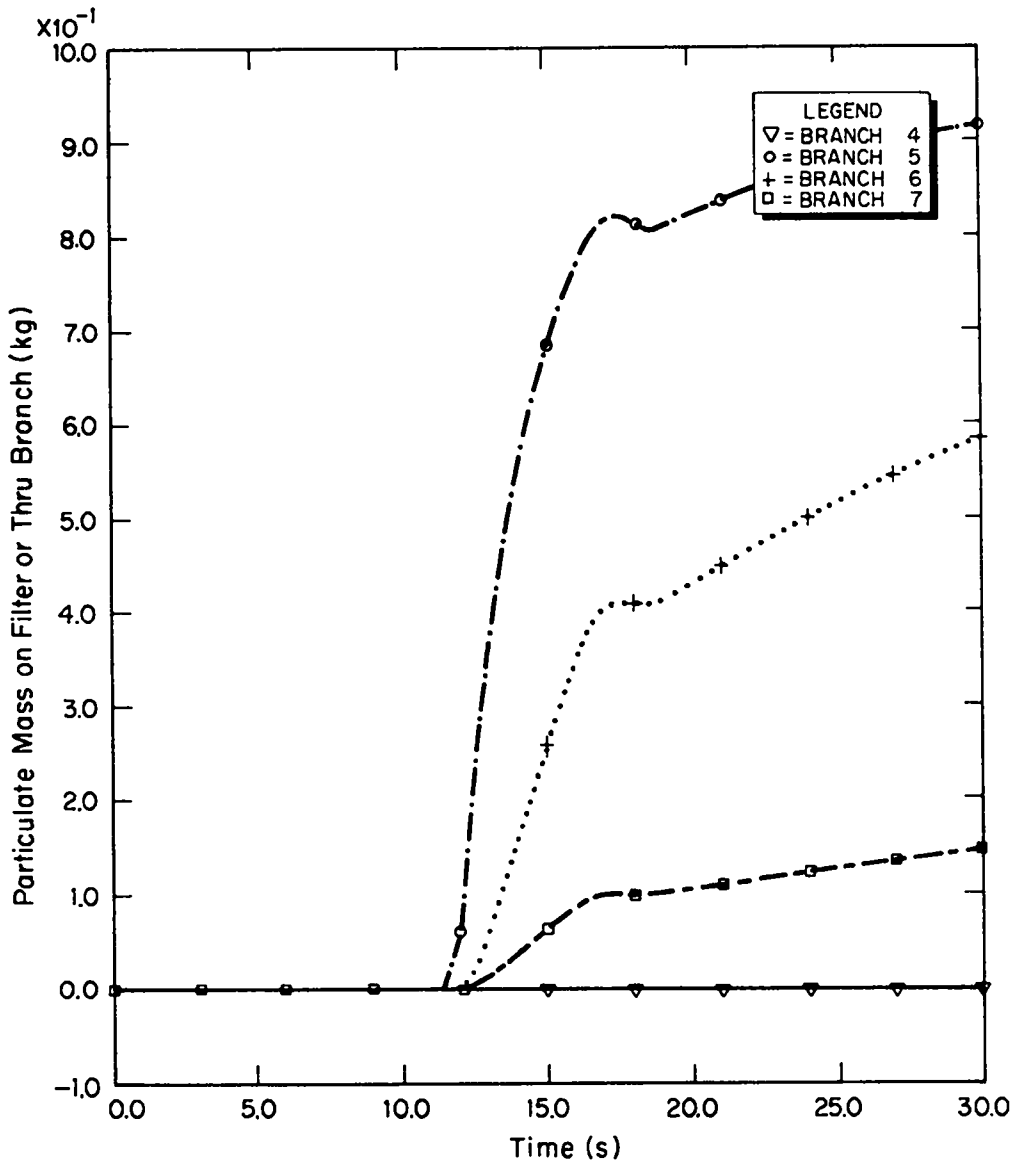


Fig. 55.  
Entrainment T(50) D(100).

curves in Fig. 55 represent the integral of their counterparts in Fig. 54. At  $t = 30$  s in this example, Fig. 55 shows that about 0.92(2.03 lb) kg of material was removed from node 5 with about 0.15 kg (0.33 lb) surviving the filter. The net reduction in concentration ahead of the filter observed here is caused by dilution and time delay only as deposition was turned off. That is, before material can flow through branch 6 (filter), the concentration in node 6 (duct volume) must be built up by material flow in branch 5 following entrainment in node 5. We observe that deposition by sedimentation was turned off in this example for simplicity and clarity but could have been turned on simultaneously with entrainment. Problem 10 shows that this  $100\text{-}\mu\text{m}$ ,  $3\text{-g/cm}^3$  ( $0.11\text{ lb/in.}^3$ ) material would have been substantially removed from suspension if deposition had been turned on.

#### Problem 10 - Aerosol Depletion

This problem illustrates TORAC's capability to account for aerosol depletion by gravitational sedimentation. The user requirements and theory for this subroutine are discussed in Sec. III.D.5. and in Appendix B, Sec. VI, below. As before, our model is shown schematically in Figs. 15 and 16. In this version of TORAC, aerosol depletion is handled in the same way for ducts and rooms. The following conditions were assumed and set up in the TORAC master input file. (See Fig. 17.)

1. Tornado of strength 127 cm w.g. (50 in. w.g.) applied at exhaust node 10.
2. From times  $t = 10$  s to 16 s, a total of 0.4 kg (0.88 lb) of aerosol is injected into the  $28.32\text{-m}^3$  ( $1000\text{-ft}^3$ )-volume room represented by node 4.
3. No material subject to entrainment anywhere.
4. The contaminant material is assumed to be composed of homogeneous, monodisperse, spherical particles with aerodynamic diameter  $D_p = 10\ \mu\text{m}$  ( $10^{-5}\text{m}$ ) and bulk density  $\rho_p = 3\ \text{g/cm}^3$  ( $0.11\ \text{lb/in}^3$ ).
5. As the contaminant material is injected, it instantly forms a homogeneous mixture with the air in room 4.
6. Deposition by sedimentation occurs in the duct lengths represented by volumes at nodes 5 and 6 only (but was not turned on for room 4).
7. The filter efficiency was set at 0.8.

In this example we illustrate the alternate user input option for material transport initiation as opposed to the other option, calculated aerodynamic entrainment, which was illustrated in Problem 9. Material is injected at node 4 to simulate accident conditions there. Deposition occurs in the two downstream duct segments. The choice of material characteristics for this example is strictly hypothetical and different from that discussed for Problem 9. (See example Problem 9 above.) The same tornado pressure function described in Problem 9 was used here. However, the material generation function goes from 0 kg/s (0 lb/min) at time  $t = 10$  s to 0.1 kg/s (13.2 lb/min) at  $t = 12$  s, stays constant until  $t = 14$  s, and returns to 0 kg/s (0 lb/min) at  $t = 16$  s. (See Fig. 17.)

The results of sample Problem 10 are shown in Fig. 52 and Figs. 56—60. That is, the tornado-induced flow time histories are identical to those discussed for Problem 9. The material concentration histories for four selected nodes are shown in Fig. 56. The aerosol concentration in room 4 begins to rise immediately at  $t = 10$  s because that is when material injection begins. As the  $28.32\text{-m}^3$  ( $1000\text{-ft}^3$ ) room 4 receives aerosol, the concentration goes up to a peak at  $t = 16$  s. Meanwhile, there is a delay while particulate-laden air drawn out of room 4 flows into duct volume 5. A dip in the concentration profiles at about  $t = 10$  s was caused by the flow reversal. Figure 57 also shows this momentary flow reversal in particulate flow rate. In Fig. 58 the material accumulations on the filter (branch 7) and passing through branches 4--6 are shown. Although 0.4 kg (0.88 lb) of aerosol is injected into room 4 during  $10 \leq t \leq 16$  s, the accumulated aerosol mass flow passing through branch 4 at  $t = 30$  s is only about 0.143 kg (0.32 lb). This is because fresh air from branch 3 is diluting the mixture in room 4 continually. By  $t = 120$  s, the accumulation of mass through branch 4 is about 0.34 kg (0.75 lb), and the concentration in node 4 is down to about  $0.0012\text{ kg/m}^3$  ( $0.000075\text{ lb/ft}^3$ ) (not shown in Fig. 58). The effect of deposition can be observed by comparing Fig. 58 with Figs. 59 and 60. Figure 59 was run for the same conditions as Figs. 56—58 except that deposition in branches 5 and 6 was shut off. Notice that the reduction in accumulation of  $10\text{ }\mu\text{m}$  material in branches 5—7 in Fig. 58 from Fig. 59 is relatively small. However, material losses resulting from sedimentation in these branches are more pronounced in Fig. 60. Figure 60 was run for the same conditions as Figs. 56—58 except that the material size used was  $100\text{ }\mu\text{m}$  instead of  $10\text{ }\mu\text{m}$ .

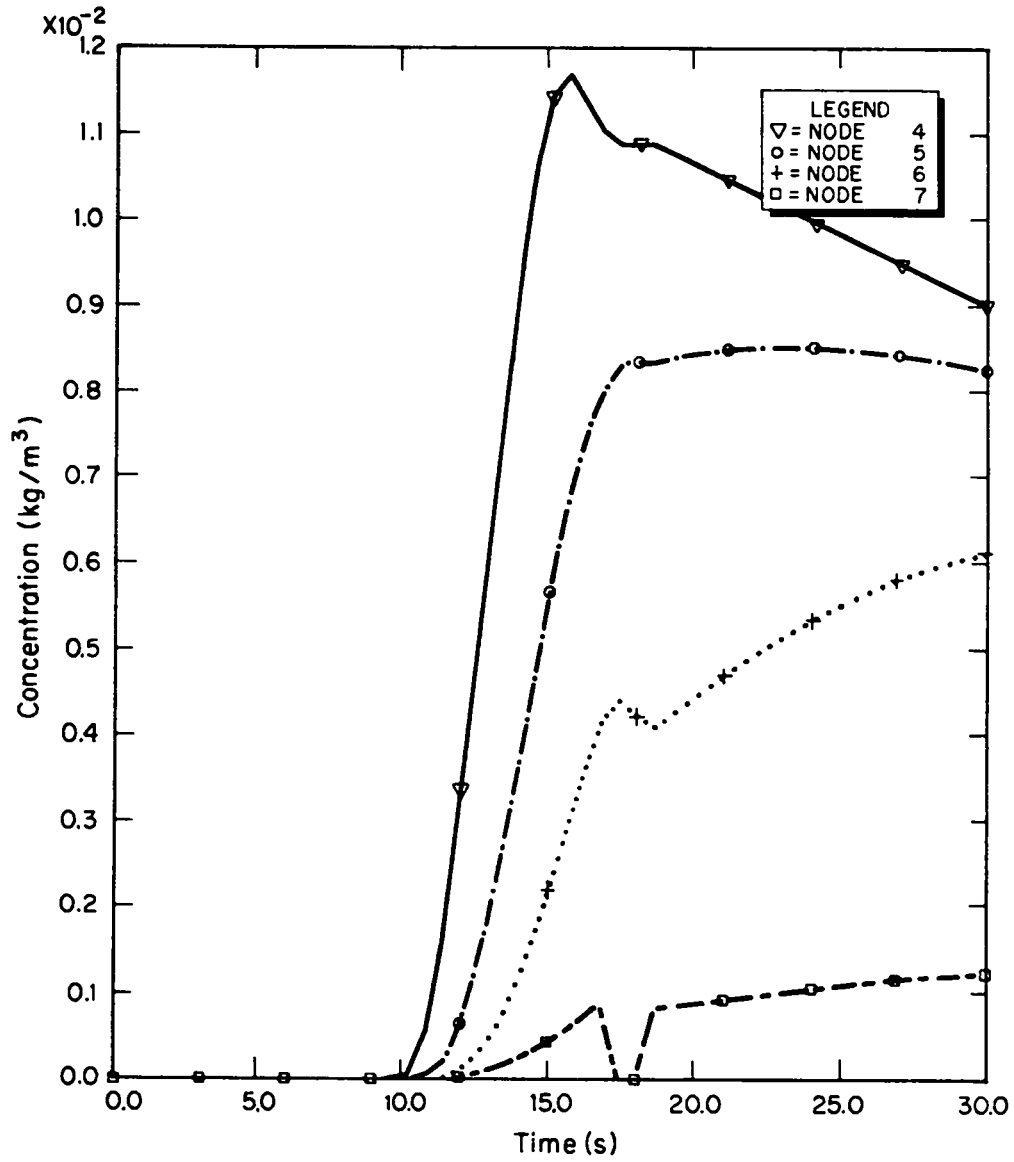


Fig. 56.  
Deposition T(50) D(10).

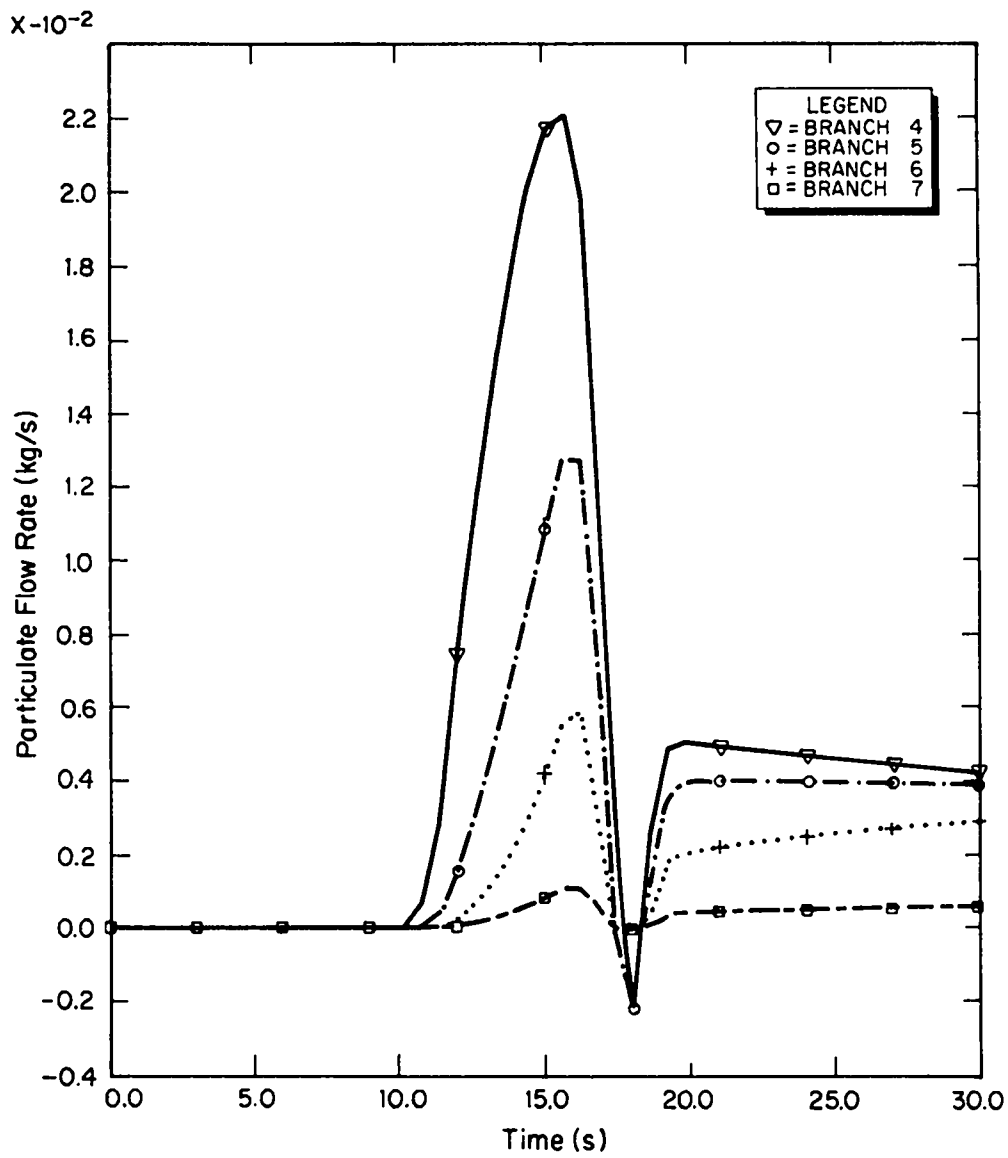


Fig. 57.  
Deposition T(50) D(10).

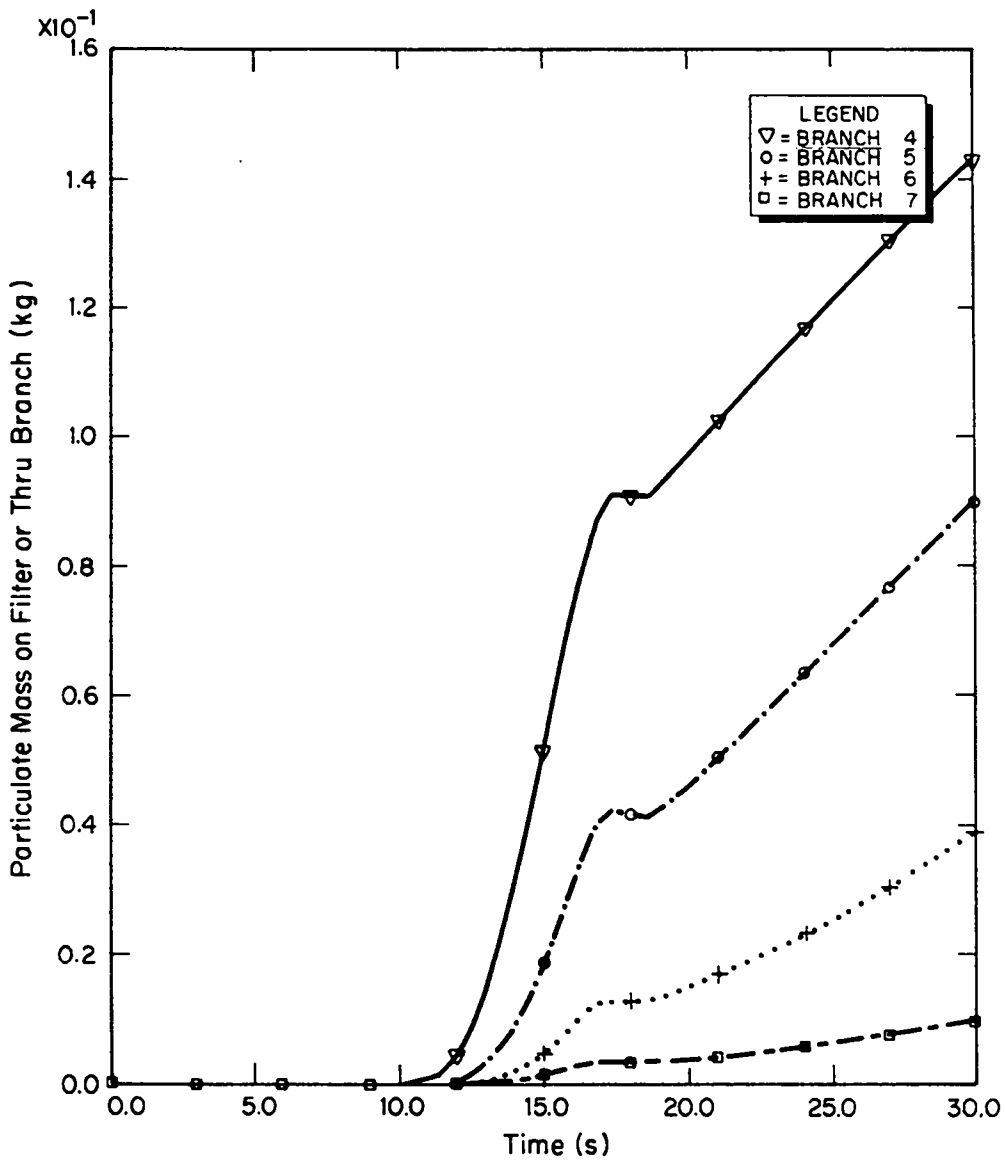


Fig. 58.  
Deposition T(50) D(10).

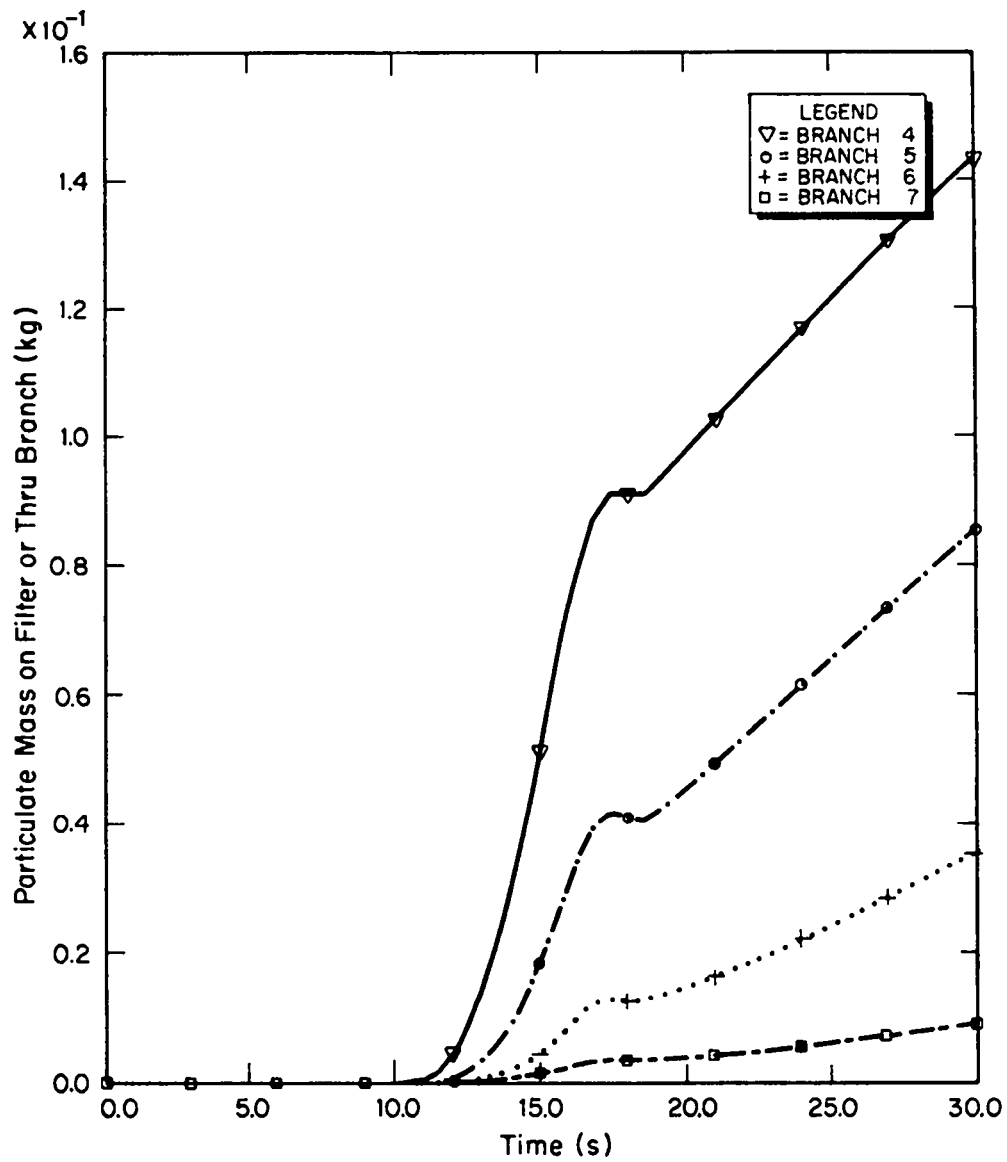


Fig. 59.  
Injection, no deposition T(50).



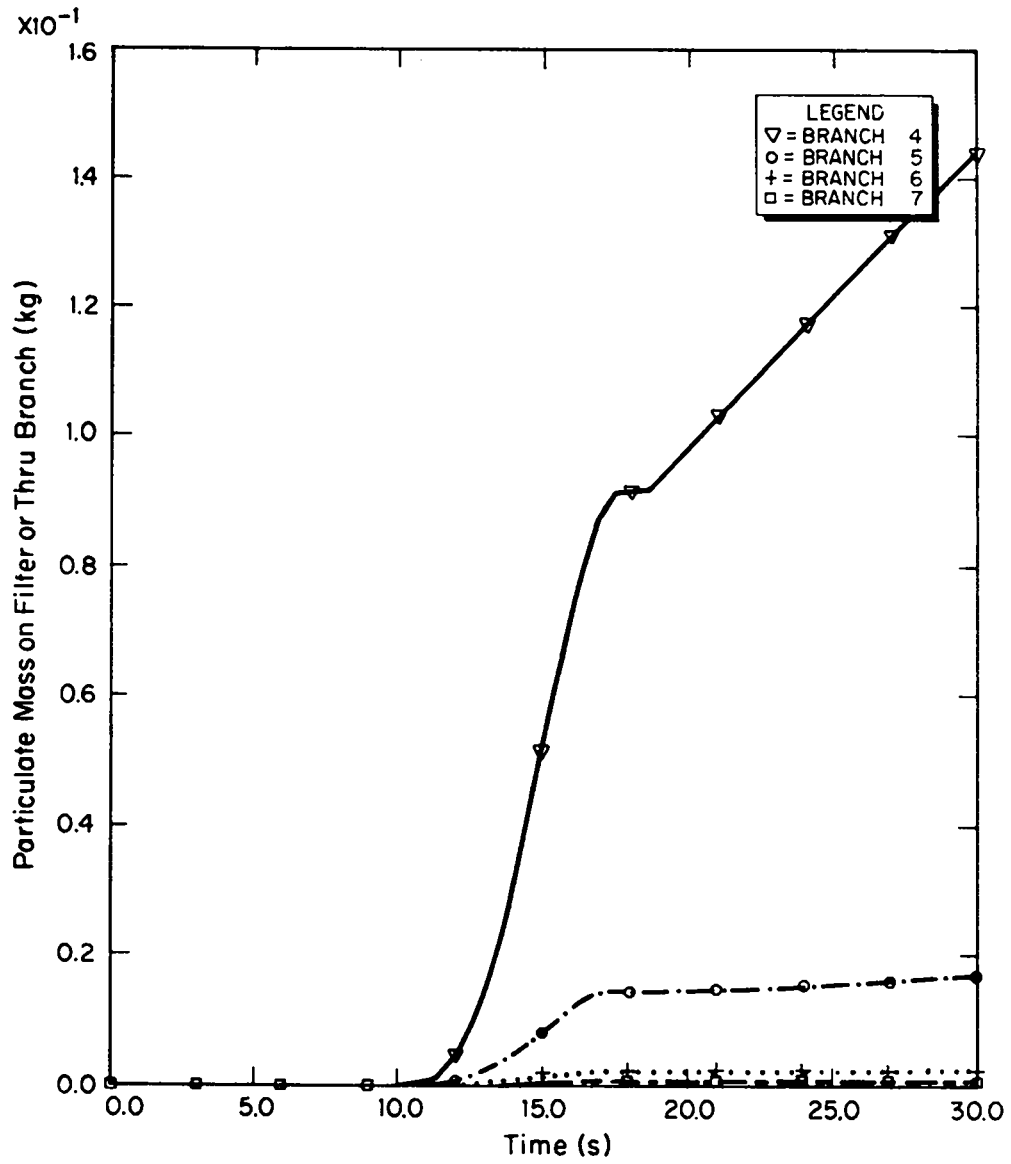


Fig. 60.  
Deposition T(50) D(100).

## APPENDIX A

### GAS DYNAMICS SUMMARY

This is a very brief summary of the gas dynamics used in the TORAC computer code. The formulation of the equations is the same as that used in the TVENT code<sup>1</sup>, and the reader should see Ref. 1 for a more detailed discussion of the theoretical and numerical formulation of the working equations.

The lumped-parameter method is the basic formulation in TVENT and TORAC that describes a ventilation system or any other air pathway. No spatial distribution of parameters is considered in this approach, but an effect of spatial distribution can be approximated. Using the lumped-parameter method, network theory includes a number of system elements, called branches, joined at certain points, called nodes. Ventilation system components that exhibit resistance, such as dampers, filters, and blowers, are located within the branches of the system. The ductwork of a ventilation system is considered a resistive element because of frictional resistance to fluid flow.

The connection points (nodes) of the system elements or branches are at the upstream and downstream ends of the branches. Components that have larger volumes, such as rooms, gloveboxes, and plenums, are located at nodal points. Therefore, a node may possess some volume or capacitance where fluid storage or compressibility may be taken into account.

The governing equations in TORAC require that the continuity equation be satisfied at every node and that a pressure-flow equation be satisfied for each element or branch. Variations in the node equations depend on whether the node represents a finite volume; the equation of state for a perfect gas must be satisfied. This variation also exists for the branches, depending on whether the branch is simply a duct or contains a filter, blower, or damper.

The relationship between pressure and flow for the elements is nonlinear and is written in the general form

$$Q_k = \beta_k (p_i - p_j)^N \quad . \quad (A-1)$$

The volumetric flow rate into branch  $k$  is represented by  $Q_k$ , the conductance by  $\beta_k$ , the pressures at the ends of the branch by  $p_i$  and  $p_j$ , and an arbitrary exponent by  $N$ . This numerical scheme uses a perturbation technique coupled with a Taylor series expansion of Eq. (A-1). For a small perturbation ( $\Delta p$ ), the correct value for pressure  $p_j$  is

$$p_j = \tilde{p}_j + \Delta \tilde{p} \quad , \quad (A-2)$$

where the sign  $\sim$  indicates a temporary value. Substituting Eq. (A-2) in Eq. (A-1) gives

$$Q_k = \beta_k (p_i - p_j - \Delta p)^N \quad . \quad (A-3)$$

Using a Taylor series expansion, Eq. (A-3) gives a linear relationship between flow and pressure as

$$Q_k = \bar{A}_k - \tilde{C}_k \Delta p \quad , \quad (A-4)$$

where  $\bar{A}_k$  and  $\tilde{C}_k$  are temporary iterative values based on previous values of pressure. The flow-pressure relationships in the branches for the ducts, dampers, filters, and blowers all can be formulated as Eq. (A-4). All flows must satisfy the continuity equation at the nodal points. Summing all flows at a nodal point allows us to solve for the perturbation pressure  $\Delta p$ . The numerical process then iterates through a set of equations for  $\Delta p$  until that value is very small. We then say that the numerical process has converged and all the governing equations are satisfied. This numerical scheme is a fully implicit iterative process.

Material transport is uncoupled from the gas dynamics and is discussed in Appendix B. After the flows are determined, the material is transported accordingly. However, we note that it may be desirable to represent a network duct as a room or series of rooms with a small, finite volume. The resistive nature of the duct is preserved through its connection to other rooms. The logic in this approach is related to the source and sink (deposition and entrainment) of material and is discussed in greater detail in Appendix B.

Summarizing, an implicit numerical scheme is used to solve for the pressure correction at each node. The iterative process continues until the pressure correction ( $\Delta p$ ) approaches zero and the system is balanced. The numerical scheme is altered slightly by using the equation of state for a node that represents a volume or some capacitance. Our approach in including material transport is to use the flow conditions determined by the gas dynamics to transport the material.

## APPENDIX B

### MATERIAL TRANSPORT THEORY

#### I. INTRODUCTION

The material transport algorithms in TORAC provide an estimate of the aerosol or gas transport within a nuclear fuel cycle facility. Ultimately, we would like to predict the quantity and physical and chemical characteristics of hazardous material that may be released from the facility as a result of tornado-induced depressurization. The transport can take place through rooms, cells, canyons, corridors, gloveboxes, and ductwork installed in the facility. In many cases, the entire flow pathway forms a complex, interconnected network system. Using TORAC, we can calculate material concentrations and material mass flow rates at any location in the network, including the supply and exhaust of the network system. Most importantly, the code will perform the transport calculations as a function of time for arbitrary user-specified pressure transients imposed on the facility boundaries. There is no need to assume steady flow as required in some material transport codes, but TORAC can be used to determine material transport under steady flow conditions if desired.

In Ref. 7, the material transport estimate is obtained in piecemeal fashion using steady flow calculations for rooms and duct segments. TORAC solves the entire network for transient flow and in doing so takes into account system interactions.

A generalized treatment of material transport under tornado-induced accident conditions could become very complex.<sup>2--4,8--11</sup> Several different types of materials could be transported. Also, more than one phase could be involved, including solids, liquids, and gases with phase transitions. Chemical reactions leading to the formation of new species could occur during transport. Further, there will be a size distribution function for each type of material that varies with time and position, depending on the relative importance of effects such as homogeneous nucleation, coagulation (material interaction), diffusion (both by Brownian motion and by turbulence), and gravitational sedimentation.<sup>2--4</sup> No currently existing computer code can handle transient flow-induced material transport in a network system subject to the possibility of all of these complications. The transport portion of TORAC also does not include this level of generality. This basic form of material transport consists of the following.

- Gas dynamics decoupled from material transport
- Homogeneous mixture and dynamic equilibrium
- Material transport limited to a single size and species
- No material interaction during transport
- Material deposition based on gravitational settling using relationships from the literature
- Turbulent and Brownian diffusion and phoretic effects are neglected
- Phase change, chemical reaction, and electrical migration not allowed
- Material entrainment can be specified arbitrarily using tabular inputs or calculated using semi-empirical relationships based on wind tunnel data

Although the material transport capability is limited in the TORAC code, this initial version does represent a significant advancement for the prediction of material movement within a nuclear facility. The code is structured in a modular fashion so that improved versions are easily incorporated. This concept is discussed in Sec. II and is followed by information on material characteristics that can be useful to the user. The following sections are detailed descriptions of the material transport modules within the code.

## II. MODULAR STRUCTURE

Movement of material by a flowing fluid involves several basic mechanisms. The primary mechanism for movement is the flow of the fluid itself; this process will carry along material and is referred to as convection. The other mechanisms involve physical models that could be upgraded as the state of the art improves. The basic mechanisms that we will consider in a tornado-induced flow environment are listed below.

- Transport initiation
- Convective transport
- Transport depletion
- Transport interaction

The material transport option in TORAC uses all of the basic mechanisms except transport interaction. In addition, the transport depletion module is restricted to gravitational settling and filtration. The detailed discussion of these mechanisms will be reserved for later sections because we wish to introduce the concept of analysis levels and the modular structure of the computer code.

The material transport capability in TORAC is composed of separate subroutines or modules that can be added or removed without disturbing other parts of the computer code (Fig. 61). The purpose of this structure is to allow us to begin with a basic material transport capability using modules that are based on relationships found in the literature. From this initial analysis level we will improve each module such that a higher analysis capability can be achieved. When they are complete, we will interchange an old module with a new one without disturbing the rest of the code.

### III. MATERIAL CHARACTERISTICS

In applying the material transport capability in TORAC, the user must identify the type (aerosol or gas), quantity, and location of material at risk. If the material is a solid or liquid aerosol, a characteristic size and density must be specified. In the simplest case, these parameters may be assumed. For example, if the user is concerned primarily with the transport of aerosols in the size range of  $D_p \leq 12 \mu\text{m}$  and densities of  $0.5 \leq \rho_p \leq 12 \text{ g/cm}^3$ , he could run TORAC for some assumed cases of  $(D_p, \rho_p)$  to determine entrainment or deposition sensitivity.

In general, the user may wish to characterize a nonideal aerosol contaminant with approximate or idealized values of  $(D_p, \rho_p)$ . Here we advise caution because there are many different ways to characterize the diameter of aerosols having an irregular shape and nonuniform density. For example, diameters representing a mean value relative to total count, surface area, volume, weight, or terminal settling velocity may be estimated based on the frequency of occurrence data.<sup>2--4,12</sup>

For the case of aerosol transport along fuel cycle facility pathways, we are interested in changes in aerosol concentration resulting from entrainment, dilution, deposition, and filtration. Entrainment, deposition, and filtration all depend on the quasi-steady aerodynamic drag characteristics of the aerosol.<sup>2--4</sup> Unless the aerosol is very small (less than  $0.5 \mu\text{m}$ ), the probability that a spherical particle or droplet will deposit depends on the magnitude of its terminal settling velocity,  $u_s$ .<sup>3</sup>

$$u_s = \rho_p D_p^2 C_g / 18\mu \quad , \quad (\text{B-1})$$

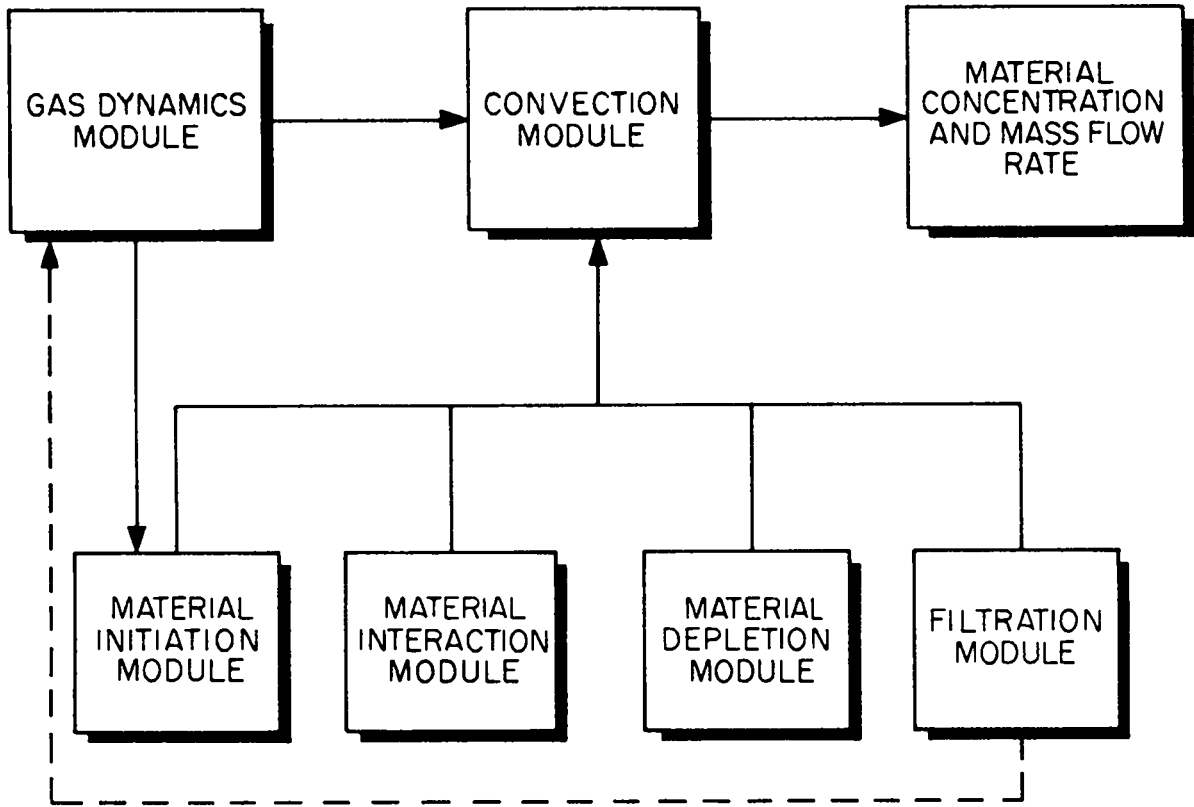


Fig. 61.  
Material transport modular structure.



where  $\rho_p$  = actual density,  
 $D_p$  = diameter,  
 $C$  = Cunningham slip factor,  
 $g$  = gravitational acceleration, and  
 $\mu$  = air dynamic viscosity.

Most aerosols--spherical or not--having the same settling velocity will be distributed throughout a ventilation system network in a similar manner. The recommended deposition parameter is aerodynamic diameter or Stokes diameter.<sup>3</sup>

- (1) Aerodynamic diameter  $D_a$  is the diameter of a sphere of unit density having the same terminal speed as the contaminant.
- (2) Stokes diameter  $D_s$  is the diameter of a sphere with the same bulk density and terminal speed as the contaminant.

These diameters are related by the equation

$$u_s = \rho_p D_s^2 C_s g / 18\mu = \rho_0 D_a^2 C_a g / 18\mu \quad , \quad (B-2)$$

where  $C_s$  and  $C_a$  are the slip factors associated with  $D_s$  and  $D_a$ , respectively, and  $\rho_0$  is unit density. For the contaminant of interest,  $D_s$  or  $D_a$  may have been measured directly using such aerodynamic classification devices as impactors, centrifuges, sedimentometers, or air elutriators. These devices are suitable for measuring the size of irregularly shaped particles. An aerodynamic diameter measurement should be based on activity if possible. Otherwise, we recommend using  $D_a$  based on mass measurements.

If count frequency data, based for example on projected area diameter for irregularly shaped particles, are available for the contaminant, then they must be converted to aerodynamic diameter. Such data should be plotted on log-probability paper and fit with a straight line. If this straight-line fit to the data is acceptable, the size distribution is approximately log-normally distributed and may be described completely by two parameters, geometric count median diameter  $D_{gc}$  and geometric standard deviation  $\sigma_g$ . Most fine particle systems

formed by comminution of a bulk material or grown by accretion have log normal size distributions; therefore, this assumption is recommended.<sup>2--4,12</sup>

Thus, the user can obtain  $D_{gc}$  and  $\sigma_g$  from log-normally distributed count frequency data. The set of Hatch-Choate transformation equations now applies. These equations relate  $D_{gc}$  and  $\sigma_g$  to a number of other median and mean diameters that may be important depending on how the toxic substance or "activity" is related to the physical properties of the particle. For example, the activity may be proportional to the total number, total surface area, or total mass of the particles. We choose to work on a mass basis. The user may calculate the geometric mass median diameter  $D_{gm}$ , the volume mean diameter  $D_v$ , and the weight mean diameter  $D_w$  from<sup>12</sup>

$$\begin{aligned} \log D_{gm} &= \log D_{gc} + 6.908 \log^2 \sigma_g, \\ \log D_v &= \log D_{gc} + 3.454 \log^2 \sigma_g, \text{ and} \\ \log D_w &= \log D_{gc} + 8.023 \log^2 \sigma_g, \end{aligned} \quad (B-3)$$

where the logarithms are calculated using base 10. The median diameters  $D_{gc}$  and  $D_{gm}$  referred to above divide the count-based and mass-based size distributions in half. For example, half of the mass of the sample lies above  $D_{gm}$  and half below. A mean diameter is the diameter of a hypothetical particle that is intended to represent the total number of particles in the sample.

In the absence of specific information on the aerodynamic properties of the aerosol of interest, Stockham<sup>12</sup> recommends using  $D_w$  as an approximation to aerodynamic size. An alternative is to convert  $D_v$  to an aerodynamic diameter. (If we assume the material density to be uniform, independent of size, and known, then the mass of the particle with size  $D_v$  is a mean mass.) To do this, use<sup>3</sup>

$$D_a = \left[ \left( \frac{6}{\pi} \right) \left( \rho_p / \rho_o \right) \left( \alpha_3 / K_r \right) \right]^{1/2} D_v, \quad (B-4)$$

where  $\alpha_3$  = volume shape factor, and

$K_r$  = resistance shape factor.

Values of  $\alpha_3$  and  $K_r$  are given in the book by Mercer where this calculation is discussed.<sup>3</sup>

We also advise caution in estimating aerosol density. The aerosol produced by accident conditions may in fact consist of flocculi and agglomerates with actual densities well below the theoretical density of the pure parent materials. The floc densities may be as much as an order of magnitude less than the normal density.<sup>12</sup> The user can find pertinent information on fuel grade powder size and density in Refs. 13--27. Useful information on droplet sizes and densities can be found in Ref. 13.

#### IV. TRANSPORT INITIATION

TORAC gives the analyst two options for transport initiation: (1) user specification of mass injection rate vs time and (2) calculated aerodynamic entrainment. These options are quite different. They require different levels of effort and judgment from the analyst. In this section we will provide background to help the user supply numbers for source-term initiation using option (1), and we will describe in detail the procedure and equations used with option (2). The primary cause of initiation is assumed to be transient flow induced by a tornado. Two examples illustrating the use of option (1) will be discussed first.

As a first example, consider a decommissioned fuel reprocessing facility with contaminated enclosures. The analyst can estimate the preaccident aerosol concentrations in these areas using the resuspension factor concept.<sup>13,14,28-30</sup> The resuspension factor  $K$  was used extensively to quantify airborne contamination levels in operational fuel cycle facilities. By definition,

$$K = \frac{\text{aerosol concentration (g/m}^3\text{)}}{\text{surface loading (g/m}^2\text{)}} , 1/\text{m} .$$

Sutter<sup>14</sup> has tabulated ranges of K that were compiled from numerous references. Her tables include values of K derived from measurements of airborne contamination resulting from numerous and varied cases of exterior wind stresses and interior mechanical stresses. Sutter's summary tables are useful for obtaining bracketing or bounding values of K. With assumed or measured values of K and surface loading, the user can calculate the airborne material concentration subject to transport. Based on the enclosure volume, a quantity or mass of contaminant subject to transport can be calculated from the concentration. This mass then can be injected using the user-specified option at the system node representing the enclosure of interest. Mass injection rate must be specified by the analyst.

Healy<sup>28</sup> reviewed many measurements and applications of this simplistic resuspension factor concept. Several of its limitations are noteworthy. First, measured values of K range over 11 orders of magnitude. For benign conditions where K is most reliable, the uncertainty is at least 2 orders of magnitude. Further, K fails to account for particle, surface, or local flow characteristics except as they existed during a particular measurement. Therefore, we recommend using a resuspension factor only for estimating preaccident airborne mass subject to transport as suggested by this example.

As a second example, consider a mixed-oxide fuel fabrication facility in which bulk MOX powder is being protected. The user may elect to model this facility using TORAC and run the code for a tornado transient without material transport. This preliminary run would supply an estimate of system flow rates and pressure drops during the accident. Some controlled areas may be subjected to abnormally high air velocities that could lead to entrainment because of aerodynamic stress. A knowledge of the air velocity time history will be useful to estimate the quantity of material made airborne.

We will summarize briefly three methods that can be used to estimate aerodynamic entrainment of aerosol material. Sutter<sup>14</sup> has reviewed and compiled data from numerous papers under the heading "aerodynamic entrainment." (We recommend this paper as a good source of reference information.) The analyst's objective here should be to estimate a quantity of material made airborne during the first part of or during the entire tornado transient. This quantity then must be converted to a mass injection rate for input to TORAC as in the first example.

The first method for estimating the quantity of material made airborne by aerodynamic entrainment is to use the "per cent airborne" and "resuspension flux" data measured by Mishima and Schwendiman.<sup>27</sup> For example, they measured entrainment of uranium dioxide powder and uranium nitrate solution at different air velocities. The application of these data will require engineering judgment. A second method for estimating entrainment is to use the results developed by Singer et al.<sup>31,32</sup> to estimate coal dust entrainment. These results are discussed by Sutter.<sup>14</sup>

Finally, the analyst may use the resuspension rate concept introduced by Sehmel.<sup>33</sup> Resuspension rate is defined as fraction of initial mass resuspended per second. By definition,

$$S = \frac{A}{G\Delta t} ,$$

where  $S$  = resuspension rate, fraction/s,  
 $A$  = mass suspended and flowing horizontally  
 through a given cross-sectional area, g,  
 $G$  = ground source mass, g, and  
 $\Delta t$  = duration of sampling, s.

Measurements of  $S$  obtained during a number of atmospheric field tests are given in Sutter's paper. The user should become familiar with the limitations of all three of the above methods so he can use them correctly.

Here we will present in detail the procedure and equations used with option (2)--calculated aerodynamic entrainment of dry powder from thick beds. This technique is modeled in a subroutine in TORAC, and it has the advantage of calculating entrainment automatically for the user. As with the three methods discussed above in the second example, our objective is to provide the material convection module with an estimate of the quantity of particulate material that can be entrained from a contaminated surface as a result of tornado-induced transient flow conditions. However, the previous three methods are not suitable for use in TORAC because they are based on steady-state measurements for specific conditions. Except for Singer's<sup>31</sup> work with coal dust, they fail to

couple unsteady flow (changing velocity) conditions to the amount of material entrained. In addition to local flow characteristics, the previous methods fail to account for material or surface characteristics in a systematic way. Thus, resuspension factor, resuspension rate, and per cent airborne would have to be measured for innumerable cases to encompass accident conditions.

The analytical method used in TORAC for calculating aerodynamic entrainment was proposed and illustrated in a fuel cycle facility application in Ref. 5. To estimate the quantity of material entrained, this method considers the following questions. (1) When does the surface material begin to move? (2) What criterion determines when material will be suspended? (3) How much material becomes suspended? A valid answer to (1) implies that one has taken into account particle, surface, and flow characteristics. Some account also must be made for the forces acting, namely, aerodynamic, interparticle (cohesion), and surface to particle (adhesion) forces. This procedure is similar to the approach taken by Travis,<sup>34</sup> who developed a computer model to predict re-entrainment and redistribution of soil contaminants as a result of eolian effects.

The first question we must answer is: When does material begin to move? Before particle motion can occur, a threshold airspeed must be equalled or exceeded so that the aerodynamic forces will be sufficient to overcome restraining forces. To relate threshold airspeed to surface effects, we introduce the friction speed

$$u_* = \sqrt{\tau/\rho} \quad , \quad (B-5)$$

where  $\tau$  = mean shear stress at the surface and

$\rho$  = fluid density.

Experimental measurements of threshold friction speed  $u_{*t}$  obtained at the onset of material movement are available for a wide range of material sizes and densities.

These measurements were plotted in Fig. 62 (from Ref. 35) and are fitted to the following semi-empirical equations.<sup>36</sup>

$$A = (0.108 + 0.0323/B - 0.00173/B^2) \quad (B-6a)$$

$$\times (1 + 0.055 / \rho_p g D_p^2)^{1/2} ,$$

where  $A = u_{*t} / \left[ (\rho_p - \rho) g D_p / \rho \right]^{1/2} ,$

$$B = u_{*t} D_p / \nu ,$$

$D_p$  = average particle diameter,

$\rho_p$  = particle density,

$g$  = gravitational acceleration, and

$\nu = \mu / \rho$  = fluid kinematic viscosity.

Equation (B-6a) holds for  $0.22 \leq B \leq 10$ . The variable A is the threshold coefficient. The variable B is the particle friction Reynolds number. For the range  $B \leq 0.22$ , Eq. (B-6b) applies:

$$A = 0.266(1 + 0.055/\rho_p g D_p^2)^{1/2} \quad (B-6b)$$

$$\times (1 + 2.123B)^{-1/2} .$$

Equations (B-6) collapse the threshold friction speed data in the appropriate range of B onto a single curve with  $D_p$  and  $\rho_p$  as parameters. Given a particular aerosol size and density, we can calculate  $u_{*t}$  from Eqs. (B-6). An iterative technique is used to solve for  $u_{*t}$  in Eqs. (B-6) because this variable appears implicitly on both sides of the equations. The value of  $\nu$  was assumed to be constant at  $\nu = 0.1454 \text{ cm}^2/\text{s}$  ( $0.02254 \text{ in.}^2/\text{s}$ ), corresponding to standard atmospheric conditions.

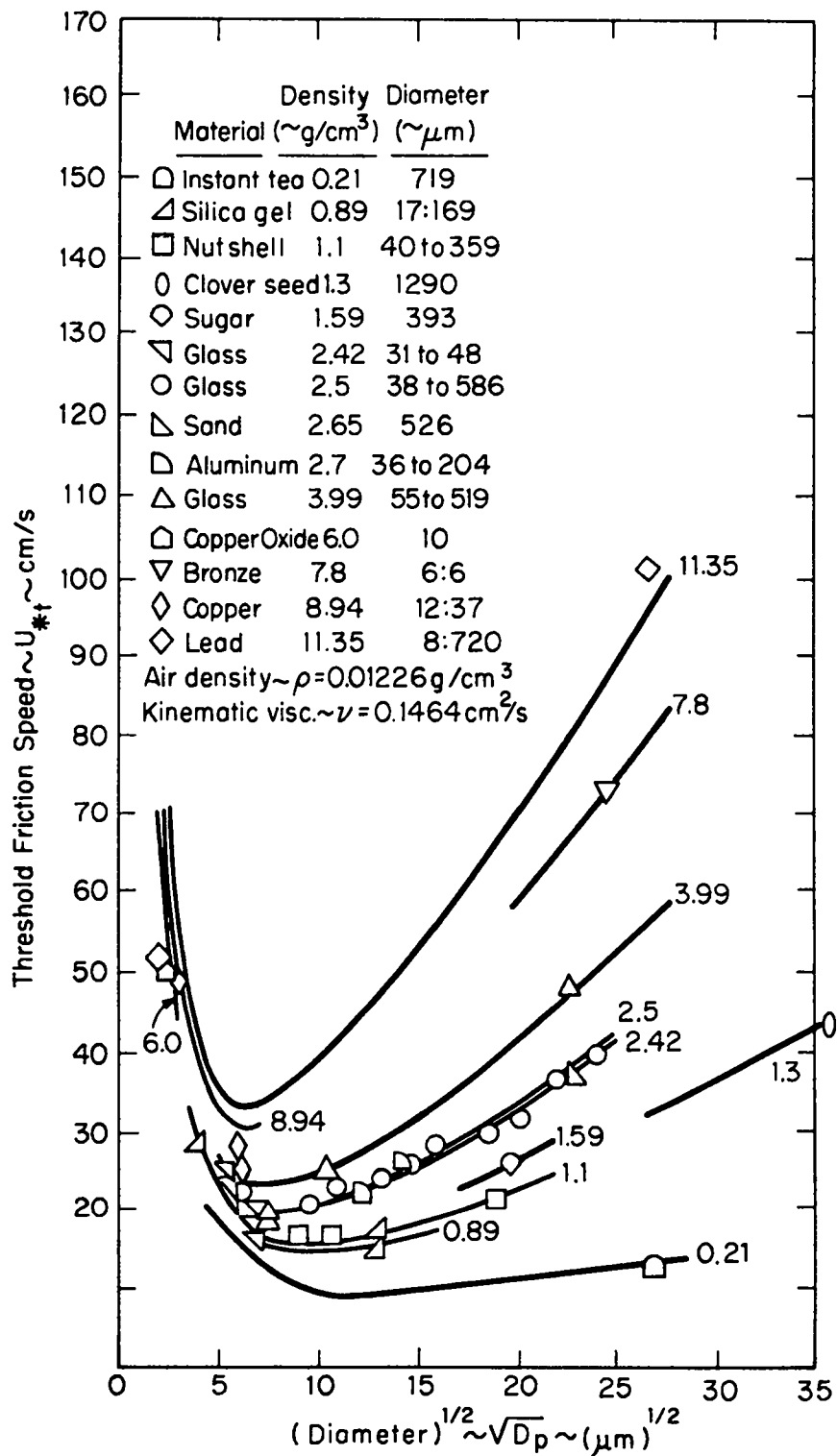


Fig. 62.  
Particulate threshold friction speed.



In  $u_{*t}$  we have a measure of when particle motion will occur and, therefore, when entrainment is possible. Under given flow and surface conditions, a value of the friction velocity exceeding the threshold friction velocity can produce entrainment. That is, entrainment can occur only when  $u_* > u_{*t}$ . We may relate  $u_*$  to the corresponding velocity at the turbulent boundary layer edge using one of the following two equations. For a smooth surface with a laminar sublayer,<sup>37</sup>

$$u(y)/u_* = (1/0.41) \ln (yu_*/\nu) + 5.0 \quad . \quad (B-7)$$

For a rough surface with no laminar sublayer,<sup>38</sup>

$$u(y)/u_* = (1/k) \ln (y/y_0) \quad , \quad (B-8)$$

where  $y$  = distance from surface,

$k = 0.4$  = Von Karman constant,

$y_0 = R/30$  = roughness length, and

$R$  = average surface roughness height,

and where the velocity  $u(y)$  is calculated by TORAC's gas dynamics module. For a duct with fully developed turbulent airflow conditions, the centerline velocity or velocity at the boundary layer edge may be 25% higher than the average or bulk velocity. This version of TORAC uses Eq. (B-8) for a rough surface with an assumed boundary layer thickness of  $y = 10$  cm and a roughness length of  $y_0 = 0.0104$  cm (0.0041 in.) (a moderately rough surface). Our use of Eq. (B-8) will lead to higher values of  $u_*$  for the same values of  $u(y)$  and  $y$  than Eq. (B-7). Because entrainment is known to depend on the difference  $(u_* - u_{*t})$ , our choice of Eq. (B-8) will lead to conservative estimates of entrained material.

The next question is: What determines whether particles go into suspension? That is, of all the particles, how do we divide those that could become airborne from those that remain close to the surface? Iversen et al.<sup>36</sup> have shown that suspension occurs as soon as the threshold speed is reached. The criterion assumed here was that suspension will occur for those particles for which  $u_s/u_* = 1$  and  $u_* > u_{*t}$ , where  $u_s$  is the particle fall or terminal speed. The friction speed  $u_*$  is of the same order of magnitude as the vertical component of turbulence in a boundary layer. Values of  $D_p < 50 \mu\text{m}$  for suspension are in agreement with measurements using soils.<sup>34</sup> In TORAC we have assumed that all of the particles are subject to suspension.

How much material becomes suspended? Travis<sup>34</sup> has suggested the following expression for  $q_v$ , the mass of particles per unit area per unit time that go into suspension.

$$q_v = q_h (c_v/u_{*t}^3 c_h) \left[ (u_*/u_{*t})^{P/3} - 1 \right] , \quad (\text{B-9})$$

where  $P$  = mass percentage of suspendable particles, and

$c_v, c_h$  = empirical constants ( $2 \times 10^{-10}$  and  $10^{-6}$ , respectively).

In Eq. (B-9),  $q_h$  is the mass of material moving horizontally through a vertical plane perpendicular to the surface per unit width per unit time and may be determined from<sup>39</sup>

$$q_h = 2.61(\rho/g)(u_* + u_{*t})^2(u_* - u_{*t}) . \quad (\text{B-10})$$

The calculated aerodynamic entrainment option of the TORAC material transport module is a subroutine that uses Eqs. (B-6) through (B-10). The steps can be summarized as follows. At a given time, the gas-dynamics module of TORAC supplies the velocity  $u(y)$  for every volume with material subject to aerodynamic

entrainment. This value of  $u(y)$  and the turbulent boundary layer velocity profile Eq. (B-8) are used to compute a surface friction velocity  $u_*$ . A characteristic value of threshold friction velocity  $u_{*t}$  for the input material characteristics is obtained from Eq. (B-6). If  $u_* \leq u_{*t}$ , no entrainment occurs. [See Eq. (B-10).] If  $u_* > u_{*t}$ , then the semi-empirical entrainment equations [Eqs. (B-9) and (B-10)] are used to estimate the vertical flux of suspendable material  $q_v$ . Knowing  $q_v$  and the floor area over which the contaminant is uniformly distributed  $A$ , we can compute the source term

$$\dot{M}_p = q_v A \quad , \quad (B-11)$$

which has the units kilograms per second. As a source term, Eq. (B-11) represents a positive contribution to the  $\dot{M}_p$  term on the right-hand side of Eq. (B-29) in Sec. V. The floor area  $A$  is assumed to be flat and free of obstacles or protuberances.

The question of how heavily a surface must be loaded before equations like Eqs. (B-6), (B-9), and (B-10) are applicable is debatable. For the realistic types of loadings such as we expect to find in many locations of a fuel cycle facility, the empirical constant in Eq. (B-10) may not be satisfactory because it was obtained for relatively thick powder beds. Furthermore, the empirical coefficients in Eq. (B-9) are suspect because they were obtained from experiments with soil particles.

The recent experimental and theoretical work underlying Eqs. (B-6) and (B-10) is believed to be the best available.<sup>35,36,39</sup> Thus, the basis for predicting  $u_{*t}$  using Eq. (B-6) is sound; however, the data base to which Eq. (B-6) was fit is sparse for small heavy particles. In principle, these uncertainties could be checked and reduced with appropriate experimentation.

## V. CONVECTION

### A. Assumptions

The usual mathematical formulation for the motion of a multiphase, multi-component material system is based on the concept of continuum mechanics with

some pertinent qualifications.<sup>9</sup> We can obtain a set of partial differential equations for some macroscopic parameters with a few phenomenological descriptions of the stress, heat flux, and diffusion plus other formulations for the physical and chemical interactions among phases and components and with the boundary. Some of the relationships are either incomplete or not yet known. Depending on the range of interest, an extensive simplification is necessary. The following assumptions are made to reduce the complexity of the problem but still enable us to meet our simple objective, namely, the capability of handling material transport without disturbing the main gas flow to any significant degree.

We define the material as any pneumatically transportable substance in a ventilation system. The material can be solid, liquid, or even gas other than the main gas stream. The individual material point is assumed to be quite small in size if it is in the condensed phase. A material cloud is an ensemble of material; throughout the ventilation system, the main body of the gas and the material cloud form a mixture. The description of the flow system is based on the continuum point of view. We will neglect all chemical reactions and physical processes such as deposition, entrainment, coalescence, material break-up, evaporation, and condensation. Material generation is a prescribed quantity; once the material cloud is formed and mixed with the main gas stream, our attention will be on the movement of the material.

Even for a dusty cloud, the volume occupied by the material is quite small compared with the gas volume. We will assume this is the case in our first model and refer to it as the disperse condition. A consequence of this is that the material motion is dominated by the aerodynamic forces (mainly drag), not by the inter-particle forces. Furthermore, the material size we most often encounter in a ventilation system falls into the micron range. For that small size, the aerodynamic relaxation time is quite small compared with the typical residence time. This means the material can respond quickly to the variation of gas velocity, and most of the time the material would have a velocity nearly identical to the gas at any location and time. Thus, we have obtained the dynamic equilibrium condition between the gas and the material cloud, and the only equation needed to find the material flow rate is the material continuity equation. We can add one more equilibrium condition; that is, the material temperature is the same as the gas, and we have a homogeneous equilibrium model for the

gas and material cloud mixture. This mixture can be treated as a simple gas with proper thermodynamic and transport properties used in all usual gas-dynamic equations.<sup>40</sup>

In principle, we could proceed to solve the set of gas-dynamic equations for the mixture. However, the mixture transport properties are not easy to determine. On the other hand, we still can obtain governing equations for the main gas stream and for the material cloud separately. Some of these equations will contain terms that express the effect of interaction between the gas stream and the material. A closer examination of these terms reveals that if the material mass fraction is quite small compared with that of the gas, then the effect of the interaction on the gas-phase flow is negligible. This is the disperse condition for the material cloud relative to the gas mass, and we shall assume so. At this point, we have achieved the complete separation of the gas-phase flow dynamics from the material cloud. The gas-dynamic aspect of the material transport problem can be solved first and then the continuity relation of the material will be used to determine the material flow. A more complete presentation of various multiphase, multicomponent flow problems is given in the literature.<sup>9,40,41</sup> All the above assumptions and steps leading to the final simplification of the material transport problem are based on those literature cited.

#### B. Continuity Equation

In a volume of  $V$ , a part of it is occupied by a material with mass  $M_p$  and volume  $V_p$  and the rest by a gas of mass  $M_g$  and volume  $V_g$ ; obviously

$$V = V_p + V_g \quad . \quad (B-12)$$

We define a volume fraction of the material

$$\alpha_p = \frac{V_p}{V} \quad , \quad (B-13)$$

and the densities (concentrations) of the material and gas based on the mixture volume,

$$\rho'_p = \frac{M_p}{V} \quad \text{and} \quad \rho'_g = \frac{M_g}{V} \quad , \quad (\text{B-14})$$

which differ from the densities based on the volume of the individual phase,

$$\rho_p = \frac{M_p}{V_p} \quad \text{and} \quad \rho_g = \frac{M_g}{V_g} \quad . \quad (\text{B-15})$$

Only  $\rho_g$  is related to the pressure and temperature through the equation of state. The mass fraction of the material is defined as

$$Y_p = \frac{M_p}{M_p + M_g} \quad . \quad (\text{B-16})$$

We can express the mass fraction in terms of volume fraction through the following relation.

$$Y_p = \left[ 1 + \left( \frac{1 - \alpha_p}{\alpha_p} \right) \left( \frac{\rho_g}{\rho_p} \right) \right]^{-1} \quad . \quad (\text{B-17})$$

Because the material-phase density of a liquid or solid is usually so much larger than the gas-phase density, the disperse condition ( $\alpha_p \ll 1$ ) does not imply the dilute condition ( $Y_p \ll 1$ ) unless

$$\alpha_p \ll \frac{\rho_g}{\rho_p} , \quad (\text{B-18})$$

which is a more stringent condition. We will assume this is the case in the current material convection model.

The velocity of a mixture is defined as follows.

$$u = \left( \rho_p' u_p + \rho_g' u_g \right) / \rho , \quad (\text{B-19})$$

with

$$\rho = \rho_p' + \rho_g' . \quad (\text{B-20})$$

$\rho$  is the density of the mixture and  $u$ ,  $u_p$ , and  $u_g$  represent the mixture velocity, material velocity, and gas velocity; they are vector quantities. Using the mass fraction  $Y_p$ , we have

$$u = Y_p u_p + (1 - Y_p) u_g . \quad (\text{B-21})$$

if  $u_p$  and  $u_g$  are of the same order of magnitude and for the dilute condition,

$$u \cong u_g . \quad (\text{B-22})$$

The mixture velocity is dominated by the gas velocity. Also from Eq. (B-20), the mixture density is roughly the same as the gas density. We expect this should be the case for a light loading situation. From now on, we shall drop the subscript g for all quantities associated with the gas phase.

The continuity equation for any phase or component in a mixture is<sup>41</sup>

$$\frac{d}{dt} \int_V \rho'_p dV = - \int_S \rho'_p \mathbf{u}_p \cdot d\mathbf{S} + \dot{M}_p \quad . \quad (\text{B-23})$$

The time derivative term on the left-hand side represents the change of the material density inside a control volume V. The first term on the right-hand side is the material flow through the boundary S of the volume V, and the last term is the material source. Assuming  $\rho_p$  is uniform over the control volume and using the same representation we have for the gas continuity equation, Eq. (B-23) becomes

$$V \frac{d\rho'_p}{dt} = \sum_i \rho'_p u_{pi} A_i + \dot{M}_p \quad . \quad (\text{B-24})$$

Here we drop the vector notion for the velocity but add subscript i to indicate the flow path connecting to that volume.  $A_i$  is the flow area, and  $u_{pi}$  is the flow velocity normal to the area. The positiveness of the flux term is referred to the flow into the volume. Again we introduce  $Y_p$  into Eq. (B-24),

$$V \frac{d}{dt} [Y_p \rho] = \sum_i Y_{pi} \rho_i u_{pi} A_i + \dot{M}_p \quad , \quad (\text{B-25})$$

or



$$V \frac{dY_p}{dt} = \frac{1}{\rho} \left[ \sum_i Y_{pi} \rho_i U_{pi} A_i + \dot{M}_p - Y_p V \frac{d\rho}{dt} \right]. \quad (B-26)$$

The last term in Eq. (B-26) is the gas density change and is determined by the gas continuity equation.

Under the dynamic equilibrium condition, the material velocity is almost identical to the gas velocity everywhere and at any instance, namely,

$$u_{pi} = u_i \quad . \quad (B-27)$$

The variable  $u_i$  represents the gas velocity in the pathway  $i$ . Substituting that into Eq. (B-26) and recalling the gas mass flow in branch  $i$ ,

$$\dot{m}_i = \rho_i u_i A_i \quad , \quad (B-28)$$

we obtain

$$V \frac{dY_p}{dt} = \frac{1}{\rho} \left[ \sum_i Y_p \dot{m}_i + \dot{M}_p - Y_p V \frac{d\rho}{dt} \right]. \quad (B-29)$$

Equation (B-29) is a differential equation for the unknown  $Y_p$ . Once the gas-dynamic quantities  $\rho$  and  $\dot{m}_i$  are known, Eq. (B-29) can be integrated to obtain  $Y_p$  at a new time. The advantage of using  $Y_p$  instead of  $\rho_p$  as unknown is that  $Y_p$  is not as subject to the effect of compressibility as  $\rho_p$ . When  $Y_p$  is calculated, the material density concentration can be obtained through

$$\rho'_p = Y_p \rho \quad . \quad (B-30)$$

The quantity mass fraction (or molar fraction) has been used extensively in fluid flow with chemical reaction.

In TORAC, we expect the air density variation to be small; therefore, we use Eq. (B-24) directly in the numerical calculation without referring to the mass fraction step.

Finally, we must emphasize again that the assumptions made about the dilute condition of material enable us to solve the gas-dynamic problem independently. The validity of the assumptions depends on the individual case that we are facing. However, we do believe that this simple model will cover a broad range of problems related to material movement in nuclear facilities.

## VI. AEROSOL DEPLETION

Because the flow Reynolds number based on the enclosure or duct hydraulic diameter and fluid bulk velocity will be greater than about 2100 for all cases of interest here, the flow always will be turbulent. We will assume that all flows are fully developed so that boundary layer or duct velocity profile shapes are constant with distance. This will be approximately true sufficiently far from inlets (20 to 50 hydraulic diameters) so that entrance effects are unimportant in our calculations.

Under these conditions, not all of the material that is made airborne at the location of material transport initiation will survive convective transport to the filtration systems or facility boundary. Depending on the aerosol aerodynamic characteristics and passage geometry, there may be a sizable reduction in aerosol concentration. As such, an enclosure or duct acts as an aerosol filter.

A number of processes that can cause aerosol depletion, and hence contribute to a material transport sink term, should be considered.<sup>2--4,10</sup> Particles that come sufficiently close to surfaces can be intercepted mechanically and stuck. Particles with enough inertia can deviate from the flow streamlines, impact, and stick to rough elements, obstacles, or bends. Particles less than about 1  $\mu\text{m}$  in size can be transported to surfaces by both turbulent (eddy) and molecular (Brownian) diffusion. Particles with size greater than about 1  $\mu\text{m}$  and being transported parallel to surfaces can be deposited because of the fluctuating velocity components normal to the surface (turbulent inertial deposition).

Also, particles moving through passages that are horizontal (or not exactly vertical) will deposit by gravitational sedimentation. Lower flow velocities enhance deposition caused by molecular diffusion and sedimentation. Unless the surfaces are sticky, the net rate of deposition will depend on the relative rates of transport and reentrainment. Except for fibrous particles or very light particles, interception may be neglected because particles large enough to be intercepted will most likely deposit as a result of inertial effects or sedimentation.

Under certain conditions, other effects may become important for the smallest particles. These effects include thermophoresis, diffusiophoresis, and electrical migration.<sup>2,10</sup> They are believed to be relatively unimportant compared with other effects.

Future versions of the TORAC material transport module will account for combined molecular and turbulent diffusion as well as aerosol interactions, but the current version is restricted to gravitational sedimentation. The particle flux  $J$  resulting from gravitational sedimentation is<sup>2</sup>

$$J = u_s n \quad , \quad (B-31)$$

where the units of  $J$  are particles per unit area per unit time,  $u_s$  is the terminal settling velocity, and  $n$  is the uniform local aerosol number concentration in particles per unit volume. If we multiply both sides of Eq. (B-31) by the homogeneous particulate mass  $m_p$ , then

$$J' = u_s \rho_p' \quad , \quad (B-32)$$

where the units of  $J'$  are mass per unit area per unit time, and  $\rho_p' = nm_p$  is the aerosol mass concentration per unit volume. The terminal settling velocity is calculated from<sup>2</sup>

$$u_s = \rho_p D_p^2 g C / 18\mu \quad , \quad (B-33)$$

where

$\rho_p$  = aerosol density,

$D_p$  = aerosol diameter,

$g$  = gravitational acceleration,

$C$  = Cunningham slip correction factor, and

$\mu$  = fluid dynamic viscosity.

The TORAC input variables for material depletion are  $\rho_p$  and  $D_p$ . These variables may be assumed or selected to be aerodynamic diameter with unit density or Stokes diameter with the material bulk density. This selection was discussed earlier. To calculate the slip correction factor, the code uses<sup>2</sup>

$$C = 1 + (2L/D_p)[A_1 + A_2 \exp(-A_3 D_p/L)] \quad , \quad (B-34)$$

where  $L$  is the molecular mean free path and the  $A$ 's are dimensionless constants based on experimental measurements of small-particle drag. The code uses

$$L = 0.065 \text{ } \mu\text{m} \quad ,$$

$$A_1 = 1.257 \quad ,$$

$$A_2 = 0.400 \quad ,$$

$$A_3 = 0.550 \quad ,$$

$$g = 981 \text{ cm/s}^2 \quad , \text{ and}$$

$$\mu = 0.0001781 \text{ g/cm s} \quad ,$$

where  $L$ ,  $\mu$ , and  $g$  are taken at standard sea level conditions.

We know  $\rho_p$  from the material transport mass balance calculation for the previous time step for each node (volume or duct). Then, knowing  $u_s$  and the projected floor area for sedimentation  $A$ , we can compute the sink term using Eq. (B-32)

$$M_p = - J'A = -u_s \rho_p A' , \quad (B-35)$$

which has the units kilograms per second. Because aerosol depletion is a sink term, we have used a minus sign in Eq. (B-35). This equation represents a negative contribution to the  $M_p$  term on the right-hand side of Eq. (B-29) in Sec. V. Aerosol depletion by sedimentation may be selected for all volumes and ducts and is calculated in the same manner.

## VII. FILTER MODEL

### A. Introduction

Experimental evidence<sup>42</sup> indicates that the pressure drop across filters commonly used for air cleaning in chemical and nuclear industries increases non-linearly at high-speed flow. This contrasts with the linear relationship that we generally observe in relatively low-speed flow regions for normal or near normal applications.<sup>1</sup> We can take an entirely experimental approach to determine all the influence coefficients for filter and flow properties. We can model the filter flow based on the principle of flow through porous media and determine the relationship between the flow rate and the pressure drop with most, if not all, pertinent parameters explicitly included. Even so, some empirical constants still are needed; for practical purposes, we can combine some filter properties into these constants and determine them by experimental means. The number of coefficients with proper filter modeling is much less than that obtained through a direct empirical method. We will review some theoretical works and then present a model that is suitable for our system.

The purpose of using air filters in a ventilation system is to remove airborne material in the air stream and to prevent hazardous material from being

released to the environment. Experience shows that the accumulation of material, usually in the condensed phase, will cause the pressure drop across a filter to increase for the same flow rate. In the case of fire or explosion, rapid flow resistance increases as the result of large amounts of material caught by a filter. This is commonly called filter plugging or clogging. After reviewing analytical work in development of filter models we will briefly review filter plugging phenomena and propose a semi-empirical formulation to describe this condition.

## B. Filter Model

The pioneering work of D'Arcy<sup>43</sup> established the foundation of the principles of fluid flow through porous media. His experimental results indicated a linear relationship between the flow rate and the pressure drop that was proportional to an empirical constant, permeability. This parallels quite well the conclusion of fully developed laminar flow through a pipe by Hagen-Poiseuille.<sup>38</sup> It is not surprising to find that many theoretical models on flow through porous media are based on D'Arcy's concept with different qualifications. Among them, the most successful is the Kozeny model.<sup>44</sup> According to his theory, the porous medium is represented by an assemblage of channels of various cross-sections with a definite length. The flow through the channels is determined by the Navier-Stokes equations, and the permeability is expressed in terms of viscosity and properties of the porous medium. However, an empirical constant is needed to include the effect of the tortuous characteristic of the medium. A modification of the Kozeny model by Carman<sup>45</sup> defined the constant, which is called tortuosity, in a more explicit way. This new model still requires an empirical coefficient to account for the uncertainty of determining various porous medium properties.

Another point of view on the pressure drop relationship of flow through a porous medium is based on drag theory with the dragging obstacles being particles or fibers. A model<sup>46</sup> using fibers as a porous medium leads to a permeability that is weakly dependent on flow rate. Because of the actual complexity of the medium, some empirical adjustment is needed for this model.

So far we have discussed D'Arcy's law and its derivatives, which are adequate only when the flow velocity is low; that is, at conditions where the pressure drop is proportional to the viscous dissipation by the porous medium. For channel flow with flow velocity increasing, the dissipation mechanism changes

from a viscous to a turbulent effect, and the pressure drop is then proportional to the kinetic energy of the stream.<sup>38</sup> Following Kozeny's reasoning in modeling porous media as channels, a quadratic relation can be established between the pressure drop and flow rate at high velocity.<sup>47</sup> Again, an empirical coefficient equivalent to the resistance factor in pipe flow under turbulence conditions is introduced. The summation of viscous effects and turbulent dissipation leads to an equation proposed by Ergun.<sup>48</sup>

$$\frac{\Delta p}{l} = 150 \frac{(1-\epsilon)^2}{\epsilon^3} \frac{\mu u_m}{d_p^2} + 1.75 \frac{(1-\epsilon)}{\epsilon^3} \frac{\rho u_m^2}{d_p} \quad , \quad (\text{B-36})$$

with

$\Delta p$  = pressure drop,

$l$  = bed length,

$g$  = gravitational constant,

$\epsilon$  = void fraction,

$\mu$  = viscosity,

$d_p$  = effective porous medium particle size,

$\rho$  = fluid density, and

$u_m$  = superficial velocity.

Superficial velocity is the flow velocity approaching the packed bed, not the average flow velocity in the interstitial region. Equation (B-36) is written in centimeter-gram-seconds units but also can be expressed in a different form:

$$\Delta p = K_L \mu \frac{Q}{A^{3/2}} + K_T \rho \frac{Q^2}{2A^2} \quad , \quad (\text{B-37})$$

where  $Q$  and  $A$  represent volume flow rate and the frontal area of the packed column, respectively. It can be seen that

$$u_m = \frac{Q}{A} \quad , \quad (B-38)$$

$$K_L = 150 \frac{(1-\epsilon)^2}{\epsilon^3} \frac{\ell A^{1/2}}{d_p^2} \quad , \quad (B-39)$$

and

$$K_T = 3.5 \frac{(1-\epsilon)}{\epsilon^3} \frac{\ell}{d_p} \quad . \quad (B-40)$$

$K_L$  and  $K_T$  are dimensionless and depend on the properties of the porous medium. Equation (B-37) is identical to the Reynolds'<sup>49</sup> expression on pipe flow in laminar and turbulent regions.

As discussed earlier, the theoretical model that we ultimately choose will use some empirical coefficients and must be included to account for the complexity and uncertainty of the porous medium. Obviously, it does not matter if we obtain  $K_L$  and  $K_T$  first from Eqs. (B-39) and (B-40) and then add experimental corrections later. We can go ahead to determine the effective  $K_L$  and  $K_T$  directly from experiment. This task is not more difficult than finding the correction factors alone because there are only two unknowns involved as presented in Eq. (B-37). From now on we will use Eq. (B-37) as the foundation of our filter model regardless of the filtration media we use as long as we can determine the two coefficients through experiment or analytical means.

A subroutine using Eq. (B-37) to represent a filter branch has been added to the TORAC code because we expect very high flow rate in the system if a tornado-induced depressurization occurs. The turbulence coefficient  $K_T$  must be read in through the input file; if it is zero, then only the laminar-dependent



portion will be used. The laminar coefficient  $K_L$  can be input or calculated for a given pressure drop and flow rate; however, the former approach is preferred. This subroutine has been checked out successfully. However, reliable data on  $K_T$  have not been obtained, and more extensive experimental work in that area is needed.

### C. Filter Plugging

The physical phenomena involving the capture of a suspended particle in an air stream by a filtration medium is complicated.<sup>50,51</sup> The porous material provides various locations for material retention—resting on the surface of the bed grain, wedged in a crevice, stopped at constrictions, or contained in a pore cavity. The normal pressure of the fluid, friction, inter-particle forces, and chemical bonding force give the required means of holding the material at a given location. The mechanisms of the suspended material reaching a retention site include gravity, inertia, hydrodynamic forces, interception, and Brownian motion. Attempting to relate the overall filter efficiency with the aforementioned mechanisms without any experimental coefficient is impractical. A phenomenological approach is more useful; that is, we assume some form of dependence on filter efficiency on the total amount of retention. We note that experimentation indicates a small increase in the efficiency for increasing retention. For normal operating conditions, we assume that filter efficiency remains constant and does not significantly affect the system flow conditions.

The same conclusion cannot be drawn about the flow resistance of a filter for a large amount of material retained on it. The increase in resistance can be quite substantial and should be dealt with properly. The plugging is related to material size, shape, phase, filter structure, and finally the quantity of captured material. Using the Carman-Kozeny filter model,<sup>45</sup> material retention reduces the specific surface, which is defined as the total surface of the bed grain per unit filter volume and thus increases the effective resistance.<sup>50</sup> We can express the general relation as follows.

$$\frac{\Delta P}{(\Delta P)_0} = f(M_a), \quad (B-41)$$

where  $(\Delta p)_0$  is the pressure drop for a clean filter [shown in Eq. (B-37)], and  $f$  is a monotonically increasing function of material mass  $M_a$  on the filter. Clearly,  $f(M_a = 0) = 1$ . For a light loading condition,  $f$  is a linear function of  $M_a$ ,

$$f(M_a) = 1 + \alpha M_a, \quad (B-42)$$

where  $\alpha$  is a coefficient dependent on filter and material properties.<sup>51</sup> More recent work of Bergman<sup>52</sup> using Davies' fibrous drag model<sup>53</sup> concludes that depends on the fiber volume fraction, fiber size, and particulate size. However, the foundation of Davies' model is still empirical. For the time being, we will postulate the phenomenological relation of Eq. (B-42) with  $\alpha$  being determined by experiment. As future data warrant, we will modify the equation with more explicit relations included.

#### D. Conclusion

We have presented a nonlinear filter model and a filter plugging model used in the TORAC computer code. The background physics, simplification, and mathematical formulation were discussed and evaluated. We are not stopping our effort here; we are continuing to modify the codes and add various features as needed. We will complement our analytical effort with extensive experimental investigation.

#### REFERENCES

1. K. H. Duerre, R. W. Andrae, and W. S. Gregory, "TVENT, A Computer Program for Analysis of Tornado-Induced Transients in Ventilation Systems," Los Alamos Scientific Laboratory report LA-7397-M (July 1978).
2. S. H. Friedlander, Smoke, Dust, and Haze (John Wiley and Sons, New York, 1977).
3. T. T. Mercer, Aerosol Technology in Hazard Evaluation (Academic Press, New York, 1973).
4. R. Dennis, "Handbook of Aerosols," Technical Information Center, Energy Research and Development Administration report TID-26608 (1978).

5. R. W. Andrae, R. A. Martin, and W. S. Gregory, "Analysis of Nuclear Facilities for Tornado-Induced Flow and Reentrainment," Los Alamos Scientific Laboratory report LA-7571-MS, NUREG/CR-0521 (January 1979).
6. E. H. Markee, Jr., J. G. Beckerley, and K. E. Sanders, "Technical Basis for Interim Regional Tornado Criteria," Nuclear Regulatory Commission report WASH-1300 (1974).
7. D. C. Kaul, Ed. "Adversary Actions in the Nuclear Power Fuel Cycles: Reference Events and Their Consequences, Vol. IV, Consequence Assessment Methodology," Science Applications Inc. report SAI-152-123-80-1 (March 1981).
8. N. A. Fuchs, The Mechanics of Aerosols (Pergamon Press Ltd., Oxford, 1964).
9. S. L. Soo, Fluid Dynamics of Multiphase Systems (Blaisdell Publishing Company, Waltham, Massachusetts, 1967).
10. C. N. Davis, Air Filtration (Academic Press, New York, 1973).
11. G. M. Hidy and J. R. Brock, The Dynamics of Aerocolloidal Systems (Pergamon Press Ltd., Oxford, 1970).
12. J. D. Stockham and E. G. Fochtman, Eds., Particle Size Analysis (Ann Arbor Science, Ann Arbor, Michigan, 1978).
13. "Accident Analysis Handbook," Los Alamos National Laboratory report NUREG/CR-2508, LA-9180-M in preparation.
14. S. L. Sutter, "Accident-Generated Particulate Materials and Their Characteristics—A Review of Background Information," Pacific Northwest Laboratory report PNL-4154 (1981).
15. J. C. Elder, M. Gonzales, and H. J. Ettinger, "Plutonium Aerosol Size Characteristics," Health Physics 27, 45-53 (1973).
16. H. J. Ettinger, J. C. Elder, and M. Gonzales, "Size Characteristics of Plutonium Aerosols," Los Alamos Scientific Laboratory report LA-DC-72-920 (1972).
17. W. B. Seefeldt, W. J. Mecham, and M. J. Steindler, "Characterization of Particulate Plutonium Released in Fuel Cycle Operations," Argonne National Laboratory report ANL-75-78 (1976).
18. E. C. Hyatt, W. D. Moss, and H. F. Schulte, "Particle Size Studies on Uranium Aerosols from Machining and Metallurgy Operations," J. Amer. Indus. Hyg. Assoc. 20(2), 99-107 (1959).
19. L. C. Schwendiman, J. Mishima, and G. E. Stegen, "Airborne Plutonium Release Postulated for Serious Accidents in a Generic Recycle Mixed Oxide Fuel Fabrication Plant," Pacific Northwest Laboratory unpublished draft report (November 1974).

20. J. M. Selby, L. D. Williams, E. C. Watson, and R. J. Hall, "Considerations in the Assessment of the Consequences of Effluents from Mixed Oxide Fuel Fabrication Plants," Pacific Northwest Laboratory report BNWL-1697 (1973).
21. J. Mishima and L. C. Schwendiman, "Airborne Release of Plutonium and its Compounds During Overheating Incidents," Pacific Northwest Laboratory report BNWL-1691, Part 1 (1972), pp. 82-87.
22. R. W. Woodard, "Plutonium Particulate Studies on Booster System No. 3 (Building 771) Filter Plenum," Dow Chemical Co. report CRDL 940610-1 (January 1971).
23. B. R. Fish, G. W. Keilholtz, W. S. Snyder, and S. D. Swisher, "Calculation of Doses Due to Accidentally Released Plutonium from an LMFBR," Oak Ridge National Laboratory report ORNL-NSIC-74 (November 1972).
24. O. J. Wick, Ed., Plutonium Handbook (Gordon and Breach Science Publishers, New York, 1967).
25. E. Walker, "A Summary of Parameters Affecting the Release and Transport of Radioactive Material from an Unplanned Accident," report by Bechtel Inc., San Francisco, California (1978).
26. L. C. Schwendiman, "Supporting Information for the Estimation of Plutonium Oxide Leak Rates Through Very Small Apertures," Battelle Pacific Northwest Laboratory report BNWL-2198 (1977).
27. J. Mishima and L. C. Schwendiman, "Some Experimental Measurements of Airborne Uranium (Representing Plutonium) in Transportation Accidents," Battelle Pacific Northwest Laboratory report BNWL-1732 (1973).
28. J. W. Healy, "Surface Contamination: Decision Levels," Los Alamos Scientific Laboratory report LA-4558-MS (September 1971).
29. B. R. Fish, Surface Contamination (Pergamon Press Ltd., Oxford, 1967).
30. R. J. Englemann and G. A. Sehmel, Atmosphere-Surface Exchange of Particulate and Gaseous Pollutants, ERDA Symposium Series Conf.-740921 (1974).
31. J. M. Singer, E. B. Cook, and J. Grumer, "Dispersal of Coal and Rock Dust Deposits," U.S. Bureau of Mines report BM-RI-7642 (1972).
32. J. M. Singer, M. E. Harris, and J. Grumer, "Dust Dispersal by Explosion-Induced Airflow, Entrainment by Air Blast," U.S. Bureau of Mines report BM-RI-8130 (1976).
33. G. A. Sehmel and F. D. Lloyd, "Particle Resuspension Rates," in Atmosphere-Surface Exchange of Particulate and Gaseous Pollutants, R. J. Englemann and G. A. Sehmel, Coordinators, ERDA Symposium Series, Conf.-740921 (1974), pp. 846-858.

34. J. R. Travis, "A Model for Predicting the Redistribution of Particulate Contaminants from Soil Surfaces," Los Alamos Scientific Laboratory report LA-6035-MS (August 1975).
35. J. D. Iversen, J. B. Pollack, R. Greeley, and B. R. White, "Saltation Threshold on Mars: The Effect of Interparticle Force, Surface Roughness, and Low Atmospheric Density," ICARUS 29, 381-393 (1976).
36. J. D. Iversen, R. Greeley, and J. B. Pollack, "Windblown Dust on Earth, Mars, and Venus," J. Atm. Sci. 33(12), 2425-2429 (1976).
37. F. M. White, Viscous Fluid Flow (McGraw-Hill Book Company, Inc., New York, 1974).
38. H. Schlichting, Boundary Layer Theory, 4th Ed. (McGraw-Hill Book Company, Inc., New York, 1960).
39. J. D. Iversen, R. Greeley, B. R. White, and J. B. Pollack, "The Effect of Vertical Distortion in the Modeling of Sedimentation Phenomena: Martian Crater Wake Streaks," J. Geophys. Res. 81 (26), 4846-4856 (1976).
40. G. B. Wallis, One-Dimensional Two-Phase Flow (McGraw-Hill Book Company, Inc., New York, 1969).
41. F. A. Williams, Combustion Theory (Addison-Wesley Publishing Company, Inc., Reading, Massachusetts, 1965).
42. W. S. Gregory, H. L. Horak, P. R. Smith, C. I. Ricketts, and W. Gill, "Investigation of HEPA Filters Subjected to Tornado Pressure Pulses", Los Alamos Scientific Laboratory report LA-7202-MS (April 1978).
43. H. D'Arcy, Les Fontaines Publiques de la Ville de Dijon (Victor Dalmont, Paris, 1856).
44. J. Kozeny, "Uber Kapillare Leitung des Wassers in Boden," Akad. Wiss. Wien, Math.-Naturw. Klases, Sitzber (Abt. IIa) 136, 271-306 (1927).
45. P. C. Carman, "Flow Through Granular Beds," Transactions of the Institution of Chemical Engineers, Vol. 15 (1937), pp. 150-166.
46. A. E. Sheidegger, The Physics of Flow Through Porous Media, 3rd Ed. (University of Toronto Press, Toronto, 1972), pp. 146-148.
47. S. P. Burke and W. B. Plummer, "Gas Flow Through Packed Columns," Industrial and Engineering Chemistry 20, 1196-1200 (1928).
48. S. Ergun, "Fluid Flow through Packed Columns," Chemical Engineering Progress 48, 89-94 (1952).
49. O. Reynolds, Papers on Mechanical and Physical Subjects (Cambridge University Press, Cambridge, Massachusetts, 1900).

50. J. P. Herzig, D. M. Leclerc and P. LeGoff, "Flow of Suspensions through Porous Media - Application to Deep Filtration," *Industrial and Engineering Chemistry* (1969).
51. J. Pich, "Theory of Aerosol Filtration," in *Aerosol Science*, C. N. Davies, Ed. (Academic Press, New York, 1966), pp. 223-285.
52. W. Bergman, H. Hebard, R. Taylor, and B. Lum, "Electrostatic Filters Generated by Electric Fields," Lawrence Livermore National Laboratory report UCRL-81926 (1979).
53. C. N. Davis, Ed., *Aerosol Science* (Academic Press, New York, 1966).

DISTRIBUTION

	<u>Copies</u>
Nuclear Regulatory Commission, RZ, Bethesda, Maryland	198
Technical Information Center, Oak Ridge, Tennessee	2
Los Alamos National Laboratory, Los Alamos, New Mexico	50
Total:	<u>250</u>

**BIBLIOGRAPHIC DATA SHEET**

NUREG/CR-4260  
LA-10435-M

2 Leave blank

3 TITLE AND SUBTITLE

TORAC User's Manual  
A Computer Code for Analyzing Tornado-Induced Flow and Material Transport in Nuclear Facilities

4 RECIPIENT'S ACCESSION NUMBER

5 DATE REPORT COMPLETED

MONTH | YEAR  
April | 1985

6 AUTHOR(S)

R.W. Andrae      R.A. Martin  
P.K. Tang        W.S. Gregory

7 DATE REPORT ISSUED

MONTH | YEAR  
May | 1985

8 PERFORMING ORGANIZATION NAME AND MAILING ADDRESS (Include Zip Code)

Los Alamos National Laboratory  
Los Alamos, NM 87545

9 PROJECT/TASK/WORK UNIT NUMBER

10 FIN NUMBER

A7029

11 SPONSORING ORGANIZATION NAME AND MAILING ADDRESS (Include Zip Code)

Division of Risk Analysis  
Office of Nuclear Regulatory Research  
U.S. Nuclear Regulatory Commission  
Washington, DC 20555

12a TYPE OF REPORT

Manual

12b PERIOD COVERED (Inclusive dates)

13 SUPPLEMENTARY NOTES

14 ABSTRACT (200 words or less)

This manual describes the TORAC computer code, which can model tornado-induced flows, pressures, and material transport within structures. Future versions of this code will have improved analysis capabilities. In addition, it is part of a family of computer codes that is designed to provide improved methods of safety analysis for the nuclear industry. TORAC is directed toward the analysis of facility ventilation systems, including inter-connected rooms and corridors.

TORAC is an improved version of the TVENT computer code. In TORAC, blowers can be turned on and off and dampers can be controlled with an arbitrary time function. The material transport capability is very basic and includes convection, depletion, entrainment, and filtration of material. The input specifications for the code and a variety of sample problems are provided.

15a KEY WORDS AND DOCUMENT ANALYSIS

15b DESCRIPTORS

16 AVAILABILITY STATEMENT

Unlimited

17 SECURITY CLASSIFICATION

(This report)  
Unclassified

18 NUMBER OF PAGES

19 SECURITY CLASSIFICATION

(This page)  
Unclassified

20 PRICE

\$



Available from

Superintendent of Documents  
U.S. Government Printing Office  
Post Office Box 37082  
Washington, D. C. 20013-7882

National Technical Information Service  
Springfield, VA 22161

Los Alamos